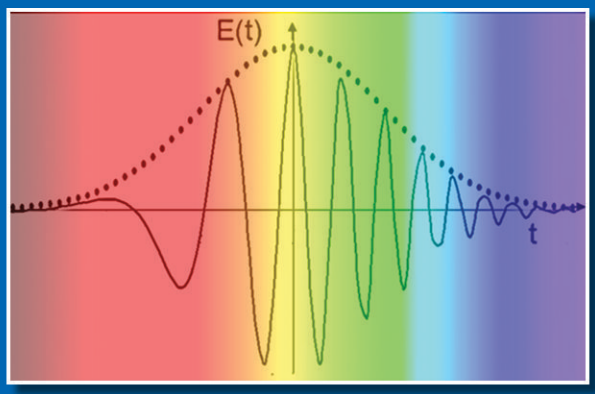
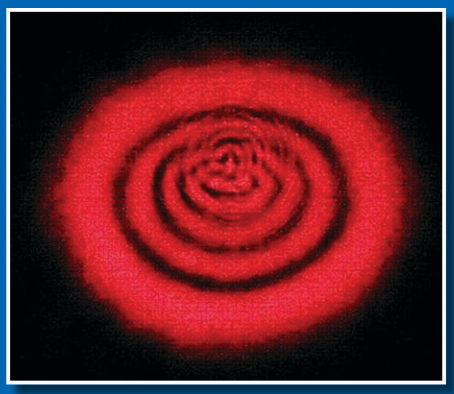
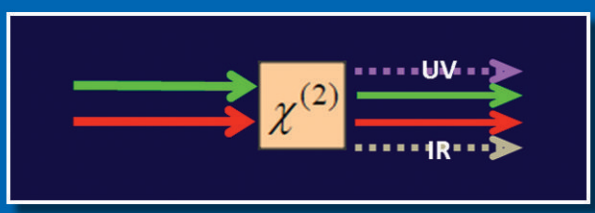
Essentials of Nonlinear Optics







Y.V.G.S. Murti
C. Vijayan

Ane Books Pvt. Ltd.

WILEY

Essentials of Nonlinear Optics

Essentials of Nonlinear Optics

Prof. YVGS Murti
Formerly Professor of Physics
Indian Institute of Technology Madras
Chennai (India)

&

Dr. C. Vijayan
Professor, Department of Physics
Indian Institute of Technology Madras
Chennai (India)

WILEY



Ane Books Pvt. Ltd.

© 2014 (Prof. YVGS Murti and Dr. C. Vijayan)

Published by

Ane Books Pvt. Ltd.

4821 Parwana Bhawan, 1st Floor
24 Ansari Road, Darya Ganj, New Delhi - 110 002, India
Tel: +91 (011) 2327 6843-44, 2324 6385
Fax: +91 (011) 2327 6863
e-mail: anebooks@vsnl.net
Website: www.anebooks.com

For

John Wiley & Sons Ltd

The Atrium, Southern Gate
Chichester, West Sussex
PO19 8SQ United Kingdom
Tel : +44 (0)1243 779777
Fax : +44 (0)1243 775878
e-mail : customer@wiley.com
Web : www.wiley.com

For distribution in rest of the world other than the Indian sub-continent

ISBN : 978-1-118-90106-9

All rights reserved. No part of this publication may be reproduced, stored in a retrieval system, or transmitted in any form or by any means, electronic, mechanical, photocopying, recording or otherwise, except as permitted by the UK Copyright, Designs and Patents Act 1988, without the prior permission of the publisher.

Designations used by companies to distinguish their products are often claimed as trademarks. All brand names and product names used in this book are trade names, service marks, trademarks or registered trademarks of their respective owners. The publisher is not associated with any product or vendor mentioned in this book.

Library Congress Cataloging-in-Publication Data

A catalogue record for this book is available from the British Library.

Printed at: Thomson Press, India

"...Jyotirgamaya..."

(Lead, kindly, *to light* !)

BrhadAraNyaka Upanishad

Preface

Nonlinear optical interaction of matter with intense optical fields forms the basis of Photonics and holds the key to a deep and comprehensive understanding of light-matter interaction as well as to the development of several significant facets of the technology of tomorrow. Training of students equipped with a clear understanding of the basic Physics involved and enthusiastic awareness of the vast scope of the field appear to be more essential than ever in view of the requirements for the delineation of the basic physical mechanisms as well as the optimal exploitation of the application potential in areas such as control, communication, and computing.

An interesting observation about the available books on Nonlinear Optics today is the wide variety in content, style, coverage of specific topics, relative emphasis of areas and the depth of treatment. Excellent classics on this topic by Bloembergen, Boyd, Shen, Butcher and Cotter, Yariv are resources providing adequate coverage and for researchers. insight. The handbooks by Sutherland and Paras Prasad, Fischer, and Zyss and Chemla and the book on Nonlinear Fiber optics by Agrawal are also worth special mention. Worthy of special mention is a very useful resource letter published recently, listing the details of all text books, reviews and other documents related to nonlinear optics with brief descriptions on each. Details of these and the recent books are given in the bibliography.

However, while teaching courses on nonlinear optics to students of both science and engineering during the past two decades, the authors have felt a strong need for an introductory level book that caters to the requirements of students at the level of the bachelors and masters courses. This book is a humble attempt in this direction and is presented as a textbook designed at college/University level for undergraduate students of Science and Engineering and a one-semester course can easily be designed based on this. Care has been taken to include rigorously features such as :

- elucidation of relevant basic principles of Physics.

- clear exposition of the ideas involved at the beginners' level.
- coverage of the physical mechanisms of nonlinearity
- overview of physical processes in emerging photonic materials
- exploratory questions and problems at the end of the chapters.

The topics covered include a detailed formalism and phenomenology of nonlinear wave mixing processes, quantum mechanics of nonlinear interaction of matter and radiation and an elucidation of specific processes as harmonic generation, optical phase conjugation, self focusing, self phase modulation and nonlinear absorption, leading to an appreciation of their application potential in areas such as tunable laser action, pulse modification, photonic switching and bistability. Major highlights of the book are detailed chapters on the symmetry aspects in nonlinear optics and on the various specific physical mechanisms of optical nonlinearity with examples of material systems in which these are operative, taking care to introduce emerging trends as well. However, an exhaustive coverage of all nonlinear optical phenomena is not attempted and topics such as Raman and Baudouin scattering are not included.

The authors are pleased to place on record the beneficial interactions with students and fellow teachers in the evolution of this book. Specifically, inputs from Professors R. Vijaya, IIT, Kanpur, C. V. Krishnamurthy and Edamana Prasad, IIT Madras, Reji Philip, IISc, Bangalore, Majles Ara, TTU, Teheran and P. Nandakumar, BITS Goa and are gratefully acknowledged. Sincere thanks are also due to students Dileep, Radhika V. Nair, Jais Tom and Radhu and post doctoral fellow Dr. Anita R. Warrier for a careful proof reading of the manuscript.

The authors have been rather slow in putting the book together and the book could not have taken the shape but for the kind indulgence of the publishers, Ane Books Pvt Ltd, and particularly Mr. A. Rathinam.

Contents

1 From Optics to Photonics **1**
1.1 The Charm and Challenge of Photonics 2
1.2 The Nature of Optical Nonlinearity 3
1.3 Overcoming the *Materials Bottleneck* 5
1.4 The Expanding Frontiers 7
1.5 Explorations 9

2 A Phenomenological View of Nonlinear Optics **11**
2.1 Optics in the Nonlinear World 12
2.1.1 Introduction 12
2.1.2 First Order Susceptibility 13
2.1.3 Second Order Susceptibility 14
2.1.4 Third Order Susceptibility 14
2.2 Time Domain Response 16
2.2.1 First Order Polarization- Time Domain Response 16
2.2.2 Higher Order Polarizations - Time Domain Response 17
2.3 Frequency Domain Response 19
2.3.1 First Order Susceptibility 19
2.3.2 Second Order Susceptibility 20
2.3.3 General Order (n) Susceptibility 20
2.4 The n^{th} order Polarization 21
2.5 Monochromatic Waves 21
2.6 Calculation of the Factor K 24
2.6.1 Optical Rectification 24
2.6.2 Second Harmonic Generation 24
2.6.3 Pockels Effect 25
2.6.4 Sum and Difference Frequency generation . . 25
2.6.5 Third Harmonic Generation 26
2.6.6 Nondegenerate Four Wave Mixing 26
2.7 Explorations 27

3 Symmetry and Susceptibility Tensors **29**
3.1 Introduction 30
3.2 Crystal Symmetry and Susceptibility Tensors 30
3.2.1 Neumann Principle 35
3.2.2 Symmetry of Second Order Susceptibility . . . 37
3.2.3 Second Harmonic Generation 40
3.2.4 Kleinman Symmetry 45
3.2.5 Symmetry of Third Order Susceptibility . . . 45
3.3 The Dielectric Permittivity Tensor 47
3.4 The Refractive Index Ellipsoid 50
3.5 Explorations 52

4 Calculation of Non-linear Susceptibilities **55**
4.1 Introduction 56
4.1.1 Physical Quantities in Quantum Physics . . . 56
4.1.2 The Projection Operator 57
4.2 The Equation of Motion 59
4.3 Ensembles of Particles 60
4.4 Time-dependent Perturbation 61
4.5 Dipolar Interaction 63
4.6 First Order Density Matrix 65
4.7 Second Order Density Matrix 66
4.8 Third Order Density Matrix 67
4.9 Double Integrals in the Expressions for Density Matrix 68
4.10 Second Harmonic Susceptibility 70
4.11 Relaxation Effects 71
4.12 Applications to Color Centers 72
4.12.1 Third Order Susceptibility 72
4.12.2 Second Order Susceptibility 74
4.13 Explorations 75

5 Nonlinear Wave Mixing Processes **77**
5.1 Introduction 78
5.2 Elements of Electromagnetism 78
5.3 Travelling Electromagnetic Waves in Free Space . . . 81
5.3.1 Energy Density in the Travelling Wave 82
5.4 Propagation of Electromagnetic Waves in Linear Materials 83

5.5 Propagation of Electromagnetic Waves in Nonlinear Materials 85
5.5.1 The Wave Equation 85
5.5.2 Energy Transfer Rate 86
5.6 Three Wave Mixing 88
5.6.1 An Approximation 89
5.7 Second Harmonic Generation 91
5.7.1 Phase Matching Schemes 93
5.7.2 Accurate Treatment of Second Harmonic Generation 95
5.8 Explorations 98

6 Optical Phase Conjugation and Bistability 101
6.1 Optical Phase Conjugation 102
6.1.1 Phase Conjugation as Time Reversal 102
6.1.2 Phase Conjugation through Four-Wave-Mixing 104
6.1.3 Practical Realization 107
6.1.4 Peculiar Properties of the Phase Conjugate Beam 109
6.1.5 The Grating Picture 112
6.1.6 Applications of Phase Conjugation 113
6.2 Optical Bistability and Photonic Switching 114
6.2.1 Refractive Index at High Intensities : An Overview 114
6.2.2 Fabry-Pėrot Etalon 117
6.2.3 Photonic Switching in a Nonlinear Fabry-Pėrot Etalon 119
6.3 Explorations 123

7 Self Focusing, Phase Modulation and Pulse Shaping 125
7.1 Self Focusing of Light 126
7.1.1 The Concept of Self Focusing 126
7.1.2 Self Trapping and Spatial Solitons 127
7.1.3 The z-scan Experiment 129
7.1.4 Analysis of the z- scan Trace 131
7.1.5 Measurement of Nonlinear Optical Absorption 133
7.1.6 Mechanisms of Nonlinear Absorption 135
7.2 Self Phase Modulation (SPM) 137
7.3 Pulse Shaping and Optical Soliton Propagation 140
7.3.1 Solitary Waves and Optical Solitons 141

7.4 Explorations 143

8 Mechanisms and Materials **147**
8.1 Introduction 148
8.2 Mechanisms of Nonlinearity 149
8.2.1 Anharmonicity of Potential 149
8.2.2 Thermal Mechanism 151
8.2.3 Orientational Mechanism 152
8.2.4 Inelastic Photon Scattering 153
8.2.5 Photorefractivity 153
8.2.6 Saturable Absorption 156
8.2.7 Band Gap Distortion (Franz-Keldysh Effect) . 157
8.2.8 Band Filling Mechanism 157
8.2.9 Non-parabolicity of Bands 158
8.2.10 Delocalization of Electrons 159
8.3 A Perspective on Newer Materials and Processes 162
8.3.1 Low Dimensional Materials 162
8.3.2 Photonic Bandgap Materials 167
8.3.3 *Slowing* of Light and the Effect on Nonlinearity 169
8.4 Explorations 171

Bibliography **173**

References **175**

Index **185**

List of Figures

3.1 Unit cell of cubic lattice with C3 axis 36
3.2 Index ellispsoid for a positive uniaxial crystal 53

4.1 Atomistic model for color centers 72
4.2 Energy level schemes for the color centers 73

6.1 A scheme for optical phase conjugation through DFWM104
6.2 Experimental set up for OPC through DWFM . . . 107
6.3 Comparison of linear and nonlinear and reflection . . 110
6.4 Time reversal in phase conjugaion 112
6.5 Two possible types of spatial *gratings* in phase conjugation 113
6.6 FP etalon and its fringe pattern 118
6.7 Transmittance of an FP etalon with a nonlinear medium as a function of RTPS 121
6.8 Optical bistability 122

7.1 Self focusing of a beam of Gaussian profile 127
7.2 Experimental setup for closed z scan 129
7.3 Typical trace of the z scan experiment 131
7.4 Experimental set up for open z-scan 134
7.5 Typical open scan traces for SA and RSA/MPA . . . 137
7.6 Unchirped pulse 138
7.7 The origin of chirp 139
7.8 Chirping of pulses 139

8.1 Beam geometry in OPC in a photorefractive crystal . 155
8.2 The grating picture for OPC in a photorefractive rystal 155
8.3 A conjugate polymer chain 159
8.4 Structure of PNA 161
8.5 Molecular engineering with PNA 161
8.6 Optical absorption spectrum of nanocrystalline CdS. The inset shows the band picture 164

8.7 A skectch of the plot between frequency and the magnitude of wave vector, showing photonic bandgap; inset : a typical 1D PBG. 168

Chapter 1

From Optics to Photonics

"And God said: Let there be light" (The Bible)
Thus there was Optics.
Einstein said: "Let it be quantized";
then there was Photonics.

Learning Objectives

- Enumeration of the important milestones in the unfolding saga of optics and photonics.
- Recognition of the significance of optical nonlinearity in ushering in the technology of photonics.
- Development of a scheme to categorize phenomena on the basis of the order of nonlinearity.
- Identification of the need for obtaining material media with optimal parameters of nonlinear response.
- Appraisal of a few promising directions of the future.

1.1 The Charm and Challenge of Photonics

Light has always fascinated man by making the world around him meaningful, useful and wonderful. Man has considered light to be divine. Light, in its various forms and with its varied capabilities, has helped us to understand the world better. On the other hand, man's quest to understand light has graduated from the traditional discipline of optics to the study of the science and technology of photonics. Classical optics is a study of phenomena that can be understood well with the wave aspect of light whereas the understanding of quantum phenomena highlighting the dual nature and the interaction of photons with electrons has opened up the era of Photonics, which deals with phenomena where the particle nature (rather than the wave nature) of light becomes particularly relevant. The grand saga continues to unfold through ages, unraveling more and more novel mysteries of light, revealing novel and intriguing aspects of and light-matter interaction and ushering in fascinating technological innovations in the process. It is the dual role of light as a carrier of energy as well as information that makes it special and both these aspects have been utilized for the development of the present civilization. A great deal of theoretical insight has been obtained on the nature of light itself and on the interaction of light with matter, which is available in several standard text books of optics. The amazing progress made recently in several new areas of optics could not have even been dreamt of in earlier days. The understanding of coherent and quantum optics and nonlinear optics, development of laser sources, production and propagation of ultrashort pulses, modern forms of spectroscopy, fiber optics, diffractive optics and integrated optics are just a few of the new areas that have changed the face of science and technology. The field continues to grow even after the celebration of a hundred years of the birth of the concept of the Photon. Topics such as singular optics, negative refraction, optical band gaps and slowing and localization of light are examples of new ideas that promise to give a totally new outlook to optics – in terms of both conceptual insight as well as scope for device applications.

The different stages of technological evolution are characterized in terms of the dominant type of tools and technologies used in each

of these stages. Having evolved from the *stone age* through the *copper age* and the *iron age*, we are probably now in the *electron age*. After having done a wonderful job, today electronic technologies have started experiencing their limits, for example, in handling the ever-growing requirements of communication in the present world. Photonics appears to hold some promise as an emerging technology in this scenario. The present technology makes use of a wide variety of hybrid circuits involving optoelectronics and electro-optics. Communications is a frontier where optical technology has proven its utility in an abundant measure. It indeed is a long way to achieving all-optical systems in various other areas of technology. The basic and relevant question is whether photons can be made to do what electrons are doing today for the mankind. Electronic circuits work on the basic principle that a given electron can influence and control the other electrons, implying that we use one current to control another current the way we want. This aspect is very clear even in the case of the simplest electronic device, the transistor, where the emitter-collector current characteristics are controlled by the base current, making it possible to develop electronic amplifiers, oscillators and other more complicated devices that continue to revolutionize the areas of control, communications and computing.

Photons obey the principle of superposition and consequently a beam of light travels in a medium without exchanging energy with any other beam that may be propagating in the same medium at the same time. There is no cross talk and hence no interaction, as a beam of photons cannot control another beam of photons. However, optical nonlinearity makes it possible to have such an interaction that can lead to energy exchange between light beams propagating simultaneously in suitable media if the intensity of light is high enough. This *wave mixing* is the basic idea of nonlinear optics.

1.2 The Nature of Optical Nonlinearity

The most significant single invention that has played a major role in the development of Photonics is perhaps that of the laser, a source of coherent radiation with high intensity and directionality. Apart from revolutionizing the technology of optics, this has also contributed immensely to the enhancement of our understanding of

basic optical processes in matter. The strong stimulus provided by light at high intensity can induce a nonlinear response in materials, leading to the occurrence of several interesting new phenomena.

The alternating electric field of the incident light beam induces a time-varying electrical polarization in the medium. Hence the polarization is expected to vary sinusoidally at the same frequency as that of the light wave. However, the response becomes complicated when the incident light has a large enough intensity and hence the amplitude of the corresponding electric vector is large enough. This causes the resulting polarization wave to deviate from a simple sinusoidal behavior, leading to the excitation of higher harmonics as well. Such an interaction results in several new *wave mixing* processes which may have the potential for use in device applications in optical data processing and computing, apart from developing new tools of probing deeper into the basic aspects of light matter-interaction by way of new kinds of spectroscopy.

The incident electromagnetic radiation with electric vector $\vec{E}(t)$ polarizes the medium and causes it to develop a time dependent electrical polarization $\vec{P}(t)$. The proportionality of this induced polarization $\vec{P}(t)$ in the medium to the electric field $\vec{E}(t)$ of the incident light beam breaks down and the resulting polarization can be considered to be made up of several contributions, represented by terms consisting of products of higher order susceptibility $\chi^{(n)}$ and the magnitude of the electric field $\vec{E}(t)$. Thus the i^{th} component of the vector $\vec{P}(t)$ (where i stands for x, y or z) is given by

$$P_i = \epsilon_0 \left\{ \chi^{(1)}_{ij} E_j + \chi^{(2)}_{ijk} E_j E_k + \chi^{(3)}_{ijkl} E_j E_k E_l + ... \right\}$$

Where $\chi^{(n)}$ is the susceptibility of n^{th} order , which is a tensor of rank $(n+1)$ with $3^{(n+1)}$ components in general. ϵ_0 is the permittivity of free space.

This mathematical formalism helps us to classify nonlinear optical processes in materials and to describe several important aspects of it in a convenient way. The components of the susceptibility tensor describe the directional dependence of optical properties of crystals and other anisotropic media. The second and subsequent terms inside the bracket in the expression for susceptibility are progressively much smaller than the first term. This means that higher

order nonlinear optical effects would vanish in the low optical intensity regime as only the first term in the expansion would be of considerable magnitude in this case. A material can be expected to exhibit n^{th} order optical nonlinearity when either of the quantities $\chi^{(n)}$ or $\vec{E}$ is large enough. The magnitude of $\vec{E}$ depends on the intensity of the laser used and $\chi^{(n)}$ is a property of the material. Thus the magnitude of nonlinearity depends both on the nature of the material as well as on the intensity of the light used.

Wave mixing processes result in second, third and even higher harmonic generation where light at frequencies of 2ω, 3ω etc. are generated from an input beam of frequency ω. Input light beams of frequencies ω_1 and ω_2 can get mixed in the medium to generate sum and difference frequencies $(\omega_1 + \omega_2)$ and $(\omega_1 - \omega_2)$ respectively. Combinations of such frequency-mixing processes are used widely in the recent technology to develop tunable solid state laser sources. White light laser pulses can be generated by femtosecond pulses using nonlinear interaction with matter. Several processes other than frequency conversion also occur in nonlinear optical media. The refractive index becomes dependent on light intensity at high intensities and this causes *self -focusing* effects in nonlinear media. This can be made use of in pulse modification applications including long-distance signal propagation in fibers. Optical phase conjugation is a third order nonlinear process by which a time-reversed replica of an incident light beam can be generated. This finds use in distortion-healing applications in adaptive optics. Nonlinear absorption processes become important at high intensities. Phenomena such as saturable absorption (SA), reverse saturable absorption (RSA) and multi-photon absorption (MPA) are observed in media when interrogated with laser beams of appropriate intensities and pulse durations. Some of these processes can be used in optical limiting in which the media act as smart materials and control their transmission characteristics depending upon the magnitude of the intensity of the incident light.

1.3 Overcoming the *Materials Bottleneck*

The most important limitation in exploiting the potential of Photonic processes to their fullest extent is the difficulty in obtaining appropriate material media. This is known as the *materials bottle-*

neck. It turns out that most of the available materials do not meet the simultaneous requirements of large as well as fast nonlinearity required for the practical devices. Many inorganic materials such as KDP, ADP, barium titanate etc. have been used from the earliest days. Organic materials and semiconductors also have been found to be excellent materials. Special molecules such as fullerenes, liquid crystals and porphyrins are also studied as promising materials.

Polymers offer a large scope for structure modification, which can be utilized to engineer materials with large and fast optical nonlinearity. The structures of certain polymers such as polyphenyl acetylene (PPA) have spatially well-spread electron clouds resulting in large values of linear as well as nonlinear susceptibility. Structure of such polymers can be modified easily by doping with other materials and/or attaching appropriate side groups to the main chain. Some of these variations are known to enhance the nonlinearity of the basic polymer by way of extending the spatial spread of electrons and hence enlarging the linear as well as nonlinear susceptibilities. A second example is that of structure variation in materials such as porphyrins and phthalocyanines which also has yielded interesting results. Porphyrins allow for incorporation of various ligands and different core metal ions, which alter the susceptibilities considerably. Incorporation of porphyrins into solid polymer membranes is found to enhance nonlinearity, besides stabilizing the materials against photodegradation and providing a convenient solid matrix. Composites of conventional optical materials with appropriate polymers appear to hold promise from the device application point of view.

One of the frontier areas of Photonic materials development today is that of *quantum engineering* of semiconductor nanostructures. Quantum wells are made of thin alternate layers of semiconductors of different values of the band gap, thus confining the electron to virtually a plane. These are now being used in a number of devices. Electrons can be further confined to one dimension by embedding a semiconductor wire or a conducting polymer chain in a material of larger band gap. Research on quantum wires and nanotubes is being pursued actively these days. Quantum dots can be formed by embedding tiny crystalline islands of semiconductors or metals (called nanoclusters) in glass or polymer matrices. These are practical realizations of the quantum mechanical concept

of *particle in a box* whose optical properties depend on the particle size. Interesting techniques of obtaining such monosize clusters have been perfected by materials scientists. Ion-exchange strategies and control of cluster formation in chemical reactions by capping with surfactants are some examples. Other techniques used widely to produce quantum dots are ion-implantation, monolayer building and molecular beam epitaxy.

Quantum confinement alters the electronic states of the semiconductor and hence influences the linear and nonlinear optical properties. The band gap is modified by the increased oscillator strength of exciton transitions leading to an effective blueshift of the absorption edge with decreasing cluster size. This results in an alteration of the effective band gap, which is also known as *bandgap engineering*. Strong quantum confinement is expected to result in considerable increase in the nonlinear susceptibilities along with a decrease in response times. Collaborative attempts by materials scientists and physicists along these directions are expected to be productive in designing novel types of photonic materials ideally suited for exploiting the fascinating possibilities of Photonics to their fullest extent.

1.4 The Expanding Frontiers

Since the pioneering work by Bloembergen, nonlinear optics has bloomed into a flourishing field of active research with wide ranging technological applications. New insights into processes, materials and applications continue to appear regularly. Though it is not possible to do justice to all important advances here, it would be appropriate to have a glimpse of a few important facets of this expanding frontier. One of the interesting challenges being addressed to in recent times is bringing down nonlinearity to low power levels. Metal-dielectric boundaries that support plasmon excitation are capable of exhibiting optical nonlinearity at low powers. Metal-core microparticles have been shown to show optical bistability with low power helium neon lasers as sources. Thin films show a variety of effects worth consideration in waveguide design. Special materials such as bacteriorhodopsin and certain porphyrin derivatives appear to be good candidates for low power nonlinearity. Liquid crystals

are known to show *giant* optical nonlinearity. Thermal variation of the local refractive index can easily show certain effects through nonlinearity of *non-electronic* origin though their applicability may be limited to situations such as nonlinear image processing and beam-profile modification where operation at high speeds may not be a serious criterion. There is also current interest in the area of low threshold optical limiters.

The availability of femtosecond laser pulses has ushered in the era of ultrafast nonlinearity where thermal mechanisms are insignificant and one can separate out purely electronic effects. Continuum generation leading to the generation of white light lasers is a process which can be excited with such sources. Periodic structures such as photonic crystals and negative refractive index materials hold promise for entirely new nonlinear optical processes. Techniques of reducing the speed of light in certain artificial materials to values much below that in vacuum have been demonstrated. Such a slowing leads to an increased interaction between light and matter and holds promises for novel modes of enhanced nonlinear optical response. Laser technology of the present day makes effective use of a variety of nonlinear wave mixing processes in the design of tunable solid state laser sources such as the Ti:Sapphire laser. Though nonlinearity often leads to problems in pulse propagation through optical fibers, clever schemes can be devised to compensate for dispersion utilizing nonlinear interaction of the fiber material, thus obtaining soliton propagation capable of revolutionizing communications technology. Image processing is another area where schemes employing nonlinear optical processes offer specific advantages. Optical communication engineers used to consider optical nonlinearity as a nuisance for their communications systems. However, recent trends are in the direction of favorably exploiting the nonlinearity of fiber-based systems.

1.5 Explorations

1. We know that the human race has evolved through various epochs of technology from the stone age, in terms of the technology used. How would you describe the present age ? What would be the next age?

2. Which, if any, do you think is the area of present day civilization where optical technology has been established to the best of available technology? Why is that Photonics is not yet the favorite technology in other areas?

3. This chapter describes how the higher order polarization in a medium interacting with intense light can be described in terms of the products of electric field components of the electromagnetic field of the incident light wave. Do you think a similar description in terms of the magnetic field components of the light wave would be worth considering? Justify.

4. What are the processes in electronics that are analogous to optical wave mixing? How would you design a device that mixes electrical signals in the form of periodic oscillations at specific frequencies using an electronic device in order to generate the second harmonic and sum-and-difference frequencies of the input signals?

5. The design of an electronic small signal amplifier is considered to be inefficient if the operating point is beyond the linear region of the characteristic curve of transistor used. In what ways can the amplified signal be affected by this? Answer with the help of appropriate sketches.

Chapter 2

A Phenomenological View of Nonlinear Optics

"In the right light, at the right time, everything is extraordinary"

Aaron Rose

In bright light, ordinary optics becomes nonlinear optics.

Learning Objectives

- Recognition of the physical processes leading to optical nonlinearity.
- Relating optical susceptibility to the time-dependence of polarization.
- Formulation of a method to characterize susceptibilities for different processes.
- Employment of the basic formalism for a phenomenological description of nonlinear optical processes.

2.1 Optics in the Nonlinear World

2.1.1 Introduction

What is the response of a material when it is placed in an optical electromagnetic field? We seek an answer to this question by considering the effect of an electric field on an atom. The electric field acting on the positive and negative charges of the atom distorts the electron charge distribution in the atom. A primary measure of this distortion is the electric dipole moment $\vec{p}$ induced in the atom by the electric field.

$$\vec{p} = q_i \vec{r_i} \tag{2.1}$$

Where q_i is the electric charge located at the point denoted by the position vector $\vec{r_i}$ and the summation is over the atomic volume. The dipole moment is the first moment of charge. An isolated atom does not have a permanent dipole moment which means that the center of the negative charge coincides with the centre of the nuclear charge. Applying an electric field $\vec{E}$ will bring about a shift in the center of the negative charges relative to the nucleus. In linear optics, the dipole moment so induced is proportional to the electric field according to

$$\vec{p} = \alpha \vec{E} \tag{2.2}$$

where α is the electronic polarizability of the atom. The overall macroscopic electric polarization $\vec{P}$ is obtained by summing such dipoles over the volume V of the sample and dividing by the volume:

$$\vec{P} = \frac{\sum \vec{p_i}}{V} \tag{2.3}$$

What is the order of magnitude of the shift in the charge distribution in the atom? Assuming a spherically uniform distribution of total charge q over a radius R, the electronic polarizability is approximately given by $\alpha \approx 4\pi\epsilon_0 R^3 q$. In an atom with the atomic number Z, the displacement Δx is given by

$$\Delta x = \frac{4\pi\epsilon_0 R^3}{Ze} E \tag{2.4}$$

where e is the electronic charge. For an electric field of magnitude $10^4\ V\ m^{-1}$, $R = 0.2\ nm$, $Z = 8$, the displacement amounts to $\approx 10^{-17} m$. At electric fields of the order of $10^8\ V\ m^{-1}$, dielectric breakdown sets in. This breakdown field is about 1% of the internal fields prevailing in materials.

How much electric field can we realize in the electromagnetic field of a laser beam? The intensity I of a beam and the amplitude E of the electric field are related by

$$I = \frac{1}{2} cn\epsilon_0 E^2 \tag{2.5}$$

where n is the refractive index. For an intensity of $I = 10^{14}\ W\ m^{-2}$ and $n = 1.5$, we get $E \approx 10^8\ V\ m^{-1}$ which is close to the breakdown strength. Thus, when we work with laser fields that are sufficiently large and yet safely within the breakdown limits, the optical response of the material may be expressed in a series expansion of the polarization in powers of the electric field:

$$\vec{P} = \epsilon_0 \left[\chi^{(1)} \vec{E} + \chi^{(2)} \vec{E}\,\vec{E} + \chi^{(3)} \vec{E}\,\vec{E}\,\vec{E} + ... \right] \tag{2.6}$$

The various electric susceptibilities $\chi^{(n)}$ correspond to linear $(n = 1)$ and n^{th} $(n = 2, 3, ..)$ order nonlinear optical polarizations of the material. Now we can look at these susceptibilities more closely and enquire about their physical manifestations. For the development of nonlinear susceptibilities, we follow closely the excellent treatment presented in the treatise of Butcher and Cotter [1990]

2.1.2 First Order Susceptibility

Linear optics of refraction, absorption and diffraction are governed by this susceptibility, which is a second rank tensor relating the three vector polarization components with the three components of the vector electric field:

$$\begin{pmatrix} P_x \\ P_y \\ P_z \end{pmatrix} = \epsilon_0 \begin{pmatrix} \chi^{(1)}_{xx} & \chi^{(1)}_{xy} & \chi^{(1)}_{xz} \\ \chi^{(1)}_{yx} & \chi^{(1)}_{yy} & \chi^{(1)}_{yz} \\ \chi^{(1)}_{zx} & \chi^{(1)}_{zy} & \chi^{(1)}_{zz} \end{pmatrix} \begin{pmatrix} E_x \\ E_y \\ E_z \end{pmatrix} \tag{2.7}$$

Thus there are nine susceptibility coefficients $\chi_{i,j}^{(1)}$ in general given by

$$P_i = \varepsilon_0 \chi_{ij}^{(1)} E_j$$

the right hand side of the equation implying summation over the full range of the repeated index (j), following the Einstein notation.

2.1.3 Second Order Susceptibility

This is a nonlinear property of the material describing how the polarization develops due to the product of two field components:

$$P_i = \varepsilon_0 \chi_{ijk}^{(2)} E_j E_k \tag{2.8}$$

Here the summation on the right hand side is over the two repeated indices j and k. This susceptibility is a third rank tensor comprising twenty seven components of $\chi^{(2)}$ in general relating the three polarization components with the nine components of the products of the electric field components. There exist many important optical properties of materials resulting from this second order response. Among these are:

i) Second Harmonic Generation: $\chi^{(2)}(-2\omega : \omega, \omega)$

ii) Parametric Mixing and Amplification:
$\chi^{(2)}(-\{\omega_1 \pm \omega_2\} : \omega_1, \omega_2)$

iii) Optical Rectification: $\chi^{(2)}(0 : \omega, -\omega)$

iv) Pockels Effect: $\chi^{(2)}(-\omega : \omega, 0)$

The angular frequencies ω appearing within the parentheses correspond to the various monochromatic electric fields that combine nonlinearly as per the notation we will elaborate later.

2.1.4 Third Order Susceptibility

This susceptibility $\chi^{(3)}$ is a fourth rank tensor with 81 coefficients in general, and it relates the polarization and the fields according to:

$$P_i = \varepsilon_0 \chi_{ijkl}^{(3)} E_j E_k E_l \tag{2.9}$$

again with the summation convention of having to sum over all the three repeated dummy indices j, k, l on the right hand side. A good number of significant and interesting nonlinear phenomena arise as consequences of the susceptibility of this order. Among these are:

i) Third Harmonic Generation (*THG*) represented by

$\chi^{(3)}(-3\omega : \omega, \omega, \omega)$,

ii) Electric Field Induced Second Harmonic Generation (*EFISH*) represented by $\chi^{(3)}(-2\omega : \omega, \omega, 0)$,

iii) Non-Degenerate Four Wave Mixing (*NDFWM*) represented by $\chi^{(3)}(-\{\omega_1 + \omega_2 \pm \omega_3\} : \omega_1, \omega_2, \pm\omega_3)$,

iv) Optical Phase Conjugation (*OPC*) represented by

$\chi^{(3)}(-\omega : \omega, \omega, -\omega)$,

v) Two Photon Absorption (*TPA*) represented by the imaginary part of $\chi^{(3)}(-\omega : \omega, -\omega, \omega)$,

vi) Stimulated Brillouin Scattering (*SBS*) represented by $\chi^{(3)}(-\{\omega \pm \Omega\} : \omega, -\omega, \omega \pm \Omega)$ and

vii) Stimulated Raman Scattering (*SRS*) represented by $\chi^{(3)}(-\{\omega \pm \Omega\} : \omega, -\omega, \omega \pm \Omega)$

Other manifestations of this response include *CARS* (Coherent Anti-Stokes Raman Scattering), Optical Bistability (*OB*) and Intensity-Dependent Refractive Index (*IDRI*). The last two govern the working of all-photonic switching devices. We may record the S. I. units of these susceptibilities:

- $\chi^{(1)}$: dimensionless
- $\chi^{(2)}$: $m\ V^{-1}$
- $\chi^{(3)}$: $m^2 V^{-2}$
- $\chi^{(n)}$: $m^{(n-1)} V^{-(n-1)}$

2.2 Time Domain Response

2.2.1 First Order Polarization- Time Domain Response

We assume that the polarization at any point in the material depends only on the local electric field. How then does the driving electric field $\vec{E}(t)$ at any time t, influence the resulting polarization $\vec{P}(t)$ as a function of time? To answer this query we expand the time-domain response in various orders of the electric field:

$$\vec{P}(t) = \vec{P}^{(1)}(t) + \vec{P}^{(2)}(t) + \vec{P}^{(3)}(t) + ... + \vec{P}^{(n)}(t) + .. \quad (2.10)$$

The elementary contribution $\overrightarrow{dP}^{(1)}(t)$ to the first order polarization $\vec{P}^{(1)}(t)$ at any time t, arising from the electric fields occurring during the time interval dt' lying between the instants t' and $t'+dt'$ is given by

$$\overrightarrow{dP}^{(1)}(t) = \epsilon_0 F^{(1)}\left(t : t'\right)\vec{E}\left(t'\right)dt' \quad (2.11)$$

Where $F^{(1)}\left(t, t'\right)$ is the first order time-domain response tensor connecting the elementary polarization prevailing at time t with the field at time t'. First we note that this tensor must be a real quantity since both the polarization and electric field are real physical entities. To obtain the finite polarization at time t, we need to integrate over time t' from $t' = -\infty$ to $t' = t$.

$$\vec{P}^{(1)}(t) = \epsilon_0 \int_{-\infty}^{t} F^{(1)}\left(t : t'\right)\vec{E}\left(t'\right)dt' \quad (2.12)$$

It may be noted that the polarization developing at any time t should depend only on the time delay between the time t' when the field is applied and time t and not on the absolute value of t'. Therefore we introduce a new symbol for this tensor :

$$F^{(1)}\left(t : t'\right) \equiv G^{(1)}\left(t - t'\right) \quad (2.13)$$

Further noting that the polarization developed at time t depends only on the fields applied at times preceding it, the tensor G should vanish for $t' > t$ (principle of causality). Therefore we set $t - t' = \tau$, and the first order time-dependent polarization becomes

$$\vec{P}^{(1)}(t) = \epsilon_0 \int_{-\infty}^{0} G^{(1)}\left(\tau'\right)\vec{E}\left(t - \tau'\right)d\tau' \quad (2.14)$$

and the Cartesian components are given by

$$P_{ij}^{(1)}(t) = \epsilon_0 \int_{-\infty}^{0} G_{ij}^{(1)}\left(\tau'\right) E_j\left(t-\tau'\right) d\tau' \tag{2.15}$$

2.2.2 Higher Order Polarizations - Time Domain Response

In a similar manner, we can consider the second order polarization at time t to arise from the electric field $\vec{E}\left(t_1'\right)$at the time t_1' as well as the electric field $\vec{E}\left(t_2'\right)$at the time t_2' to be given by

$$\vec{P}^{(2)}(t) = \epsilon_0 \int_{-\infty}^{t}\int_{-\infty}^{t} F^{(2)}\left(t:t_1',t_2'\right)\vec{E}\left(t_1'\right)\vec{E}\left(t_2'\right)dt_1'dt_2' \tag{2.16}$$

The response function $F^{(2)}$ is a third rank tensor and its components $F_{ijk}^{(2)}$ relate the components $P_i^{(2)}$ of the second order polarization with the two field components E_j and E_k according to

$$P_i^{(2)}(t) = \epsilon_0 \int_{-\infty}^{t}\int_{-\infty}^{t} F_{ijk}^{(2)}\left(t:t_1',t_2'\right)E_j\left(t_1'\right)E_k\left(t_2'\right)dt_1'dt_2' \tag{2.17}$$

From the way the two field components appear in the above equation, it is clear that the physical situation would remain unaltered if we interchange $E_j\left(t_1'\right)$ and $E_k\left(t_2'\right)$ so much so the tensor component $F_{ijk}^{(2)}\left(t:t_1',t_2'\right)$should be invariant under the exchange of the pairs$\left(j,t_1'\right)$and $\left(k,t_2'\right)$.

$$F_{ijk}^{(2)}\left(t:t_1',t_2'\right) = F_{ikj}^{(2)}\left(t:t_2',t_1'\right) \tag{2.18}$$

This means that an intrinsic permutation property of the tensor. As mentioned in the case of the first order response, the polarization at any time t, would depend only on the time intervals $\left(t-t_1'\right)$and $\left(t-t_2'\right)$but not on the particular values of t_1' and t_2'. We may thus introduce the response function $G^{(2)}$ by

$$F^{(2)}\left(t:\tau_1',\tau_2'\right) \equiv G^{(2)}\left(t-t_1',t-t_2'\right) \tag{2.19}$$

In terms of this G function, the polarization may be written as $\vec{P}^{(2)}(t) =$

$$\epsilon_0 \int_{-\infty}^{t} \int_{-\infty}^{t} G^{(2)}\left(t-t_1^{'}, t-t_2^{'}\right) \vec{E}\left(t-t_1^{'}\right) \vec{E}\left(t-t_2^{'}\right) dt_1^{'} dt_2^{'} \tag{2.20}$$

The principle of casualty requires that $G^{(2)}$ should vanish whenever $t_1^{'} > t$ or $t_2^{'} > t$. We therefore introduce the time difference variables $t - t_1^{'} = \tau_1^{'}$ and $t - t_2^{'} = \tau_2^{'}$, to rewrite the above equation as $P^{(2)}(t) =$

$$\epsilon_0 \int_{-\infty}^{0} \int_{-\infty}^{0} G^{(2)}\left(\tau_1^{'}, \tau_2^{'}\right) \vec{E}\left(t-\tau_1^{'}\right) \vec{E}\left(t-\tau_2^{'}\right) d\tau_1^{'} d\tau_2^{'} \tag{2.21}$$

with the proviso that $G^{(2)}$ obey the intrinsic permutation symmetry for the components:

$$G_{ijk}^{(2)}\left(\tau_1^{'}, \tau_2^{'}\right) = G_{ikj}^{(2)}\left(\tau_2^{'}, \tau_1^{'}\right) \tag{2.22}$$

We can now generalize the relationships to a nonlinearity of order n and write the polarization $\vec{P}^{(n)}(t)$ as:

$$\epsilon_0 \int_{-\infty}^{t} \ldots \int_{-\infty}^{t} F^{(n)}\left(t : t_1^{'}, t_2^{'}, .. t_n^{'}\right) \vec{E}\left(t_1^{'}\right) \vec{E}\left(t_2^{'}\right) .. \vec{E}\left(t_n^{'}\right) dt_1^{'} dt_2^{'} .. dt_n^{'} \tag{2.23}$$

Since the field terms may be written in $n!$ possible different orders we can define the tensor components by

$$F_{ijkl}^{(n)}\left(t : t_1^{'}, t_2^{'}, .. t_n^{'}\right) = \frac{1}{n!} \sum F_{ijkl}^{(n)}\left(t : t_1^{'}, t_2^{'}, .. t_n^{'}\right) \tag{2.24}$$

the summation on the right hand side being over the terms obtained by performing the $n!$ permutations of the n pairs $\left(i, t_1^{'}\right)$, $\left(j, t_2^{'}\right)$,$\left(k, t_3^{'}\right)$, .

Again using the time invariance of the tensor $G^{(n)}\left(t-t_1^{'}, .. t-t_n^{'}\right)$, in general, we have $P^{(n)}(t) =$

$$\epsilon_0 \int_{-\infty}^{0} \ldots \int_{-\infty}^{0} G^{(n)}\left(\tau_1^{'}, .. \tau_n^{'}\right) \vec{E}\left(t-\tau_1^{'}\right) .. \vec{E}\left(t-\tau_n^{'}\right) d\tau_1^{'} .. d\tau_n^{'} \tag{2.25}$$

2.3 Frequency Domain Response

2.3.1 First Order Susceptibility

To move from the time domain to the frequency domain, we use the Fourier integral representation for the electric field

$$\vec{E}(t) = \int_{-\infty}^{\infty} d\omega \vec{E}(\omega) e^{-i\omega t} \tag{2.26}$$

where the Fourier component $\vec{E}(\omega)$ is given by

$$\vec{E}(\omega) = \frac{1}{2\pi} \int_{-\infty}^{\infty} d\tau \vec{E}(\tau) e^{-i\omega\tau} \tag{2.27}$$

We also note the identity property

$$\frac{1}{2\pi} \int_{-\infty}^{\infty} dx e^{-ix(\tau - t)} = \delta(\tau - t) \tag{2.28}$$

Besides, the fact that the electric field $\vec{E}(t)$ is real demands that the complex conjugate of $\vec{E}(\omega)$ satisfies the equality

$$\left(\vec{E}(\omega)\right)^* = \vec{E}(-\omega) \tag{2.29}$$

Substituting the Fourier representation of the time-dependent electric field as given above, in the equation for the first order time-dependent polarization immediately yields

$$\vec{P}^{(1)}(t) = \epsilon_0 \int_{-\infty}^{\infty} \int_{-\infty}^{\infty} G^{(1)}(\tau) \vec{E}(\omega) e^{-i\omega(t-\tau)} d\omega d\tau \tag{2.30}$$

Introducing the first order susceptibility in the frequency domain

$$\chi^{(1)}(-\omega_d : \omega) = \int_{-\infty}^{\infty} d\tau G^{(1)}(\tau) e^{i\omega\tau} \tag{2.31}$$

in the above equation results in

$$\vec{P}^{(1)}(t) = \epsilon_0 \int_{-\infty}^{\infty} \chi^{(1)}(-\omega_d : \omega) \vec{E}(\omega) e^{-i\omega_d t} d\omega \tag{2.32}$$

Here is ω_d the angular frequency of the driving field. Again the susceptibility should obey the reality condition:

$$\left\{\chi^{(1)}(-\omega_d : \omega)\right\}^* = \chi^{(1)}(\omega_d^* : -\omega^*) \tag{2.33}$$

2.3.2 Second Order Susceptibility

In a similar manner we can introduce the second order susceptibility, by first writing the Fourier representation of the polarization.

$$\begin{aligned}\overrightarrow{p}^{(2)}(t) &= \varepsilon_0 \int_{-\infty}^{\infty}\int_{-\infty}^{\infty}\int_{-\infty}^{\infty}\int_{-\infty}^{\infty} G^{(2)}(\tau_1,\tau_2) \\ &\quad \overrightarrow{E}(\omega_1)\,\overrightarrow{E}(\omega_2)\, e^{-i\{\omega_1(t-\tau_1)+\omega_2(t-\tau_2)\}} d\omega_1 d\omega_2 d\tau_1 d\tau_2\end{aligned}$$

Second order susceptibility $\chi^{(2)}(-\omega_d : \omega_1, \omega_2)$ is defined as

$$\int_{-\infty}^{\infty}\int_{-\infty}^{\infty} d\tau_1 d\tau_2 G^{(2)}(\tau_1,\tau_2)\, e^{i\{\omega_1\tau_1+\omega_2\tau_2\}}$$

with the condition

$$\omega_d = \omega_1 + \omega_2 \tag{2.34}$$

2.3.3 General Order (n) Susceptibility

Generalizing the above development to the n^{th} order response, we have the polarization given by

$$\begin{aligned}\overrightarrow{P}^{(n)}(t) &= \epsilon_0 \int_{-\infty}^{\infty} \ldots \int_{-\infty}^{\infty} \chi^{(n)}(-\omega_d : \omega_1, \omega_2..\omega_n) \\ &\quad \overrightarrow{E}(\omega_1)\,\overrightarrow{E}(\omega_2)\,..\overrightarrow{E}(\omega_n)\, e^{-i\omega_d t} d\omega_1 d\omega_2..d\omega_n\end{aligned}$$

where the n^{th} order susceptibility is $\chi^{(n)}(-\omega_d : \omega_1, \omega_2..\omega_n)$ is the n^{th} order susceptibility, defines as

$$\int_{-\infty}^{\infty} \ldots \int_{-\infty}^{\infty} G^{(n)}\left(\tau_1'..\tau_n'\right) e^{i(\omega_1\tau_1+\omega_2\tau_2+..+\omega_n\tau_n)} d\tau_1 d\tau_2..d\tau_n$$

And the reality condition is

$$\left\{\chi^{(n)}(-\omega_d : \omega_1, \omega_2..\omega_n)\right\}^* = \chi^{(n)}(\omega_d^* : -\omega_1^*, -\omega_2^*.. - \omega_n^*) \tag{2.35}$$

The intrinsic permutation symmetry obeyed by the susceptibility components means that $\chi^{(n)}_{ijkl...}(-\omega_d : \omega_1, \omega_2..\omega_n)$ is invariant under the permutations of the pairs (j, ω_1), (k, ω_2) and so on.

2.4 The n^{th} order Polarization

The Fourier transform is

$$\vec{P}^{(n)}(t) = \int_{-\infty}^{\infty} \vec{P}^{(n)}(\omega)\, e^{-i\omega t} d\omega \tag{2.36}$$

where the Fourier amplitudes are

$$\vec{P}^{(n)}(\omega) = \frac{1}{2\pi} \int_{-\infty}^{\infty} \vec{P}^{(n)}(t)\, e^{i\omega t} dt \tag{2.37}$$

Now let us substitute the Fourier expansion of the electric fields in the above equation to get $\vec{P}^{(n)}(\omega)$ as equal to

$$\frac{1}{2\pi} \int_{-\infty}^{\infty} e^{i\omega t} dt \epsilon_0 \int_{-\infty}^{\infty} .. \int_{-\infty}^{\infty} \chi^{(n)}(-\omega_d : \omega_1, \omega_2 .. \omega_n)$$
$$\vec{E}(\omega_1)\, \vec{E}(\omega_2) .. \vec{E}(\omega_n)\, e^{-i\omega_d t} d\omega_1 d\omega_2 .. d\omega_n$$

Alternatively, we write (using the identity property given earlier),

$$\begin{aligned} \vec{P}^{(n)}(\omega) &= \epsilon_0 \int_{-\infty}^{\infty} .. \int_{-\infty}^{\infty} \chi^{(n)}(-\omega_d : \omega_1, \omega_2 .. \omega_n) \\ &\quad \vec{E}(\omega_1)\, \vec{E}(\omega_2) .. \vec{E}(\omega_n)\, \delta(\omega - \omega_d)\, d\omega_1 d\omega_2 .. d\omega_n \end{aligned}$$

The polarization components are $P_{\alpha}^{(n)}(\omega) = \ :$

$$\sum_{\beta_1 .. \beta_n} \epsilon_0 \int_{-\infty}^{\infty} .. \int_{-\infty}^{\infty} \chi_{\alpha\beta_1 .. \beta_n}^{(n)}(-\omega_d : \omega_1, \omega_2 .. \omega_n) \tag{2.38}$$
$$E_{\beta_1}(\omega_1) .. E_{\beta_n}(\omega_n)\, \delta(\omega - \omega_d)\, d\omega_1 d\omega_2 .. d\omega_n$$

2.5 Monochromatic Waves

Since the time-dependent electric field is real it can be expressed in terms of harmonic electromagnetic waves of angular frequency ω' as

$$\vec{E}(t) = \frac{1}{2} \sum_{\omega' > 0} \left[\vec{E}_{\omega'} e^{-i\omega' t} + \vec{E}_{-\omega'} e^{+i\omega' t} \right] \tag{2.39}$$

with the requirement $\vec{E}_{-\omega'} = \vec{E}^*_{\omega'}$. It follows from the Fourier transformation of $\vec{E}(t)$, that

$$\vec{E}(\omega) = \frac{1}{2}\sum_{\omega' \geq 0}\left[\vec{E}_{\omega'}\delta\left(\omega - \omega'\right) + \vec{E}_{-\omega'}\delta\left(\omega + \omega'\right)\right] \tag{2.40}$$

It may be noted that we should not get confused between $\vec{E}_{\omega'}$ which are amplitudes of the electric field with units of $V\ m^{-1}$ and $\vec{E}(\omega)$ which are Fourier component amplitudes with the units of $V\ m^{-1}s$.

The intensity of the wave at the angular frequency is given by$I_{\omega'} =$

$$\epsilon_0 cn\left(\omega'\right)\left\langle\frac{1}{2}\left[\vec{E}_{\omega'}e^{-i\omega' t} + \vec{E}^*_{\omega'}e^{+i\omega' t}\right]\cdot\left[\vec{E}_{\omega'}e^{-i\omega' t} + \vec{E}^*_{\omega'}e^{+i\omega' t}\right]\right\rangle \tag{2.41}$$

The angular brackets imply averaging over one wave cycle, which gives a factor of (1/2) for the harmonic fields. The refractive index $n\left(\omega'\right)$ is the refractive index at the angular frequency ω'. The expression for the intensity thus takes the form

$$I_{\omega'} = \frac{1}{2}\epsilon_0 cn\left(\omega'\right)\left|\vec{E}_{\omega'}\right|^2 \tag{2.42}$$

in units of $W\ m^{-2}$. For the harmonic fields impressed as above, the polarization may be written as

$$\vec{P}^{(n)}(t) = \frac{1}{2}\sum_{\omega \geq 0}\left[\vec{P}_{\omega}e^{-i\omega t} + \vec{P}_{-\omega}e^{+i\omega t}\right] \tag{2.43}$$

Again, since the polarization $\vec{P}^{(n)}(t)$ is real, it is necessary that $\vec{P}_{-\omega} = \left(\vec{P}_{\omega}\right)^*$. The Cartesian components of the n^{th} order polarization at the driving angular frequency ω_d are thus given by$\left\{\vec{P}^{(n)}_{\omega_d}\right\}_{\alpha} =$

$$2\epsilon_0\sum_{\beta_1..\beta_n}\left(\chi^{(n)}_{\alpha\beta_1..\beta_n}\left(-\omega_d;\omega_1,\omega_2,..\omega_n\right)\frac{1}{2}E_{\omega_1\beta_1}E_{\omega_2\beta_2}..\frac{1}{2}E_{\omega_n\beta_n}\right.$$
$$\left.+\chi^{(n)}_{\alpha\beta_1..\beta_n}\left(-\omega_d;\omega_2,\omega_1,..\omega_n\right)\frac{1}{2}E_{\omega_2\beta_1}E_{\omega_1\beta_2}..\frac{1}{2}E_{\omega_n\beta_n}\right.$$
$$+\text{further distinguishable terms}$$

with the driving frequency related to the component frequencies by the conservation condition

$$\omega_d = \omega_1 + \omega_2 + .. + \omega_n \tag{2.44}$$

A note of explanation is in order here. In the above expansion for $\vec{P}^{(n)}_{\omega_d}$ we are considering only such angular frequencies that satisfy this condition and the right hand side contains only distinguishable terms corresponding to each of the distinct arrangements of $\omega_1, \omega_2, ..., \omega_n$ whose sum equals ω_d . The number of distinguishable terms will be less if two are more frequencies are the same. Note that a frequency and its negative are considered distinct. To illustrate, let us assume that $\omega_1 = \omega_2$. Then the second term is indistinguishable from the first term. Intrinsic permutation symmetry allows us to freely exchange pairs such as (β_1, ω_1) and (β_2, ω_2). As a result the first two terms become in fact equal. We therefore see that as a consequence of the intrinsic permutation symmetry, two or more terms may become equal, but which are included in the expansion as they are distinguishable. Accordingly, we write only one term in place of such distinguishable but equal terms, which are obtained by permutation of the set of frequencies and multiply the expansion by an appropriate factor that takes care of this fact. Taking care of this factor, the factor 2 in front as well as the (1/2) factors on the right hand side [Ward and New, 1969], the expression for the polarization $\left\{ \vec{P}^{(n)}_{\omega_d} \right\}_\alpha$ becomes

$$\epsilon_0 \sum_{\beta_1 .. \beta_n} \sum_{\omega} K\left(-\omega_d; \omega_1, \omega_2, .. \omega_n\right)$$
$$\chi^{(n)}_{\alpha\beta_1 .. \beta_n}\left(-\omega_d; \omega_1, \omega_2, .. \omega_n\right) E_{\omega_1\beta_1} E_{\omega_2\beta_2} .. E_{\omega_n\beta_n} \tag{2.45}$$

The summation over ω implies summation over all distinct sets of frequencies that meet our conditions. The numerical factor K can be computed in each case using the general formula given by Ward and New:

$$K\left(-\omega_d; \omega_1, \omega_2, .. \omega_n\right) = 2^{l+m-n} p \tag{2.46}$$

Here p is the number of distinct permutations of the angular frequencies, n is the order of nonlinearity; $l = 1$ if $\omega_d \neq 0$ and

$l = 0$ if $\omega_d = 0$. m is the number of the set of $n\omega_j$ that are zero. For instance, if none of the frequencies as well as the driving frequency is zero ($m = 0, l = 1$), and all the component frequencies are different, then $K = 2^{1-n}n!$.

2.6 Calculation of the Factor K

We illustrate the calculation of the numerical factor K in a few cases [Butcher and Cotter, 1990].

2.6.1 Optical Rectification

This is a second order process with $n = 2$, in which is no output wave emitted, $\omega_d = 0$ and so $l = 0$. The result of this process is merely the development of a DC polarization in the medium and the corresponding susceptibility is denoted as $\chi^{(2)}(0; \omega, -\omega)$. This is viewed as a difference frequency generation process with the only input being a strong optical wave at a frequency ω . Thus neither of the component frequencies is zero so that $m = 0$. $p = 2! = 2$. As a consequence,

$$K = 2^{0+0-2}2! = \frac{1}{2} \tag{2.47}$$

Explicitly the polarization is given by

$$P_{0\alpha}^{(2)} = \epsilon_0 \sum_{\beta_1,\beta_2} \chi_{\alpha\beta_1\beta_2}^{(2)}(0 : \omega, -\omega) \left[\frac{1}{2}E_{\omega\beta_1}\frac{1}{2}E_{-\omega\beta_2} + \frac{1}{2}E_{-\omega\beta_1}\frac{1}{2}E_{\omega\beta_2}\right] \tag{2.48}$$

which simplifies to

$$P_{0\alpha}^{(2)} = \epsilon_0 \sum_{\beta_1,\beta_2} \frac{1}{2}\chi_{\alpha\beta_1\beta_2}^{(2)}(0 : \omega, -\omega) E_{\omega\beta_1}E_{-\omega\beta_2} \tag{2.49}$$

illustrating the use of the K factor.

2.6.2 Second Harmonic Generation

The second order polarization is given by

$$\left\{P_{2\omega}^{(2)}\right\}_\alpha = 2\epsilon_0 \sum_{\beta_1,\beta_2} \chi_{\alpha\beta_1\beta_2}^{(2)}(-2\omega : \omega, \omega) \frac{1}{2}E_{\omega\beta_1}\frac{1}{2}E_{\omega\beta_2} \tag{2.50}$$

The K factor equals

$$K = 2^{1+0-2}1! = \frac{1}{2} \tag{2.51}$$

because $n = 2$, $m = 0$, as no frequency is zero and $l = 1$ since $\omega_d = 2\omega \neq 0$ and $p = 1!$

2.6.3 Pockels Effect

The Pockels effect occurs in the presence of a DC electrostatic field (i.e. of zero frequency) and does not alter the frequency ω of the input beam. The susceptibility in this case is denoted as $\chi^{(2)}(-\omega; 0, \omega)$. The corresponding polarization is given by

$$\left\{P_{\omega}^{(2)}\right\}_{\alpha} = 2\epsilon_0 \sum_{\beta_1,\beta_2} \chi^{(2)}_{\alpha\beta_1\beta_2}(-\omega : 0, \omega)\left[E_{0\beta_1}\frac{1}{2}E_{\omega\beta_2} + \frac{1}{2}E_{\omega\beta_1}E_{0\beta_2}\right] \tag{2.52}$$

and the K factor is$K = 2^{1+1-2}2! = 2$.

$$\left\{P_{\omega}^{(2)}\right\}_{\alpha} = \epsilon_0 \sum_{\beta_1,\beta_2} 2\chi^{(2)}_{\alpha\beta_1\beta_2}(-\omega : 0, \omega)\, E_{0\beta_1}E_{\omega\beta_2} \tag{2.53}$$

2.6.4 Sum and Difference Frequency generation

Input frequencies ω_1 and ω_2 get mixed to generate an output frequency $\omega_3 = \omega_1, \pm\omega_2$ and $\chi^{(2)}_{\alpha\beta_1\beta_2}(-\omega_3 : \omega_1, \pm\omega_2)$ is the corresponding susceptibility. The polarization $\left\{P^{(2)}_{\omega_3}\right\}_{\alpha}$ and for the case of sum frequency generation can be written as :

$$2\epsilon_0 \sum_{\beta_1,\beta_2} \chi^{(2)}_{\alpha\beta_1\beta_2}(-\omega_3 : \omega_1, \omega_2)\left[\frac{1}{2}E_{\omega_1\beta_1}\frac{1}{2}E_{\omega_2\beta_2} + \frac{1}{2}E_{\omega_2\beta_1}E_{\omega_1\beta_2}\right] \tag{2.54}$$

and the K factor is

$$K = 2^{1+0-2}2! = 1 \tag{2.55}$$

The susceptibility is $\chi^{(2)}_{\alpha\beta_1\beta_2}(-\omega_3 : \omega_1, -\omega_2)$ and the K factor equals 1 for the case of difference frequency generation.

2.6.5 Third Harmonic Generation

Three input waves of frequency ω combine together to provide an output wave of frequency 3ω and the susceptibility involved is $\chi^{(3)}_{\alpha\beta_1\beta_2\beta_3}(-3\omega:\omega,\omega,\omega)$. The third order polarization $\left\{P^{(3)}_{3\omega}\right\}_\alpha$ in this case is equal to

$$2\epsilon_0 \sum_{\beta_1,\beta_2,\beta_3} \chi^{(3)}_{\alpha\beta_1\beta_2\beta_3}(-3\omega:\omega,\omega,\omega)\left[\frac{1}{2}E_{\omega_1\beta_1}\frac{1}{2}E_{\omega_2\beta_2}\frac{1}{2}E_{\omega_3\beta_3}+\ldots\right]$$

$$K = 2^{1+0-3}1! = \frac{1}{4} \tag{2.56}$$

2.6.6 Nondegenerate Four Wave Mixing

This is an effect arising from third order nonlinearity and is denoted by

$$\chi^{(3)}_{\alpha\beta_1\beta_2\beta_3}(-\omega_4:\omega_1,\omega_2,\omega_3)\,. \tag{2.57}$$

The relevant polarization $\left\{P^{(3)}_{\omega_4}\right\}_\alpha$ is given by

$$2\epsilon_0 \sum_{\beta_1,\beta_2,\beta_3} \chi^{(3)}_{\alpha\beta_1\beta_2\beta_3}(-\omega_4:\omega_1,\omega_2,\omega_3)\left[\frac{1}{2}E_{\omega_1\beta_1}\frac{1}{2}E_{\omega_2\beta_2}\frac{1}{2}E_{\omega_3\beta_3}+\ldots\right]$$

The K factor is

$$K = 2^{1+0-3}3! = \frac{3}{2} \tag{2.58}$$

A table of the K values for several nonlinear effects as given in Butcher and Cotter [1969] as follows:

Process	n	$-\omega_d;\omega_1,...,\omega_n$	K
Linear optics	1	$-\omega,\omega$	1
Optical rectification	2	$0;\omega,-\omega$	1/2
Pockels effect	2	$-\omega;0,\omega$	2
Frequency mixing, 2^{nd} order	2	$-\omega_3;\omega_1,\pm\omega_2$	1
DC Kerr effect	3	$-\omega;0,0,\omega$	3
EFISH	3	$-2\omega;0,\omega,\omega$	3/2
THG	3	$-3\omega;\omega,\omega,\omega$	1/4
NDFWM	3	$-\omega_4;\omega_1,\omega_2,\omega_3$	3/2
Frequency mixing , 3^{rd} order	3	$-\omega_3;\pm\omega_1,\omega_2,\omega_3$	3/4
CARS	3	$-\omega_{AS};\omega_P,\omega_P,-\omega_S$	3/4
Kerr effect, *SRS*, *SBS*	3	$-\omega_S;\omega_P,-\omega_P,\omega_S$	3/2
DFWM	3	$-\omega;\omega,-\omega,\omega$	3/4
TPA	3	$(-\omega_1;-\omega_2,\omega_2,\omega_1)$	3/2
TPE	3	$-\omega;-\omega,\omega,\omega$	3/4
FHG	5	$-5\omega;\omega,\omega,\omega,\omega,\omega$	1/16
SHRS	5	$-\omega_S;\omega_{P_1},\omega_{P_2},-\omega_{P_2},-\omega_{P_1},\omega_S$	15/2
SHRS	5	$-\omega_S;\omega_P,\omega_P,-\omega_P,-\omega_P,\omega_S$	15/8
n^{th} harmonic generation	n	$-n\omega;\omega,...\omega$	2^{1-n}

It may be noted that the table gives values of K for the process specified, with the angular frequencies labeled , $\omega_1,\omega_2,...$ with the understanding the frequencies have different values. If the frequencies are equal, then the same symbol is used to express that fact explicitly. Otherwise, it is necessary to understand that the frequencies are different.

2.7 Explorations

1. Assuming a spherically uniform distribution of total charge q over a radius R, show that the electronic polarizability is approximately given by $\alpha \approx 4\pi\epsilon_0 R^3 q$. Given that dielectric breakdown sets in most materials typically at electric fields of the order of $10^8\ V\ m^{-1}$, estimate the intensity of optical fields at which this would occur.

2. a) Write explicitly how the y-component of linear dielectric polarization induced in a medium of dielectric constat ϵ_r is related to the z-component of the optical electric field of the interacting light wave.

b) Which are the components of the interacting optical electric fields that determine the magnitude of the z-component of the second order polarization induced in a medium with a large $\chi^{(2)}$?

3. Write down explicitly the relationship between the polarization and the optical electric fields involved in the process of difference frequency generation where the output frequency is given by the difference between the two input frequencies.

4. What are the requirements of causality and reality important at a fundamental level? What do these imply for the complex nature of the response tensor and susceptibility tensor?

5. Arrive at the units and dimensions of the coefficients of n^{th} order nonlinear optical susceptibility, from first principles.

6. Consider a material medium exhibiting seond order nonlinearity with susceptibility $\chi^{(2)}$. Find the resulting first order as well as second order polarization in the material when a harmonic electric field of magnitude $E = E_0 \cos(\omega t)$ at a frequency ω interacts with this material.

7. What is is the origin of the Ward and New K-factor in nonlinear optics? In what way is this factor different for (a) Third harmonic generation and and third order sum frequency generation and (b) for Pockels effect and Kerr effect ? What would be the K-factor for a linear optical process ?

8. Show that K-factor for n^{th} harmomnic generation would always have a value smaller than for the sum-frequency generation (with all input frequencies beign different from one another) of the n^{th} order.

Chapter 3

Symmetry and Susceptibility Tensors

"You can observe a lot by just watching".

Yogi Berra

...and reduce the apparent complexities around you.

Learning Objectives

- Recognition of the role of symmetry in determining the number of independent tensor elements of nonlinear susceptibility.
- Employment of Neumann principle to examine how certain tensor elements are related to one another.
- Enumeration of the independent and nonvanishing tensor components in media belonging to specific crystal classes.
- Description of the propagation of light in a uniaxial crystal using the concept of indicatrix.

3.1 Introduction

In this chapter, we learn about the influence of the spatial symmetry of material media on the nature optical nonlinearity exhibited by them. We have seen that n^{th} order nonlinearity is governed by a tensor of rank $(n+1)$ with $3^{(n+1)}$ tensor components in general. It would indeed be very inconvenient if we have to consider such a large number of quantities to describe nonlinearity. For example, it appears we need to specify 81 tensor components to characterize the third order susceptibility of a medium. However, it can be shown that only a much smaller number would be actually required in most materials and for example, one independent element is sufficient to describe third order nonlinearity in media in the form of transparent liquids. This reduction is brought about by understanding how the inherent symmetry in the material medium makes several of the tensor components related to one another.

3.2 Crystal Symmetry and Susceptibility Tensors

We know that crystalline solids have atoms arranged in a periodic way but with varying kinds of spatial symmetry. Thus there are seven crystal systems. All crystalline solids come under one of these systems: triclinic, monoclinic, rhombohedral, orthorhombic, tetragonal, hexagonal, and cubic crystal systems. The symmetry is greatest in cubic crystals and least in the triclinic system. There are 32 different local symmetry types based on the rotational, reflectional and inversion symmetry around a point in the crystal. These 32 crystal classes are also called 32 point groups. Physical properties have in general, a tensor character, depending on their phenomenological nature. Optical linear susceptibility itself is represented by a second order tensor with 9 independent components. Property symmetry and intrinsic symmetry based on its thermodynamic properties reduces the number of components to only 6 independent coefficients. Neumann criterion on physical property tensors could reduce this number further depending on the point group symmetry (crystal class) to which the crystal belongs. We follow closely the excellent treatment of this subject to be found in the article by Smith [1958].

Let us see how a physical property tensor transforms under a symmetry operation. Toward this purpose, we first consider the linear optical susceptibility tensor and cubic crystals. The linear optical susceptibility tensor connects the vector electric field with the vector electric polarization, as given in the previous chapter:

$$\vec{P} = \epsilon_0 \chi^{(1)} \vec{E} \tag{3.1}$$

The Cartesian components of the polarization are given by

$$P_i = \epsilon_0 \chi_{ij}^{(1)} E_j \tag{3.2}$$

where we sum over the repeated suffix (j) on the right hand side. To be specific, we get the equations for the three polarization components as

$$P_1 = \epsilon_0 \chi_{11}^{(1)} E_1 + \epsilon_0 \chi_{12}^{(1)} E_2 + \epsilon_0 \chi_{13}^{(1)} E_3 \tag{3.3}$$

$$P_2 = \epsilon_0 \chi_{21}^{(1)} E_1 + \epsilon_0 \chi_{22}^{(1)} E_2 + \epsilon_0 \chi_{23}^{(1)} E_3 \tag{3.4}$$

$$P_3 = \epsilon_0 \chi_{31}^{(1)} E_1 + \epsilon_0 \chi_{32}^{(1)} E_2 + \epsilon_0 \chi_{33}^{(1)} E_3 \tag{3.5}$$

The susceptibility, accordingly is given as a second order tensor with the matrix represented by

$$\chi^{(1)} = \begin{pmatrix} \chi_{11}^{(1)} & \chi_{12}^{(1)} & \chi_{13}^{(1)} \\ \chi_{21}^{(1)} & \chi_{22}^{(1)} & \chi_{23}^{(1)} \\ \chi_{31}^{(1)} & \chi_{32}^{(1)} & \chi_{33}^{(1)} \end{pmatrix} \tag{3.6}$$

with 9 components $(\chi_{ij}^{(1)})$. Owing to the intrinsic symmetry of the susceptibility, we have $\chi_{ij}^{(1)} = \chi_{ji}^{(1)}$ with the result, the nine components reduce to 6 components in general: three diagonal components $\chi_{11}^{(1)}, \chi_{22}^{(1)}, \chi_{33}^{(1)}$ and three non-diagonal components $\chi_{12}^{(1)} = \chi_{21}^{(1)}, \chi_{23}^{(1)} = \chi_{32}^{(1)}, \chi_{31}^{(1)} = \chi_{13}^{(1)}$. For convenience, sometimes, we adopt a reduced suffix convention in which the components are labelled as $\chi_{11}^{(1)} \equiv \chi_1^{(1)}$, $\chi_{22}^{(1)} \equiv \chi_2^{(1)}$, $\chi_{33}^{(1)} \equiv \chi_3^{(1)}$, $\chi_{23}^{(1)} \equiv \chi_4^{(1)}$, $\chi_{31}^{(1)} \equiv \chi_5^{(1)}$, and $\chi_{12}^{(1)} \equiv \chi_6^{(1)}$. Notice the order of labelling these components: the diagonal components are in the order of 11, 22, 33 followed by the non-diagonal components in the order of the missing suffix.

How does a property tensor transform under any symmetry operation? Consider a right-handed set of Cartesian axes termed

X_1, X_2, X_3 (corresponding respectively to the XYZ axes. A rotation of the axes system through the angle θ about the X_3 axis transforms a vector, say, an electric field $\vec{E} = E_1\,\hat{i} + E_2\,\hat{j} + E_3\,\hat{k}$, as follows

$$\begin{pmatrix} E_1' \\ E_2' \\ E_3' \end{pmatrix} = \begin{pmatrix} \cos\theta & \sin\theta & 0 \\ -\sin\theta & \cos\theta & 0 \\ 0 & 0 & 1 \end{pmatrix} \begin{pmatrix} E_1 \\ E_2 \\ E_3 \end{pmatrix} \tag{3.7}$$

where the components of the electric field after the rotation, i.e. in the new axes are labelled as primed components (E_1', E_2', E_3'). If it is a 4-fold rotation about the X_3 axis, then the new transformed values of the electric field will be given by substituting $\theta = 90^0$ in the above equation. For a symmetry operation such as reflection in a mirror with its normal along the X_3 axis, the equation for the vector transformation is given by

$$\begin{pmatrix} E_1' \\ E_2' \\ E_3' \end{pmatrix} = \begin{pmatrix} 1 & 0 & 0 \\ 0 & 0 & 0 \\ 0 & 0 & -1 \end{pmatrix} \begin{pmatrix} E_1 \\ E_2 \\ E_3 \end{pmatrix} \tag{3.8}$$

In general any symmetry operation on the crystal, or conversely on the axes, can be represented by a vector transformation matrix a

$$\begin{pmatrix} E_1' \\ E_2' \\ E_3' \end{pmatrix} = \begin{pmatrix} a_{11} & a_{12} & a_{13} \\ a_{21} & a_{22} & a_{23} \\ a_{31} & a_{32} & a_{33} \end{pmatrix} \begin{pmatrix} E_1 \\ E_2 \\ E_3 \end{pmatrix} \tag{3.9}$$

We can see that for the rotation operation (Eq.3.7), $a_{11} = \cos\theta$, $a_{12} = \sin\theta$, $a_{13} = 0$, $a_{21} = -\sin\theta$, $a_{22} = \cos\theta$ and so on. An alternative way of performing the transformation for any such operation is to use the components, one by one, instead of transforming the entire matrix in one go. This component transformation is given by

$$E_i' = a_{ij} E_j \tag{3.10}$$

wherein, we used the implicit Einstein summation convention of summation over the repeated index. Any vector transforms according to the equations given above for the matrix and for the components. Note that a vector is a tensor of rank 1 and all first rank physical quantities undergo transformation as just given.

Now we go back to the linear first order optical susceptibility as defined in Eq.3.1 and following equations for the components of the

matrix. Since polarization $\vec{P}$ is a vector, it also undergoes transformation like a vector illustrated above for the electric field as an example. Now how does the susceptibility tensor components $\chi_{ij}^{(1)}$ and matrix χ transform in a given axes transformation represented by the transformation matrix a? To answer this we perform the following mathematical tricks. In the new axes system (X_1', X_2', X_3') obtained by the transformation a, we have

$$P' = \epsilon_0 \chi^{(1)'} E' \tag{3.11}$$

where the new matrix of the susceptibility measured in the new axes is $\chi^{(1)'}$, P' and E' being the matrices respectively for the polarization and electric field as measured in the new axes. To obtain a relation between the transformed matrix $\chi^{(1)'}$ and the matrix before the transformation χ, we note that $P' = aP$, and $E' = aE$. So we pre-multiply the equation $P = \epsilon_0 \chi^{(1)} E$ with the matrix a to get

$$aP = \epsilon_0 a \chi^{(1)} E \tag{3.12}$$

Now insert the matrix product $a^{-1}a$ in between $\chi^{(1)}$ and E in the above equation to find

$$aP = \epsilon_0 a \chi^{(1)} a^{-1} a E \tag{3.13}$$

We are allowed to do this because a^{-1} being the inverse of a, $a^{-1}a = I$, the identity matrix. Notice that aE in the above equation is just equal to E'. Also $aP = P'$. As such, we may rewrite the above equation as

$$P' = \epsilon_0 a \chi^{(1)} a^{-1} E' \tag{3.14}$$

Now compare this equation with the Eq.3.11 to realize that the new susceptibility matrix is related to the old susceptibility matrix by the transformation equation

$$\chi^{(1)'} = a \chi^{(1)} a^{-1} \tag{3.15}$$

We may develop the transformation relations between the components of the susceptibility matrix in a similar manner. Note the vector components transform as $P_i' = a_{ij} P_j$ and $E_i' = a_{ij} E_j$ as we may learn from Eq.3.10. Thus the susceptibility components in the original axes are given by Eq.3.2: $P_i = \epsilon_0 \chi_{ij}^{(1)} E_j$. We need to obtain the relation between the components of $\chi^{(1)'}$ and the components of $\chi^{(1)}$. The components $\chi_{ij}^{(1)'}$ relate P_i' with the components E_j' by

$$P_i' = \epsilon_0 \chi_{ik}^{(1)'} E_k' \tag{3.16}$$

We know that the reverse of the transformation of vectors from axes X_1', X_2', X_3' to axes X_1, X_2, X_3 is given by $E = a^{-1}E'$ and $P = a^{-1}P'$ which leads to the relations for their components as $E_i = a_{ji}E_j'$. Accordingly, $E_k' = a_{kl}E_l$. Note that the suffix k here is fixed at the chosen value and the suffix l is a dummy suffix and is to be summed over its full range of $l = 1, 2, 3$. We can therefore use any other label in place of this dummy label l other than the fixed label k (in this case).

Starting with $P_i' = a_{ij}P_j$, we have, since $P_j = \epsilon_0\chi_{jk}E_k$, $P_i' = a_{ij}\epsilon_0\chi_{jk}E_k$. Further, since $E_k = a_{lk}E_l'$, this gives $P_i' = a_{ij}\epsilon_0\chi_{jk}a_{lk}E_l'$. Hence we see that from Eq.3.16, that

$$\chi_{il}^{(1)'} = a_{ij}a_{lk}\chi_{jk} \tag{3.17}$$

In the above equation, the right hand side has the dummy labels j, k and we have to sum over the full range of each of these dummy variable suffices. For convenience we may re-write the above transformation of the susceptibility tensor by changing the suffixes, as follows:

$$\chi_{ij}^{(1)'} = a_{ik}a_{jl}\chi_{kl} \tag{3.18}$$

Now the fixed indices are any chosen pair ij and dummy suffixes are kl. As an example, suppose we wish to know the expression for the susceptibility tensor component $\chi_{12}^{(1)'}$ in the new axes system: It is given by

$$\begin{aligned}
\chi_{12}^{(1)'} &= a_{1k}a_{2l}\chi_{kl} = a_{11}a_{21}\chi_{11} + a_{11}a_{22}\chi_{12} + a_{11}a_{23}\chi_{13} && (3.19)\\
&+a_{12}a_{21}\chi_{21} + a_{12}a_{22}\chi_{22} + a_{12}a_{23}\chi_{23} && (3.20)\\
&+a_{13}a_{21}\chi_{31} + a_{13}a_{22}\chi_{32} + a_{13}a_{23}\chi_{33} && (3.21)
\end{aligned}$$

Notice that there are nine terms because we have allowed the two dummy indices k and l to take the values $1, 2, 3$ each.

The equation 3.18 is the law of transformation for first order optical susceptibility. What are the transformation laws for non-linear susceptibilities?

For the second order susceptibility, the transformation law is given by

$$\chi_{ijk}^{(2)'} = a_{il}a_{jm}a_{kn}\chi_{lmn} \tag{3.22}$$

It is easy to remember once you understand the structure of the law. For any given (chosen) component of the second order susceptibility fixed by the index triplet ijk, the right hand side

has additive terms obtained by allowing the dummy indices lmn each to take their full range of values $(1-3)$, leading to a total of $3 \times 3 \times 3 = 27$ terms with corresponding χ_{lmn} components of the tensor in the original axes system.

The transformation law for the third order susceptibility is

$$\chi^{(3)'}_{ijkl} = a_{im}a_{jn}a_{ko}a_{lp}\chi_{mnop} \tag{3.23}$$

Here again, for a chosen component of the third order susceptibility tensor, the transformation from the measurement axes $(X_1X_2X_3)$ to the axis set $(X'_1X'_2X'_3)$involves adding $3\times3\times3\times3 = 81$ susceptibility components on the right hand side, along with the appropriate coefficients of the axes transformation matrix a.

3.2.1 Neumann Principle

The Neumann principle [Neumann, 1885] asserts that macroscopic physical properties of a crystal must exhibit at least the symmetry of the point group to which the crystal belongs. The property is expected to exhibit the symmetry of the point group or more but not less. The hypothesis is plausible because the point group symmetry of a crystal is the symmetry of the atomic arrangement around a point in the crystal. For example, if there is a three-fold symmetry about a certain axis at a point in the crystal, then rotating the crystal through the angle of 120^0 about that axis would give rise to a new orientation and atomic structure of the crystal sample which is identical to the orientation before the rotation. The crystal is said to be invariant under the above symmetry operation. This must be true for every symmetry element present in the point group.

We can make use of the principle to learn about the effect of symmetry on the optical susceptibilities. First consider the first order susceptibility. Let us see what the principle bodes for the linear susceptibility in cubic crystals. In a cubic crystal, there are five point groups for all of which there is a common essential symmetry element: a three-fold symmetry about the body diagonals of the cubic unit cell. The Neumann principle demands that since the crystal possesses this symmetry, the property also must exhibit this symmetry. Measure the optical susceptibility of a cubic crystal using the Cartesian axes $(X_1X_2X_3)$ usually chosen to be along the crystallographic axes, i.e. along the sides of the cubic unit cell. Now rotate the crystal about one of its body diagonals by the angle 120^0. And re-measure the susceptibility. Since the crystal is

invariant under this rotation, the measured property also must be invariant. You should get the same values as before the operation. That is what the principle tells us.

However, we can follow an equivalent procedure of keeping the crystal stationary and rotating the measuring axes about the body diagonal through the angle 120^0. This procedure is more convenient for our purpose, as illustrated in what follows. Fig.3.1 shows the bare unit cell of a cubic crystal with our measuring axes placed along the standard crystallographic (a, b, c) directions or in the usual crystallographic Miller notation respectively along the [100], [010], [001] directions, with the origin placed at a cube corner. Note since we have a cubic cell, the sides are all equal $(a = b = c)$.

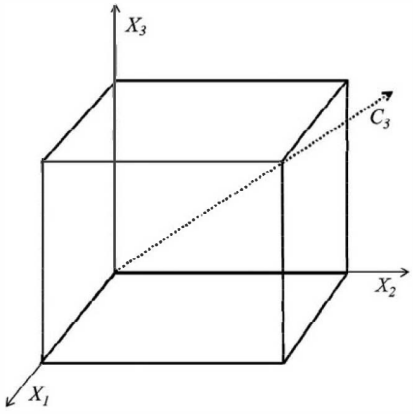


Figure 3.1: Unit cell of cubic lattice with C3 axis

Fig.3.1 gives a sketch of the unit cell of a cubic crystal with the axes $(X_1X_2X_3)$, and the three-fold symmetry axis C_3 oriented along a body diagonal starting from the origin of the axes O. A rotation of the axes about this axis through the angle 120^0 counterclockwise, would take the X_1 axis to occupy the place of the X_2 axis., giving $X_1^{'} = X_2$. The X_2 axis in turn would go to place itself along the former X_3 axis: to give $X_2^{'} = X_3$. And the new position of the X_3 axis coincides with the former position of the X_1 axis leading to $X_3^{'} = X_1$. As such the transformation of coordinates and hence of a vector is given by the set of equations $x_1^{'} = x_2$, $x_2^{'} = x_3$, and $x_3^{'} = x_1$. The matrix equation for these relations is therefore given by

$$\begin{pmatrix} x_1' \\ x_2' \\ x_3' \end{pmatrix} = \begin{pmatrix} 0 & 1 & 0 \\ 0 & 0 & 1 \\ 1 & 0 & 0 \end{pmatrix} \begin{pmatrix} x_1 \\ x_2 \\ x_3 \end{pmatrix} \tag{3.24}$$

The axis transformation matrix is thus given by

$$a \equiv \begin{pmatrix} 0 & 1 & 0 \\ 0 & 0 & 1 \\ 1 & 0 & 0 \end{pmatrix} \tag{3.25}$$

We deduce that for this rotation operation, $a_{11} = 0$, $a_{12} = 1$, $a_{13} = 0$, $a_{21} = 0$, $a_{22} = 0$, $a_{23} = 1$, $a_{31} = 1$, $a_{32} = 0$, $a_{33} = 0$.

Let us now see how the linear susceptibility tensor coefficients transform under this symmetry operation. We apply equation 3.18.

$\chi_{11}' = a_{1k}a_{1l}\,\chi_{kl} = a_{11}a_{11}\,\chi_{11} + a_{11}a_{12}\,\chi_{12} + a_{11}a_{13}\,\chi_{13} + a_{12}a_{11}\,\chi_{21} + a_{12}a_{12}\,\chi_{22} + a_{12}a_{13}\,\chi_{23} + a_{13}a_{11}\,\chi_{31} + a_{13}a_{12}\,\chi_{32} + a_{13}a_{13}\,\chi_{33}$. Substituting the values of the a_{ij} coefficients in the above equation gives immediately $\chi_{11}' = \chi_{22}$. In a similar manner, we find $\chi_{22}' = \chi_{33}$ and $\chi_{33}' = \chi_{11}$.

Now we go to the Neumann principle. The principle tells us that $\chi_{11}' = \chi_{11}$, $\chi_{22}' = \chi_{22}$ and $\chi_{33}' = \chi_{33}$. Together with the above result of transformation, this requirement leads us to conclude that the three diagonal components must be equal: $\chi_{11} = \chi_{22} = \chi_{33}$.

In a similar manner we may investigate the effect of the other symmetry operations corresponding to the elements of symmetry present in the cubic point groups to find that all the non-diagonal components must be zero in order to satisfy the Neumann principle. The final conclusion for the linear optical susceptibility is in the case of all cubic crystals,

$$\chi = \begin{pmatrix} \chi_{11} & 0 & 0 \\ 0 & \chi_{11} & 0 \\ 0 & 0 & \chi_{11} \end{pmatrix} \tag{3.26}$$

3.2.2 Symmetry of Second Order Susceptibility

Now we examine the symmetry of the second order optical susceptibility in the case of crystals belonging to the point group C_4. In this group, there is only one symmetry element, namely, a four-fold rotational symmetry about the crystallographic c axis. We place our measuring Cartesian axes such that the X_3 (Z axis) falls

along this c axis (also known as the [001] axis) and the other two axes X_1 (X axis) and X_2 (Y) axis along respectively the crystallographic a and b axes. The origin is placed at one cell corner. The four-fold rotational symmetry means that when we rotate the entire crystal through the angle 90^0 about this axis (X_3), the crystal is invariant (appears the same) so that the same values obtain for any macroscopic measured physical property of the crystal. The physical property of any crystal belonging to the crystal class C_4 is thus invariant under rotation of the axes system through the angle 90^0 about the X_3 axis.

First we write the a matrix for the transformation of the axes, by substituting $\theta = 90^0$ in the a matrix of equation 3.7. We get then

$$a \equiv \begin{pmatrix} 0 & 1 & 0 \\ -1 & 0 & 0 \\ 0 & 0 & 1 \end{pmatrix} \tag{3.27}$$

We have the nonzero elements of the a matrix $a_{12} = 1$, $a_{21} = -1$, $a_{33} = 1$. We start by considering the component χ_{111}. according to the transformation given by Eq.3.22, we find

$$\chi'_{111} = a_{1j}a_{1k}a_{1l}\chi_{jkl} \tag{3.28}$$

wherein, we need to sum over all possible values of the dummy indices jkl. While we could get 27 terms, this number is drastically reduced (to only one term) because of the zeros in the a matrix, given above. Thus we have

$$\chi'_{111} = a_{12}a_{12}a_{12}\chi_{222} = \chi_{222} \tag{3.29}$$

As a consequence of the Neumann principle, the component χ'_{111} resulting from the rotation operation should be equal to the same value as the component before the rotation, since the rotational operation is a symmetry operation. Which means that Neumann principle demands that $\chi'_{111} = \chi_{111}$. In view of the result given in the above equation (Eq.3.29), this means that $\chi_{111} = \chi_{222}$.

Next let us apply the same symmetry operation on the component χ_{222}:

$$\chi'_{222} = a_{2j}a_{2k}a_{2l}\chi_{jkl} = a_{21}a_{21}a_{2l}\chi_{111} = -\chi_{111} \tag{3.30}$$

since the only non-zero element of the second row of the matrix (Eq.3.27)is $a_{21} = -1$. Now use Neumann principle which requires

$\chi'_{222} = \chi_{222}$. In view of the above result, this gives $\chi_{222} = -\chi_{111}$. But the conclusion we have arrived at from the consideration of the component of the χ_{111} is $\chi_{111} = \chi_{222}$. Both these conclusions must be right and that leads us to the only possible solution that $\chi_{111} = \chi_{222} = 0$.

Application of the rotation operation on the component χ_{333} gives the result $\chi'_{333} = \chi_{333}$ and Neumann principle does not give any extra information on this component χ_{333}. Thus we conclude that χ_{333} exists for crystals having the point group C_4.

Consider the component χ_{112}. Applying the four-fold symmetry operation on this component, we have

$$\chi'_{112} = a_{1j}a_{1k}a_{2l}\chi_{jkl} = a_{12}a_{12}a_{21}\chi_{221} = (1)(1)(-1) = -\chi_{221} \quad (3.31)$$

Since according to Neumann principle, $\chi'_{112} = \chi_{112}$; $\chi_{112} = -\chi_{221}$.

Now apply the same symmetry operation on the component χ_{221} to find

$$\chi'_{221} = a_{2j}a_{2k}a_{1l}\chi_{jkl} = a_{21}a_{21}a_{12}\chi_{221} = (-1)(-1)(1)\chi_{112} = \chi_{112} \quad (3.32)$$

Neumann principle requires that $\chi'_{221} = \chi_{221}$. Hence we get from the above result, $\chi_{221} = \chi_{112}$

This, together with the previous result that $\chi_{112} = -\chi_{221}$ we are led to conclude that the above equations become valid only if $\chi_{221} = \chi_{112} = 0$.

If we proceed in the same manner with the components χ_{223} and χ_{113}, we do not get any added information leaving us with the conclusion that these two components can exist in the point group C_4.

The overall result of such an investigation on the effect of the crystal symmetry on the susceptibility tensor is that $\chi^{(2)}$ can be represented by the matrix

$$\begin{pmatrix} 0 & 0 & 0 & \chi^{(2)}_{123} & \chi^{(2)}_{132} & \chi^{(2)}_{131} & \chi^{(2)}_{113} & 0 & 0 \\ 0 & 0 & 0 & \chi^{(2)}_{113} & \chi^{(2)}_{131} & -\chi^{(2)}_{132} & -\chi^{(2)}_{123} & 0 & 0 \\ \chi^{(2)}_{311} & \chi^{(2)}_{311} & \chi^{(2)}_{333} & 0 & 0 & 0 & 0 & \chi^{(2)}_{312} & -\chi^{(2)}_{312} \end{pmatrix} \quad (3.33)$$

While the above treatment is most general, there is a further simplification in the case of some second order properties owing to inherent symmetry of the process. We illustrate this by considering the second harmonic generation.

3.2.3 Second Harmonic Generation

Recall how we defined the second order susceptibility for second harmonic generation in terms of the second harmonic polarization given by

$$P_{2\omega}^{(2)} = \epsilon_0 K\left(-2\omega;\omega,\omega\right)\chi^{(2)}\left(-2\omega;\omega,\omega\right)E_\omega E_\omega \tag{3.34}$$

where the K factor has the value $K = \frac{1}{2}$. In the literature, an alternative tensor d is used for second harmonic generation as defined by

$$P_{2\omega}^{(2)} = \epsilon_0 d\left(-2\omega;\omega,\omega\right)E_\omega E_\omega \tag{3.35}$$

Hence we see that $d\left(-2\omega;\omega,\omega\right) = \frac{1}{2}\chi^{(2)}\left(-2\omega;\omega,\omega\right)$. The components of the second harmonic polarization are given by

$$P_\mu^{(2)} = \epsilon_0 d_{\mu m}\left(-2\omega;\omega,\omega\right)E_\mu E_m \tag{3.36}$$

In view of an intrinsic permutation symmetry, we write the matrix equation as

$$\begin{pmatrix} P_1 \\ P_2 \\ P_3 \end{pmatrix} = \epsilon_0 \begin{bmatrix} d_{11} & d_{12} & d_{13} & d_{14} & d_{15} & d_{16} \\ d_{21} & d_{22} & d_{23} & d_{24} & d_{25} & d_{26} \\ d_{31} & d_{32} & d_{33} & d_{34} & d_{35} & d_{36} \end{bmatrix} \begin{pmatrix} E_1^2 \\ E_2^2 \\ E_3^2 \\ 2E_2E_3 \\ 2E_3E_1 \\ 2E_1E_2 \end{pmatrix} \tag{3.37}$$

wherein, we have used a contracted notation for the products of the electric field components: μm : $11 \equiv 1$, $22 \equiv 2$, $33 \equiv 3$, $23 \equiv 4$, $31 \equiv 5$, $12 \equiv 6$. with this notation, the number of coefficients of the d matrix become reduced from 27 to 18. We have used the fact that owing to the permutation symmetry, $E_{\omega 3}E_{\omega 2} + E_{\omega 2}E_{\omega 3} = 2E_{\omega 2}E_{\omega 3}$. Similarly, $E_{\omega 3}E_{\omega 1} + E_{\omega 1}E_{\omega 3} = 2E_{\omega 3}E_{\omega 1}$ and $E_{\omega 1}E_{\omega 2} + E_{\omega 2}E_{\omega 1} = 2E_{\omega 1}E_{\omega 2}$. This is what has been used above.

We may consider crystals belonging to the point group symmetry, for this application. Recalling the axes transformation matrix a for the four-fold rotation about the X_3 axis,

$$a = \begin{pmatrix} 0 & 1 & 0 \\ -1 & 0 & 0 \\ 0 & 0 & 1 \end{pmatrix} \tag{3.38}$$

The effect of this symmetry operation on d_{14} is given by

$$d_{14}' = d_{123}' = a_{1j}a_{2k}a_{3l}d_{jkl} = a_{12}a_{21}a_{33}d_{213} = -d_{213} = -d_{25} \tag{3.39}$$

Thus $d'_{14} = -d_{25}$ and Neumann principle requires that $d'_{14} = d_{14}$ because the above transformation is a symmetry operation. Therefore, we get $d_{14} = -d_{25}$.

The effect of the same transformation on the element d_{25} is given by

$$d'_{25} = d'_{231} = a_{2j}a_{3k}a_{1l}d_{jkl} = a_{21}a_{33}a_{12}d_{132} = -d_{132} = -d_{14} \quad (3.40)$$

Neumann principle then leads to $d_{231} = -d_{132}$ which means in terms of the short notation, $d_{25} = -d_{14}$.

Now for the element d_{15}:

$$d'_{15} = d'_{131} = a_{1j}a_{3k}a_{1l}d_{jkl} = a_{12}a_{33}a_{12}d_{232} = d_{232} = d_{24} \quad (3.41)$$

Again Neumann principle yields $d_{15} = d_{24}$.

Similarly, we have

$$d'_{16} = d'_{112} = a_{1j}a_{1k}a_{2l}d_{jkl} = a_{12}a_{12}a_{21}d_{221} = -d_{221} = -d_{26} \quad (3.42)$$

Neumann principle then gives $d_{16} = -d_{26}$.

Similarly,

$$d'_{26} = d'_{212} = a_{2j}a_{1k}a_{2l}d_{jkl} = a_{21}a_{12}a_{21}d_{121} = d_{121} = d_{16} \quad (3.43)$$

Neumann principle ($d'_{26} = d_{26}$) then gives $d_{26} = d_{16}$. This coupled with the above result then means that these elements both must be equal to zero: $d_{16} = 0$, $d_{26} = 0$.

Further,

$$d'_{31} = d'_{311} = a_{3j}a_{1k}a_{1l}d_{jkl} = a_{33}a_{12}a_{12}d_{322} = d_{322} = d_{32} \quad (3.44)$$

which by virtue of the Neumann principle gives $d_{31} = d_{32}$.

The element d_{33} undergoes the transformation due to the 4-fold rotation as

$$d'_{33} = d'_{333} = a_{3j}a_{3k}a_{3l}d_{jkl} = a_{33}a_{33}a_{33}d_{333} = d_{333} = d_{33} \quad (3.45)$$

which does not change anything. The element d_{35} becomes under the above symmetry operation:

$$d'_{35} = d'_{331} = a_{3j}a_{3k}a_{1l}d_{jkl} = a_{33}a_{33}a_{12}d_{332} = d_{332} = d_{34} \quad (3.46)$$

By Neumann principle, this means that $d_{35} = d_{34}$. The element d_{34} under the same operation becomes

$$d'_{34} = d'_{332} = a_{3j}a_{3k}a_{2l}d_{jkl} = a_{33}a_{33}a_{21}d_{331} = -d_{331} = -d_{35} \quad (3.47)$$

Neumann principle then gives $d_{34} = -d_{35}$. Together with the just previous result, it transpires that $d_{35} = 0$ and $d_{34} = 0$.

Consider the elements d_{11}, d_{22}.

$$d'_{11} = d'_{111} = a_{1j}a_{1k}a_{1l}d_{jkl} = a_{12}a_{12}a_{12}d_{222} = d_{222} = d_{22} \tag{3.48}$$

$$d'_{22} = d'_{222} = a_{2j}a_{2k}a_{2l}d_{jkl} = a_{21}a_{21}a_{21}d_{111} = -d_{111} = -d_{11} \tag{3.49}$$

Neumann principle requires that $d'_{11} = d_{11}$ and $d'_{22} = d_{22}$. Accordingly the above results lead us to conclude that both relations are satisfied only if $d_{11} = d_{22} = 0$.

d_{13} transforms as

$$d'_{13} = d'_{133} = a_{1j}a_{3k}a_{3l}d_{jkl} = a_{12}a_{33}a_{33}d_{233} = d_{233} = d_{23} \tag{3.50}$$

d_{23} transforms as

$$d'_{23} = d'_{233} = a_{2j}a_{3k}a_{3l}d_{jkl} = a_{21}a_{33}a_{33}d_{133} = -d_{133} = -d_{13} \tag{3.51}$$

Both the above results in conjunction with the Neumann principle give us that $d_{13} = 0$ and $d_{23} = 0$. The transformation of d_{12} is given by

$$d'_{12} = d'_{122} = a_{1j}a_{2k}a_{2l}d_{jkl} = a_{12}a_{21}a_{21}d_{211} = d_{211} = d_{21} \tag{3.52}$$

d_{21} transforms as

$$d'_{21} = d'_{211} = a_{2j}a_{1k}a_{1l}d_{jkl} = a_{21}a_{12}a_{12}d_{331} = -d_{122} = -d_{12} \tag{3.53}$$

Neumann principle applied in the two cases above leads us to conclude that $d_{12} = 0$ and $d_{21} = 0$.

Collecting all the above conclusions then reduces the d matrix for the symmetry C_4 to

$$d = \begin{pmatrix} 0 & 0 & 0 & d_{14} & d_{15} & 0 \\ 0 & 0 & 0 & d_{15} & -d_{14} & 0 \\ d_{31} & d_{31} & d_{33} & 0 & 0 & 0 \end{pmatrix} \tag{3.54}$$

The C_4 point group belongs to one of seven tetragonal crystal classes. How does the d matrix look like for all the crystallographic point groups? We answer this question by giving the results.

For all centrosymmetric crystals (11 point groups), all d elements become zero. Inversion symmetry means that (xyz) transform to $(-X,-Y,-Z)$. The corresponding axes transformation matrix is

$$a = \begin{pmatrix} -1 & 0 & 0 \\ 0 & -1 & 0 \\ 0 & 0 & -1 \end{pmatrix} \tag{3.55}$$

Under such an inversion symmetry operation, the second order susceptibility tensor components become

$$\chi^{(2)'}_{ijk} = a_{il}a_{jm}a_{kn}\chi_{lmn} = a_{ii}a_{jj}a_{kk}\chi^{(2)}_{ijk} = (-1)(-1)(-1)\chi^{(2)}_{ijk} = -\chi^{(2)}_{ijk} \tag{3.56}$$

Neumann principle asserts that $\chi^{(2)'}_{ijk} = \chi^{(2)}_{ijk}$ and the above result of the inversion symmetry operation requires that $\chi^{(2)}_{ijk} = -\chi^{(2)}_{ijk}$ which can be valid only if the coefficients $\chi^{(2)}_{ijk}$ are all equal to zero. The eleven centrosymmetric point groups are: $C_i(S_2)$, C_{2h}, D_{2h}, C_{4h}, D_{4h}, $S_6(C_{3i})$, D_{3d}, C_{6h}, D_{6h}, T_h, O_h.

Triclinic system:

Group C_1: All the 18 d coefficients are non-vanishing. There is no crystallographic symmetry and therefore there is no reduction on that account.

Monoclinic system:

There are two point groups: C_2 and m.

C_2 group: The 2-fold rotation axis is conventionally chosen to lie along the X_2 (Y axis). In such a case, there are 8 non-vanishing independent components: d_{14}, d_{16}, d_{21}, d_{22}, d_{23}, d_{25}, d_{34}, d_{36}. All the other elements are zero. If the C_2 axis is placed along the X_3 axis, these become instead, d_{14}, d_{15}, d_{24}, d_{25}, d_{31}, d_{32}, d_{33}, d_{36}. All other elements are zero.

m group: If the mirror is perpendicular to the X_2 (Y) axis, then there are 10 non-vanishing elements: d_{11}, d_{12}, d_{13}, d_{15}, d_{24}, d_{26}, d_{31}, d_{32}, d_{33}, d_{35}, the other elements being equal to zero.

On the other hand, if the mirror plane is normal to the $X_3(Z)$ axis instead, the above non-vanishing elements become d_{11}, d_{12}, d_{13}, d_{16}, d_{21}, d_{22}, d_{23}, d_{26}, d_{34}, d_{35}, the other elements being equal to zero.

Orthorhombic system:

There are two point groups: C_{2h} and C_{2v}.

D_2 group: This class has only 3 non-zero d matrix elements: d_{14}, d_{25}, d_{36}, the other elements being all equal to zero.

C_{2v} group: There are 5 independent non-zero components for this group: d_{15}, d_{24}, d_{31}, d_{32}, d_{33}. All other components vanish by virtue of symmetry.

Tetragonal system:

There are five non-centrosymmetric groups in this system.

C_4 group: We have already illustrated the derivation of the non-vanishing elements of this group. There are only 4 independent elements here:$d_{14} = -d_{25}$, $d_{15} = d_{24}$, $d_{31} = d_{32}$ and d_{33}.

S_4 group: Here again there are 4 independent elements in the d matrix: $d_{14} = d_{25}$, $d_{15} = -d_{24}$, $d_{31} = -d_{32}$, and d_{36}.

D_4 group: Only 1 independent coefficient with non-vanishing elements: $d_{14} = -d_{25}$.

C_{4v} group: There are 3 independent d components: $d_{15} = d_{24}$, $d_{31} = d_{32}$ and d_{33}.

D_{2d} group: Only 2 independent coefficients exist: $d_{14} = d_{25}$, d_{36}.

Rhombohedral (trigonal) system:

C_3 group: There are 6 independent d elements with internal relations as follows. $d_{11} = -d_{12} = d_{26}$, $d_{14} = -d_{25}$, $d_{15} = d_{24}$, $d_{16} = d_{21} = -d_{22}$, $d_{31} = d_{32}$, d_{33}.

D_3 group: Only 2 coefficients are independent: $d_{11} = -d_{12} = -d_{26}$, $d_{14} = -d_{25}$.

C_{3v} group: The reflection plane is taken to be perpendicular to the X_1(X axis). There exist 4 independent components, as given by $d_{15} = d_{24}$, $d_{16} = d_{21} = -d_{22}$, $d_{31} = d_{32}$, d_{33}.

Hexagonal system:

C_6 group: This group has 4 independent components, as given by $d_{14} = -d_{25}$, $d_{15} = d_{24}$, $d_{31} = d_{32}$, d_{33}.

C_{6v} group: Only 3 independent elements exist in this group, as given by $d_{15} = d_{24}$, $d_{31} = d_{32}$, d_{33}.

D_6 group: Only 1 independent d component as given by $d_{14} = -d_{25}$.

C_{3h} group: 2 independent components as $d_{11} = -d_{12} = d_{26}$, $d_{16} = d_{21} = -d_{22}$.

D_{3h} group: with the mirror plane perpendicular to the X_1 axis. Only 1 independent d element exists: $d_{16} = d_{21} = -d_{22}$.

Cubic system:

O group: No non-vanishing d coefficients possible by virtue of the symmetry

T group and T_d group: Only one independent d matrix element exists with the relations $d_{14} = d_{25} = d_{36}$.

3.2.4 Kleinman Symmetry

Kleinman [1962] showed that there exists an additional simplification of the d matrix if the mechanism is purely electronic in origin. Writing the third order term in energy $U^{(3)}$ as a function of ionic displacement ξ and electric field magnitude E

$$U^{(3)}(\xi) = -\frac{1}{3}\sum_{ijk} d_{ijk}E_iE_jE_k \tag{3.57}$$

and the corresponding non-linear polarization $P^{(3)}$ as

$$P_k^{(3)} = \sum_{ij} d_{ijk}E_iE_j \tag{3.58}$$

he argued that since there is no physical distinction between terms obtained by rearranging the field components in any order, only 10 independent coefficients exist in general for the d matrix as given below:

$$d = \begin{pmatrix} d_{11} & d_{12} & d_{13} & d_{14} & d_{15} & d_{16} \\ d_{16} & d_{22} & d_{23} & d_{24} & d_{14} & d_{12} \\ d_{15} & d_{24} & d_{33} & d_{23} & d_{13} & d_{14} \end{pmatrix} \tag{3.59}$$

The column matrix on which this matrix operates has the elements E_1^2, E_2^2, E_3^2, $2E_2E_3$, $2E_3E_1$, $2E_1E_2$. Note that besides the elements d_{11}, d_{22}, d_{33}, the only other independent elements are d_{12}, d_{13}, d_{14}, d_{15}, d_{16}, d_{23}, d_{24}. It has been suggested that the above relations are valid if the mixing electric field frequencies are well above the ionic resonance frequencies and far from the electronic resonances. Thus it is essential for the Kleinman relations to hold good that the ionic contribution to the nonlinearity be negligible and electronic absorption is absent at the operating frequencies.

If we combine the Kleinman symmetry with what has been deduced above from Neumann criterion, further simplification results. For example, for the crystal Rochelle salt which belongs to the orthorhombic group D_2, the three independent d elements become equal, since $d_{14} = d_{25} = d_{36}$. In the case of crystal KDP (potassium dihydrogen phosphate), which belongs to the class D_{2d}, only one independent coefficient $d_{14} = d_{36}$ remains.

3.2.5 Symmetry of Third Order Susceptibility

The effect of crystal symmetry in reducing the number of independent components of the susceptibility tensor can be obtained in a

manner similar to what has been illustrated above for the linear and second order susceptibility. Therefore, without going through all the detailed calculations, we illustrate with a few cases and finally state the final situation for cubic crystals and isotropic materials.

Cubic system:

The common (minimum) symmetry of all cubic point groups is the presence of 3 - fold rotation axes along the body diagonals of the cubic unit cell and 2 -fold rotational symmetry axes parallel to face diagonals. We first see the effect of the triad axes on the susceptibility components χ_{1111}; χ_{2222}, χ_{3333}. Using Eq.3.23 for the transformation and Eq.3.25 for the a matrix,

$$\chi'_{1111} = a_{1i}a_{1j}a_{1k}a_{1l}\chi_{ijkl} = a_{12}a_{12}a_{12}a_{12}\chi_{2222} = \chi_{2222} \tag{3.60}$$

because $a_{12} = 1$ (Eq.3.25). Since Neumann principle requires the component to be unchanged, we get $\chi_{1111} = \chi_{2222}$. For the component χ_{2222},

$$\chi'_{2222} = a_{2i}a_{2j}a_{2k}a_{2l}\chi_{ijkl} = a_{23}a_{23}a_{23}a_{23}\chi_{3333} = \chi_{3333} \tag{3.61}$$

because $a_{23} = 1$ (Eq.3.25). And similarly,

$$\chi'_{3333} = a_{3i}a_{3j}a_{3k}a_{3l}\chi_{ijkl} = a_{31}a_{31}a_{31}a_{31}\chi_{1111} = \chi_{1111} \tag{3.62}$$

because $a_{31} = 1$. Neumann principle coupled with the above three equations thereby lead to $\chi_{1111} = \chi_{2222} = \chi_{3333}$.

The component χ_{1122} transforms as

$$\chi'_{1122} = a_{1i}a_{1j}a_{2k}a_{2l}\chi_{ijkl} = a_{12}a_{12}a_{23}a_{23}\chi_{2233} = \chi_{2233} \tag{3.63}$$

in which we have used the data of the matrix of Eq.3.25.

Similarly, the component χ_{2233} and χ_{3311} transform under this symmetry operation according to

$$\chi'_{2233} = a_{2i}a_{2j}a_{3k}a_{3l}\chi_{ijkl} = a_{23}a_{23}a_{31}a_{31}\chi_{3311} = \chi_{3311} \tag{3.64}$$

$$\chi'_{3311} = a_{3i}a_{3j}a_{1k}a_{1l}\chi_{ijkl} = a_{31}a_{31}a_{12}a_{12}\chi_{1122} = \chi_{1122} \tag{3.65}$$

Along with the Neumann principle, all these equations give us the condition that $\chi_{1122} = \chi_{2233} = \chi_{3311}$. One can verify the other results quoted below.

Point groups T and T_d

21 non-vanishing with 7 independent coefficients exist. These are given by

$\chi_{1111} = \chi_{2222} = \chi_{3333}$
$\chi_{2233} = \chi_{3311} = \chi_{1122}$
$\chi_{3322} = \chi_{1133} = \chi_{2211}$
$\chi_{2323} = \chi_{3131} = \chi_{1212}$
$\chi_{3232} = \chi_{1313} = \chi_{2121}$
$\chi_{2332} = \chi_{3113} = \chi_{1223}$
$\chi_{3223} = \chi_{1331} = \chi_{2112}$

Point groups O, T_d, O_h

There are 21 non-vanishing coefficients with 4 of them being independent. These are:

$\chi_{1111} = \chi_{2222} = \chi_{3333}$
$\chi_{2233} = \chi_{3322} = \chi_{3311} = \chi_{1133} = \chi_{1122} = \chi_{2211}$
$\chi_{2323} = \chi_{3232} = \chi_{3131} = \chi_{1313} = \chi_{1212} = \chi_{2121}$
$\chi_{2332} = \chi_{3223} = \chi_{3113} = \chi_{1331} = \chi_{1221} = \chi_{2112}$

In isotropic media such as polycrystals and homogeneous liquids or gases, there is a further simplification. Only three independent coefficients but 21 non-zero components exist for this tensor. These are given by the same set of components given above for the above cubic groups but with the additional restriction given by

$\chi_{1111} = \chi_{1122} + \chi_{1212} + \chi_{1221}$.

3.3 The Dielectric Permittivity Tensor

We introduce here the linear dielectric permittivity tensor and the refractive index ellipsoid for use in a latter chapter. The electric displacement vector $\vec{D}$ of a dielectric having the polarization $\vec{P}$ under an electric field $\vec{E}$ is given by

$$\vec{D} = \epsilon_0 \vec{E} + \vec{P} \tag{3.66}$$

and

$$\vec{D} = \epsilon \vec{E} = \epsilon_r \epsilon_0 \vec{E} \tag{3.67}$$

where ϵ is the permittivity of the material and ϵ_r the relative permittivity (same as the dielectric constant). Since we write the polarization as

$$\vec{P} = \epsilon_0 \chi \vec{E} \tag{3.68}$$

we have

$$\epsilon = \epsilon_0 (1 + \chi) \tag{3.69}$$

$$\epsilon_r = (1 + \chi) \tag{3.70}$$

where ϵ_r and χ are dimensionless properties of the material. The tensor nature of the permittivity is evident when we write the displacement and the electric field in terms of their components in an arbitrary set of Cartesian axes X_1, X_2, X_3:

$$D_1 = \epsilon_{11}E_1 + \epsilon_{12}E_2 + \epsilon_{13}E_3 \tag{3.71}$$

$$D_2 = \epsilon_{21}E_1 + \epsilon_{22}E_2 + \epsilon_{23}E_3 \tag{3.72}$$

$$D_3 = \epsilon_{31}E_1 + \epsilon_{32}E_2 + \epsilon_{33}E_3 \tag{3.73}$$

or in matrix form

$$\begin{pmatrix} D_1 \\ D_2 \\ D_3 \end{pmatrix} = \begin{pmatrix} \epsilon_{11} & \epsilon_{12} & \epsilon_{13} \\ \epsilon_{21} & \epsilon_{212} & \epsilon_{23} \\ \epsilon_{31} & \epsilon_{32} & \epsilon_{33} \end{pmatrix} \begin{pmatrix} E_1 \\ E_2 \\ E_3 \end{pmatrix} \tag{3.74}$$

which may expressed in short form for the components

$$D_i = \epsilon_{ij}E_j \tag{3.75}$$

with the understanding that the sum is over the repeated index $(j = 1, 2, 3)$.

Energy considerations lead us to discover that the ϵ matrix is symmetric with $\epsilon_{ij} = \epsilon_{ji}$, as shown below.

The energy density stored in the electric field in the medium may be written as

$$u_E = \frac{1}{2}\vec{E} \cdot \vec{D} \tag{3.76}$$

or

$$u_E = \frac{1}{2}(E_1D_1 + E_2D_2 + E_3D_3) \tag{3.77}$$

In view of the relations $D_i = \epsilon_{ij}E_j$, the above equation becomes

$$u_E = \frac{1}{2}E_i\epsilon_{ij}E_j \tag{3.78}$$

wherein, the summation is over both the indices (repeated) i and j. We now take the time derivative of the energy density:

$$\frac{du_E}{dt} = \frac{1}{2}\left[\frac{dE_i}{dt}\epsilon_{ij}E_j + E_i\epsilon_{ij}\frac{dE_j}{dt}\right] \tag{3.79}$$

or

$$\frac{du_E}{dt} = \frac{1}{2}\epsilon_{ij}\left[\frac{dE_i}{dt}E_j + E_i\frac{dE_j}{dt}\right] \tag{3.80}$$

The terms $\frac{1}{2}\epsilon_{12}\left[\frac{dE_1}{dt}E_2 + E_1\frac{dE_2}{dt}\right]$ and $\frac{1}{2}\epsilon_{21}\left[\frac{dE_2}{dt}E_1 + E_2\frac{dE_1}{dt}\right]$ are obviously equivalent. So, we conclude that $\epsilon_{12} = \epsilon_{21}$. Similarly, $\epsilon_{23} = \epsilon_{32}$ and $\epsilon_{31} = \epsilon_{13}$. This makes the permittivity matrix symmetric with only six independent components in general: the three diagonal components $\epsilon_{11}, \epsilon_{22}, \epsilon_{33}$ and the three non-diagonal components $\epsilon_{12}\,(=\epsilon_{21})$, $\epsilon_{23}\,(=\epsilon_{32})$ and $\epsilon_{31}\,(=\epsilon_{13})$. Now the stored energy density may be written as

$$u_E = \frac{1}{2}\left[\epsilon_{11}E_1^2 + \epsilon_{22}E_2^2 + \epsilon_{33}E_3^2 + 2\epsilon_{12}E_1E_2 + 2\epsilon_{23}E_2E_3 + 2\epsilon_{31}E_3E_1\right] \tag{3.81}$$

The ϵ matrix can however be diagonalized by means of a principal axes transformation. That is , there exist a set of new axes X_1', X_2', X_3' in which the permittivity matrix is diagonal:

$$\epsilon' = \begin{pmatrix} \epsilon_{11}' & 0 & 0 \\ 0 & \epsilon_{22}' & 0 \\ 0 & 0 & \epsilon_{33}' \end{pmatrix} \tag{3.82}$$

And the energy density of the electric field becomes

$$u_E = \frac{1}{2}\left\{\epsilon_{11}'\left(E_1'\right)^2 + \epsilon_{22}'\left(E_2'\right)^2 + \epsilon_{33}'\left(E_3'\right)^2\right\} \tag{3.83}$$

The displacement matrix is given by

$$\begin{pmatrix} D_1' \\ D_2' \\ D_3' \end{pmatrix} = \begin{pmatrix} \epsilon_{11}' & 0 & 0 \\ 0 & \epsilon_{22}' & 0 \\ 0 & 0 & \epsilon_{33}' \end{pmatrix} \begin{pmatrix} E_1' \\ E_2' \\ E_3' \end{pmatrix} \tag{3.84}$$

Alternatively,

$$u_E = \frac{1}{2}\left(\frac{\left(D_1'\right)^2}{\epsilon_{11}'} + \frac{\left(D_2'\right)^2}{\epsilon_{22}'} + \frac{\left(D_3'\right)^2}{\epsilon_{33}'}\right) \tag{3.85}$$

For convenience in use, we rename all the components as measured from the principal axes as follows: $\epsilon_{11}' = \epsilon_x'$, $\epsilon_{22}' = \epsilon_y'$ and $\epsilon_{33}' = \epsilon_z'$. Also $D_1' = D_x$, $D_2' = D_y$ and $D_3' = D_z$. With this simplified notation, remembering that we are now working in the new principal axes frame in which the permittivity tensor is diagonal, we have for the energy density

$$u_E = \frac{1}{2}\left(\frac{D_x^2}{\epsilon_x'} + \frac{D_y^2}{\epsilon_y'} + \frac{D_z^2}{\epsilon_z'}\right) \tag{3.86}$$

3.4 The Refractive Index Ellipsoid

Consider a travelling plane harmonic wave of angular frequency ω with the wave vector $\vec{k}$ and the electric field having the magnitude given by

$$E = E_0 e^{i\left(\omega t - \vec{k}\cdot\vec{r}\right)} \tag{3.87}$$

The phase velocity of this wave is obviously equal to

$$\vec{v}_p = \frac{c}{n}\hat{k} \tag{3.88}$$

where n is the refractive index and $\hat{k}$ is the unit vector along the direction of propagation. Also we note that

$$\hat{k} = \frac{c}{\omega n}\vec{k} \tag{3.89}$$

since $\frac{\omega}{|\vec{k}|} = v_p = \frac{c}{n}$.

In the equation for the energy density given above, we now put $\epsilon_x' = \epsilon_x\epsilon_0$, $\epsilon_y' = \epsilon_y\epsilon_0$, and $\epsilon_z' = \epsilon_z\epsilon_0$, where ϵ_x, ϵ_y and ϵ_z are the principal relative dielectric constants (relative primitivities). It is shown in standard electromagnetic theory, that $\epsilon_i' = \left(n_i'\right)^2$ $(i =$

$1, 2, 3$), n_i being the principal refractive indices. The energy density equation now is written as

$$u_E \epsilon_0 = \frac{1}{2}\left(\frac{D_x^2}{\epsilon_x} + \frac{D_y^2}{\epsilon_y} + \frac{D_z^2}{\epsilon_z}\right) \tag{3.90}$$

Writing

$$\frac{\vec{D}}{\sqrt{2u_E\epsilon_0}} = \vec{r} \tag{3.91}$$

we have

$$D_x = \sqrt{2u_E\epsilon_0}\, x \tag{3.92}$$
$$D_y = \sqrt{2u_E\epsilon_0}\, y \tag{3.93}$$
$$D_z = \sqrt{2u_E\epsilon_0}\, z \tag{3.94}$$

leading to

$$1 = \frac{x^2}{\epsilon_x} + \frac{y^2}{\epsilon_y} + \frac{z^2}{\epsilon_z} \tag{3.95}$$

Thus the form of the refractive index ellipsoid or the *optical indicatrix* is defined by

$$\frac{x^2}{n_x^2} + \frac{y^2}{n_y^2} + \frac{z^2}{n_z^2} = 1 \tag{3.96}$$

The axes of this ellipsoid are n_x, n_y, n_z. We can use the index ellipsoid to find the *ordinary* and *extraordinary* refractive indices of a crystal in an given direction of propagation, as follows. First find the plane normal to the wave vector $\vec{k}$. The intersection of this plane with the ellipsoid is an ellipse. The semi-major and the semi-minor axes of this ellipse represent the two refractive indices n_1 and n_2.

Uni-axial crystals belong to those crystal classes having a unique rotational symmetry axis. Choosing this symmetry axis (also called the optic axis) as the Z axis, the refractive index is n_e for displacement D in this direction (*extraordinary* ray) and n_o (*ordinary* refractive index) for any direction of $\vec{D}$ normal to the symmetry axis. The index ellipsoid for uni-axial crystals thus becomes

$$\frac{x^2}{n_O^2} + \frac{y^2}{n_O^2} + \frac{z^2}{n_e^2} = 1 \tag{3.97}$$

This represents the index ellipsoid is an ellipsoid of revolution for the extraordinary ray and a sphere for the ordinary ray. Given any direction of propagation $\widehat{k}$, the value of $n_e(\theta)$ can be obtained by the intersection of $\widehat{k}$ with the surface ellipsoid. For the ordinary ray, however, n_O is a constant independent of direction. For propagation of the electromagnetic wave in the direction $\widehat{k}$ that makes an angle θ with the optic axis, the refractive index can then be expressed as a function of this angle θ by the equation

$$\frac{1}{n_e^2(\theta)} = \frac{\cos^2\theta}{n_O^2} + \frac{\sin^2\theta}{n_e^2} \tag{3.98}$$

This equation results from the geometry of the ellipse. At $\theta = 0^0$, for a wave travelling along the optic axis, $n_e(\theta) = n_O$ and at $\theta = 90^0$, $n_e(\theta) = n_e(90^0) = n_{e,\max}$. Please note that here The surface representing the value of $n_e(\theta)$ and $n_O(\theta)$ is an ellipse described by the equation given above. For a positive uni-axial crystal (defined by $n_e \geq n_O$), the ellipse is sketched in Fig.2.1. In the case of a negative uni-axial crystal, the ellipsoid of the *extraordinary* ray index is contained within the sphere of the *ordinary* ray index.

3.5 Explorations

1. 1. How would the tensor element $\chi^{(2)}_{ijk}$ transform under the coordinate transformation $x \dashrightarrow -x$, $y \rightarrow -y$ and $z \dashrightarrow -z$? What is the implication of this for the observation of second harmonic generation in crystals with inversion symmetry? What does this imply for the availability of suitable materials for second order processes? How about the susceptibility of other even orders?

2. Look for examples of physical properties other than optical properties that would not be exhibited by crystals with inversion symmetry and try to give a physical explanation in each case.

3. a) Give examples of quantum mechanical operators which are (i) real and (ii) imaginary.

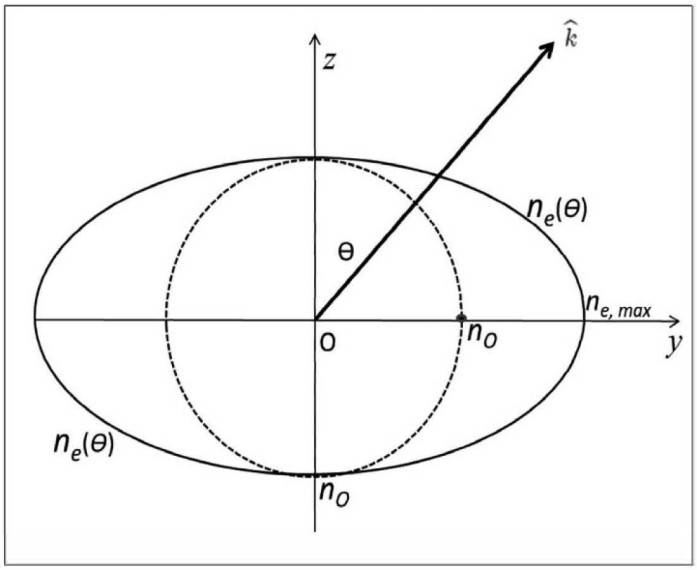


Figure 3.2: Index ellispsoid for a positive uniaxial crystal

b) How do they change under time reversal?

c) What do you conclude from this?

d) What is the relevance of this in the context of nonlinear optics?

4. Consider the process in which three input waves of frequencies ω_1 , $-\omega_2$ and ω_3 , mix together to give ω_σ , their algebraic sum. Illustrate how (a) intrinsic permutation symmetry and (b) overall permutation symmetry (assuming transparency at all frequencies involved) lead to a reduction in the number of independent components.

5. How many quantities do you have to measure in an experiment to measure the linear optical refractive index of a triclinic crystal? How will this number reduced in the case of (a) A crystal of NaCl and (b) water?

6. Arrive at the number of independent components of third order nonlinear optical susceptibility for a liquid medium. What about the fourth order susceptibility? (*Hint*: finding the answer is a lot easier in this case !)

7. How is an *ellipsoid-of-revolution* different from any other ellipsoid geometrically? Sketch the index ellipsoid for a negative uniaxial crystal. Show clearly the geometry of the figures corresponding to the propagation of ordinary and extra ordinary rays along different directions.

Chapter 4

Calculation of Non-linear Susceptibilities

"The fundamental laws necessary for the mathematical treatment of a large part of physics are thus completely known, and the difficulty lies only in the fact that application of these laws leads to equations that are too complex to be solved"

Paul Adrian Dirac

But then, one has to do it anyway.

Learning Objectives

- Identification of the quantum mechanical origin of nonlinear optical susceptibilities.
- Formulation of the equation of motion using the parity operator.
- Construction of density matrices corresponding to the different orders of nonlinearity.
- Derivation of expressions for nonlinear susceptibilities.
- Employment of the density matrix formulation to characterize optical nonlinearity of a color center system.

4.1 Introduction

In this chapter, we discuss how to evaluate non-linear optical susceptibilities of various orders from the atomic properties using quantum mechanical techniques. Toward this purpose, specifically we introduce the density operator (matrix) method of treating statistical ensembles of atoms quantum mechanically. We refer the reader to the books by Bloembergen [1996] and Marcuse [1970] for an excellent treatment of this subject, based on which we develop the subject here.

4.1.1 Physical Quantities in Quantum Physics

In classical physics, the physical behavior of a particle is completely determined once we know its initial state and all the forces acting on it, by solving the Newton's laws of motion or their variants - the Lagrange equations or the Hamilton's equations of motion. On the other hand, quantum physics takes a probabilistic view of the fundamental measurement process and allows us only to find the probable values ('*the expectation values*') of the physical quantities associated with a particle for comparison with the experimentally measured quantities. The quantum dynamical equations of motion involve operators corresponding to each physical variable. For example, the operator for the position vector $\overrightarrow{r}$ is $\overrightarrow{r}$ itself. The linear momentum components are represented by the operators: $-i\hbar\frac{\partial}{\partial x}$ for p_x, $-i\hbar\frac{\partial}{\partial y}$ for p_y, $-i\hbar\frac{\partial}{\partial z}$ for p_z. Here $\hbar = \frac{h}{2\pi}$, h being Planck's constant. The potential energy operator is $V(x)$ for $V(x)$, etc. The expectation value of any physical quantity associated with a particle in a state described by the wavefunction ψ is given by

$$\langle R \rangle = \int \psi^* \widetilde{R} \psi d\tau \tag{4.1}$$

$$\langle R \rangle = \left\langle \psi | \widetilde{R} | \psi \right\rangle \tag{4.2}$$

where $\widetilde{R}$ is the operator that represents the physical quantity in question. The integration is to be carried out over the full domain of space τ including any spin variables wherever it is appropriate. The alternative equation follows the Dirac bracket notation.

4.1.2 The Projection Operator

Instead of using the wavefunction ψ itself, we can find the expectation values $\langle R \rangle$ by an alternative route. Consider an arbitrary wavefunction θ. The contribution of ψ to the expansion of θ is defined by

$$\widetilde{P}(\psi)\,\theta = \psi \int d\tau \psi^* \theta \tag{4.3}$$

$$\widetilde{P}\theta = |\psi\rangle\langle\psi|\theta\rangle \tag{4.4}$$

where $\widetilde{P}(\psi)$ is the projection operator.

Now let us consider a set of wavefunctions $\{u_i\}$. This set is said to be orthonormal if

$$\int d\tau u_i^* u_j = \delta_{ij} \tag{4.5}$$

The set is said to be complete if we can expand any arbitrary wavefunction ψ in terms of $\{u_i\}$:

$$\psi = \sum_i a_i u_i \tag{4.6}$$

$$|\psi\rangle = \sum_i |u_i\rangle\psi\,\langle u_i|\psi\rangle \tag{4.7}$$

where the expansion coefficients a_i are given by

$$a_i = \int d\tau u_i^* \psi \tag{4.8}$$

$$a_i = \langle u_i|\psi\rangle \tag{4.9}$$

The matrix elements of an operator R in the representation $\{u_i\}$ are given by

$$R_{ij} = \int d\tau u_i^* \widetilde{R} u_j \tag{4.10}$$

$$R_{ij} = \left\langle i|\widetilde{R}|j\right\rangle \tag{4.11}$$

Accordingly the matrix elements of the projection operator are given by

$$P_{ji} = \int d\tau u_j^* \widetilde{P}(\psi) u_i \tag{4.12}$$

$$P_{ji} = \left\langle j|\widetilde{P}|i\right\rangle \tag{4.13}$$

Substituting for the projection operator and using the relations for the coefficients a_i, the above equation for the matrix elements simplifies as follows:

$$a_i = \int d\tau u_i^* \psi \tag{4.14}$$

$$P_{ji} = \int d\tau u_j^* \psi \int d\tau \psi^* u_i = a_j a_i^* \tag{4.15}$$

The expectation value of an operator can be now written alternatively, by making use of the projection operator.

$$\left\langle \widetilde{R} \right\rangle = \int d\tau \psi^* \widetilde{R} \psi = \int d\tau \sum_i a_i^* u_i^* \widetilde{R} \sum_j a_j u_j \tag{4.16}$$

$$= \sum_i \sum_j a_i^* a_j R_{ij} \tag{4.17}$$

wherein we have made use of the relations

$$\psi = \sum_i a_i u_i \tag{4.18}$$

$$\int d\tau u_i^* \widetilde{R} u_j = R_{ij} \tag{4.19}$$

We have already shown in equation 4.15 that $P_{ji} = a_j a_i^*$. Therefore, we re-write the expectation value of $\widetilde{R}$ as

$$\left\langle \widetilde{R} \right\rangle = \sum_i \sum_j P(\psi)_{ji} R_{ij} = \sum_j \left\{ \widetilde{P}(\psi) \widetilde{R} \right\}_{jj} \tag{4.20}$$

or we have the good result that

$$\left\langle \widetilde{R} \right\rangle = Tr \left\{ \widetilde{P}(\psi) \widetilde{R} \right\} \tag{4.21}$$

which is independent of the representation.

4.2 The Equation of Motion

Starting with the time-dependent Schroedinger wave equation

$$i\hbar\frac{d\psi}{dt} = \widetilde{H}\psi \tag{4.22}$$

we are going to develop an equation of motion for the projection operator. Consider the equation defining the projection operator

$$\widetilde{P}(\psi)\,\theta = \psi\int d\tau\psi^*\theta \tag{4.23}$$

where we take θ to be independent of time t.

Differentiating the above equation with respect to time t,

$$\frac{d}{dt}\widetilde{P}(\psi)\,\theta = \frac{d\psi}{dt}\int d\tau\psi^*\theta + \psi\int d\tau\frac{d\psi^*}{dt}\theta \tag{4.24}$$

Multiplying throughout with $i\hbar$ gives

$$i\hbar\frac{d}{dt}\widetilde{P}(\psi)\,\theta = i\hbar\frac{d\psi}{dt}\int d\tau\psi^*\theta + i\hbar\psi\int d\tau\frac{d\psi^*}{dt}\theta \tag{4.25}$$

The time-dependent Schroedinger equation 4.22 and its complex conjugate are given by

$$i\hbar\frac{d\psi}{dt} = \widetilde{H}\psi \tag{4.26}$$

$$-i\hbar\frac{d\psi^*}{dt} = \left(\widetilde{H}\psi\right)^* \tag{4.27}$$

Then we get

$$i\hbar\frac{d}{dt}\widetilde{P}(\psi)\,\theta = \widetilde{H}\psi\int d\tau\psi^*\theta - \psi\int d\tau\left(\widetilde{H}\psi\right)^*\theta \tag{4.28}$$

The first term on the right hand side becomes $\widetilde{H}P(\psi)\,\theta$ following from the equation 4.23. The second term on the right is

$$-\psi\int d\tau\left(\widetilde{H}\psi\right)^*\theta = -\psi\left(\int d\tau\theta^*\widetilde{H}\psi\right)^* \tag{4.29}$$

$$= -\psi\int d\tau\psi^*\widetilde{H}\theta = \widetilde{P}(\psi)\,\widetilde{H}\theta \tag{4.30}$$

Because the Hamiltonian operator like all operators representing real physical variables, is Hermitian, obeys the property

$$\left(\int d\tau \psi^* \widetilde{R} \phi\right)^* = \int d\tau \phi^* \widetilde{R} \psi \tag{4.31}$$

Finally, thus we have the result for the equation of motion of the projection operator:

$$i\hbar \frac{d}{dt} \widetilde{P}(\psi)\,\theta = \widetilde{H}\widetilde{P}(\psi)\,\theta - \widetilde{P}(\psi)\,\widetilde{H}\theta \tag{4.32}$$

Since the function θ is arbitrary, we may now write equation of motion for the operator itself:

$$i\hbar \frac{d}{dt} \widetilde{P}(\psi) = \left[\widetilde{H}, \widetilde{P}(\psi)\right] \tag{4.33}$$

4.3 Ensembles of Particles

The expectation values and the equation of motion we have been considering so far refer to the quantum mechanical mean of the physical quantities associated with a single particle. However, when we deal with an ensemble of particles, we must introduce the necessary modifications to take care of the fact that all the particles may not be in the same quantum state. The particles may be distributed amongst the various available quantum states described corresponding wavefunction. The probabilities p_n of occupation of the states ψ_n are determined by the appropriate statistical distribution law (Fermi-Dirac or Bose-Einstein) valid for the system of particles under study.

We therefore rewrite the expectation value of the operator $\widetilde{R}$ by multiplying each trace with the probability factor and summing over all the states:

$$\left\langle \widetilde{R} \right\rangle = \sum_n p_n Tr\left[\widetilde{P}(\psi_n)\,\widetilde{R}\right] \tag{4.34}$$

The density operator $\widetilde{\rho}$ is now introduced by

$$\widetilde{\rho} = \sum_n p_n \widetilde{P}(\psi_n) \tag{4.35}$$

The ensemble expectation value of the operator $\widetilde{R}$ now becomes

$$\left\langle \widetilde{R} \right\rangle = Tr\left(\widetilde{\rho}\,\widetilde{R}\right) \tag{4.36}$$

which follows from the rules of linear combination of matrix traces.

Assuming that the occupation probabilities p_n of the states ψ_n are fixed (for example by prescribing the temperature and the energy eigen values) and do not change with time, we find the equation of motion of the density operator. Differentiating the equation 4.35 with respect to time, and multiplying the equation with $i\hbar$, we get

$$i\hbar \frac{d\widetilde{\rho}}{dt} = \sum_n p_n \left[\widetilde{H}, \widetilde{P}(\psi_n)\right] \tag{4.37}$$

The equation 4.33 is used to obtain the above result. This can be alternatively written as

$$i\hbar \frac{d\widetilde{\rho}}{dt} = \left[\widetilde{H}, \sum_n p_n \widetilde{P}\psi_n\right] \tag{4.38}$$

$$i\hbar \frac{d\widetilde{\rho}}{dt} = \left[\widetilde{H}, \widetilde{\rho}\right] \tag{4.39}$$

which follows from the definition of $\widetilde{\rho}$ given by equation 4.35.

4.4 Time-dependent Perturbation

When an atom is placed in an electromagnetic field, an electric polarization is induced and we wish to calculate this polarization using quantum mechanical perturbation techniques. Assuming the perturbation is small, we develop expressions for the polarization which are non-linear in the electric field $\vec{E}$ of the electromagnetic wave. Specifically, we wish to find the polarizations which are second order (quadratic) in $\vec{E}$, third order (cubic) in $\vec{E}$ and so on.

While treating the atomic response quantum physically, we adopt the usually convenient approach of treating the field classically.

Suppose the atomic system initially ($t = 0$) has the density matrix given by $\widetilde{\rho}_0$ and the Hamiltonian is given by $\widetilde{H}_0$. It is subject to a time-dependent perturbation $\widetilde{H}_p(t)$. Note that the electromagnetic field is a time-varying quantity and sinusoidal if it is monochromatic. The perturbed Hamiltonian my be written as

$$\widetilde{H} = \widetilde{H}_0 + \widetilde{H}_p(t) \tag{4.40}$$

Substituting this in the equation 4.39, we have

$$i\hbar \frac{d\widetilde{\rho}}{dt} = \left[\widetilde{H}_0, \widetilde{\rho}\right] + \left[\widetilde{H}_p, \widetilde{\rho}\right] \tag{4.41}$$

In order to solve this equation, we write the density matrix in a perturbation series, the terms of which are in increasing powers of the field:

$$\widetilde{\rho} = \widetilde{\rho}_0 + \widetilde{\rho}^{(1)}(t) + \widetilde{\rho}^{(2)}(t) + \widetilde{\rho}^{(3)}(t) + ... + \widetilde{\rho}^{(n)}(t) \tag{4.42}$$

In this series, thus, ρ_0 is the initial constant density term; $\widetilde{\rho}^{(1)}(t)$ is linear in the perturbation $\widetilde{H}_p$; $\widetilde{\rho}^{(2)}(t)$ is quadratic in $\widetilde{H}_p$; $\widetilde{\rho}^{(3)}(t)$ is cubic in $\widetilde{H}_p$ and so on. The initial state may now be specified by

$$t = 0, \widetilde{\rho}^{(n)} = 0, n = 1, 2, 3, .. \tag{4.43}$$

Now let us substitute this series expansion in the equation of motion of the density operator, viz., the equation 4.41 and equating therms of the same order in H_p on either side of the equation, we get

$$i\hbar \frac{d\widetilde{\rho}_0}{dt} = \left[\widetilde{H}_0, \widetilde{\rho}_0\right] \tag{4.44}$$

$$i\hbar \frac{d\widetilde{\rho}^{(1)}}{dt} = \left[\widetilde{H}_0, \widetilde{\rho}^{(1)}\right] + \left[\widetilde{H}_p, \widetilde{\rho}_0\right] \tag{4.45}$$

$$i\hbar\frac{d\widetilde{\rho}^{(2)}}{dt} = \left[\widetilde{H}_0, \widetilde{\rho}^{(2)}\right] + \left[\widetilde{H}_p, \widetilde{\rho}^{(1)}\right] \tag{4.46}$$

and so on. For the n^{th} order density matrix,

$$i\hbar\frac{d\widetilde{\rho}}{dt} = \left[\widetilde{H}_0, \widetilde{\rho}^{(n)}\right] + \left[\widetilde{H}_p, \widetilde{\rho}^{(n-1)}\right] \tag{4.47}$$

4.5 Dipolar Interaction

The perturbation Hamiltonian $\widetilde{H}_p$ can now be specifically identified. If the induced electric dipole moment is $\overrightarrow{p}$, the potential energy U in the electric field $\overrightarrow{E}$ is $U = -\overrightarrow{p}.\overrightarrow{E}$ and the perturbation Hamiltonian $\widetilde{H}_p$ is the corresponding operator equal to U itself.

$$\widetilde{H}_p = -\overrightarrow{p}.\overrightarrow{E} \tag{4.48}$$

The equation of motion the equation (4.41) of the density operator thus becomes

$$i\hbar\frac{d\widetilde{\rho}}{dt} = \left[\widetilde{H}_0, \widetilde{\rho}\right] + \left[-\overrightarrow{p}.\overrightarrow{E}, \widetilde{\rho}\right] \tag{4.49}$$

Expanding the commutator bracket, the $(ij)^{th}$ element of the density matrix is then given by

$$i\hbar\frac{d\rho_{ij}}{dt} = [H_0, \widetilde{\rho}]_{ij} + \left[\widetilde{H}_p, \widetilde{\rho}\right]_{ij} \tag{4.50}$$

$$i\hbar\frac{d\widetilde{\rho}_{ij}}{dt} = \left(\widetilde{H}_0\widetilde{\rho}\right)_{ij} - \left(\widetilde{\rho}\widetilde{H}_0\right)_{ij} + (\widetilde{\rho}p - p\widetilde{\rho})_{ij}\, E \tag{4.51}$$

The dot product of the dipole moment and electric field vectors is replaced by pE in the above. This is valid when the dipole is induced by the field. For example if $\overrightarrow{E} = E\widehat{k}$, $\overrightarrow{p} = ez\widehat{k}$ and $\widetilde{H}_p = -ezE$. Later on , we may well use the dot product in place of pE.

The unperturbed Hamiltonian $\widetilde{H}_0$ is diagonal in the energy representation, *i.e.* $\widetilde{H}_{0ik} = \widetilde{H}_{0ii}$. Accordingly the first two terms in the above equation 4.51 become

$$\left(\widetilde{H}_0\widetilde{\rho}\right)_{ij} = \sum_k H_{0ik}\rho_{kj} = H_{0ii}\rho_{ij} \tag{4.52}$$

$$\left(\widetilde{\rho}\widetilde{H}_0\right)_{ij} = \sum_k \rho_{ik}H_{0kj} = \rho_{ij}H_{0jj} \tag{4.53}$$

Further, H_{0ii} and H_{0jj} may be replaced by their respective energy eigenvalues W_i and W_j. Also, $(\widetilde{\rho}p)_{ij} = \sum_k \rho_{ik}p_{kj}$. Using all these, the equation 4.51 becomes

$$i\hbar\frac{d\rho_{ij}}{dt} = (W_i - W_j)\,\rho_{ij} + \sum_k \left(\rho_{ik}p_{kj} - p_{ik}\rho_{kj}\right) E \tag{4.54}$$

At this stage, let us introduce the matrix $\widetilde{\rho}$ related to $\widetilde{\rho}$ by

$$\rho_{ij} = \sigma_{ij}e^{-i\omega_{ij}t} \tag{4.55}$$

Substituting this in the equation 4.54,

$$i\hbar\frac{d}{dt}\left(\sigma_{ij}e^{-i\omega_{ij}t}\right) = (W_i - W_j)\,\sigma_{ij}e^{-i\omega_{ij}t} \tag{4.56}$$

$$+\sum_k \left(\sigma_{ik}e^{-i\omega_{ik}t}p_{kj} - p_{ik}\sigma_{kj}e^{-i\omega_{kj}t}\right) E \tag{4.57}$$

Carrying out the indicated differentiation with respect to time on the left hand side of the equation,

$$i\hbar e^{-i\omega_{ij}t}\frac{d\sigma_{ij}}{dt} + i\hbar\left(-i\omega_{ij}\right)\sigma_{ij}e^{-i\omega_{ij}t}$$

$$= (W_i - W_j)\,\sigma_{ij}e^{-i\omega_{ij}t} + \sum_k \left(\sigma_{ik}e^{-i\omega_{ik}t}p_{kj} - p_{ik}\sigma_{kj}e^{-i\omega_{kj}t}\right) E \tag{4.58}$$

Note since $\hbar\omega_{ij} = W_i - W_j$, the second term on the left cancels with the first term on the right, reducing the equation to

$$\frac{d\sigma_{ij}}{dt} = \frac{1}{i\hbar}\sum_k \left(\sigma_{ik}e^{-i\omega_{ik}t}p_{kj} - p_{ik}\sigma_{kj}e^{-i\omega_{kj}t}\right) Ee^{i\omega_{ij}t} \tag{4.59}$$

Now we make further use of the relationships $\omega_{ij} = \frac{W_i - W_j}{\hbar}$, $\omega_{ik} = \frac{W_i - W_k}{\hbar}$ and $\omega_{kj} = \frac{W_k - W_j}{\hbar}$ to see that $\omega_{ij} - \omega_{ik} = \omega_{kj}$ and $\omega_{ij} - \omega_{kj} = \omega_{ik}$. These substitutions lead us from the above equation to

$$\frac{d\sigma_{ij}}{dt} = \frac{1}{i\hbar} \sum_k \left(\sigma_{ik} e^{i\omega_{kj}t} p_{kj} - p_{ik} \sigma_{kj} e^{i\omega_{ik}t} \right) E \tag{4.60}$$

Now we re-write the product of the dipole moment and electric field by their dot product to convert the above equation to

$$\frac{d\sigma_{ij}}{dt} = \frac{1}{i\hbar} \sum_k \left(\sigma_{ik} e^{i\omega_{kj}t} \vec{p}_{kj} - \vec{p}_{ik} \sigma_{kj} e^{i\omega_{ik}t} \right) \cdot \vec{E} \tag{4.61}$$

4.6 First Order Density Matrix

When the system is unperturbed, the initial values of the matrix elements are given by

$$\sigma_{ik} = \sigma^0_{ii} \delta_{ik}, \sigma_{kj} = \sigma^0_{jj} \delta_{kj}, t = 0 \tag{4.62}$$

In order to obtain the first order solutions, we replace σ_{ik} and σ_{kj} terms on the right hand side of the equation by their initial values as given by the equation 4.62. This approximation results in

$$\frac{d\sigma_{ij}}{dt} = \frac{1}{i\hbar} \sum_k \left(\sigma^0_{ii} \delta_{ik} e^{i\omega_{kj}t} \vec{p}_{kj} - \vec{p}_{ik} \sigma^0_{jj} \delta_{kj} e^{i\omega_{ik}t} \right) \cdot \vec{E} \tag{4.63}$$

This results in the summation retaining the terms given in

$$\frac{d\sigma^{(1)}_{ij}}{dt} = \frac{1}{i\hbar} \left(\sigma^0_{ii} e^{i\omega_{ij}t} \vec{p}_{ij} - \vec{p}_{ij} \sigma^0_{jj} e^{i\omega_{ij}t} \right) \cdot \vec{E} \tag{4.64}$$

$$\frac{d\sigma^{(1)}_{ij}}{dt} = \frac{1}{i\hbar} \left(\sigma^0_{ii} - \sigma^0_{jj} \right) \vec{p}_{ij} \cdot \vec{E} e^{i\omega_{ij}t} \tag{4.65}$$

Integrating this with respect to time yields the first order value of the matrix elements.

$$\sigma^{(1)}_{ij} = \sigma^{\bullet}_{ij} + \frac{1}{i\hbar} \left(\sigma^0_{ii} - \sigma^0_{jj} \right) \vec{p}_{ij} \cdot \int_0^t \vec{E} e^{i\omega_{ij}\tau} d\tau \tag{4.66}$$

The first term on the right is the initial value given by $\sigma_{ij}^0 = \sigma_{ii}^0 \delta_{ij}$. Inserting this, we have

$$\sigma_{ij}^{(1)} = \sigma_{ii}^0 \delta_{ij} + \frac{1}{i\hbar} \left(\sigma_{ii}^0 - \sigma_{jj}^0\right) \vec{p}_{ij} \cdot \int_0^t \vec{E} e^{i\omega_{ij}\tau} d\tau \tag{4.67}$$

4.7 Second Order Density Matrix

To get the second order matrix elements $\sigma_{ij}^{(2)}$, we substitute the first order solution values $\sigma_{ij}^{(1)}$ for σ_{ij} on the right hand side of equation 4.61:

$$\begin{aligned}\frac{d\sigma_{ij}}{dt} &= \frac{1}{i\hbar} \sum_k \left[\left(\sigma_{ii}^0 \delta_{ik} + \frac{1}{i\hbar} \left(\sigma_{ii}^0 - \sigma_{kk}^0\right) \vec{p}_{ik} \cdot \int_0^t \vec{E} e^{i\omega_{ik}\tau} d\tau \right) \vec{p}_{kj} e^{i\omega_{ik}\tau} \cdot \vec{E} \right] \\ &\quad - \frac{1}{i\hbar} \sum_k \left[\left\{ \sigma_{jj}^0 \delta_{kj} + \frac{1}{i\hbar} \left(\sigma_{kk}^0 - \sigma_{jj}^0\right) \vec{p}_{kj} \cdot \int_0^t \vec{E} e^{i\omega_{kj}\tau} d\tau \right\} \vec{p}_{ik} e^{i\omega_{ik}t} \cdot \vec{E} \right]\end{aligned}$$

$$\begin{aligned}\frac{d\sigma_{ij}}{dt} &= \frac{1}{i\hbar} \left(\sigma_{ii}^0 \vec{p}_{ij} e^{i\omega_{ij}t} \cdot \vec{E} - \vec{p}_{ij} \sigma_{jj}^0 e^{i\omega_{ij}t} \cdot \vec{E} \right) \qquad (4.68) \\ &\quad - \frac{1}{\hbar^2} \sum_k [\left(\left(\sigma_{ii}^0 - \sigma_{kk}^0\right) \vec{p}_{ik} \cdot \int_0^t \vec{E} e^{i\omega_{ik}\tau} d\tau \right) \vec{p}_{kj} e^{i\omega_{kj}t} \cdot \vec{E} \\ &\quad + \frac{1}{\hbar^2} \sum_k \left(\left(\sigma_{kk}^0 - \sigma_{jj}^0\right) \vec{p}_{kj} \cdot \int_0^t \vec{E} e^{i\omega_{kj}\tau} d\tau \right) \vec{p}_{ik} e^{i\omega_{ik}t} \cdot \vec{E} \qquad (4.69)\end{aligned}$$

Now we may integrate this with respect to time, giving the density matrix up to the second order in the electric field as $\sigma_{ij} =$

$$\begin{aligned}&\sigma_{ii}^0 \delta_{ij} + \frac{1}{i\hbar} \left(\sigma_{ii}^0 - \sigma_{jj}^0\right) \vec{p}_{ij} \cdot \int_0^t \vec{E} e^{i\omega_{ij}\tau} d\tau \\ &- \frac{1}{\hbar^2} \sum_k \int_0^t d\tau \left(\vec{p}_{ik} \cdot \vec{E} \left(\sigma_{ii}^0 - \sigma_{kk}^0\right) e^{i\omega_{kj}\tau} \vec{p}_{kj} \cdot \int_0^\tau \vec{E} e^{i\omega_{ik}\xi} d\xi \right) \\ &+ \frac{1}{\hbar^2} \sum_k \int_0^t d\tau \left(\vec{p}_{ik} \cdot \vec{E} \left(\sigma_{kk}^0 - \sigma_{jj}^0\right) e^{i\omega_{ik}\tau} \vec{p}_{kj} \cdot \int_0^\tau \vec{E} e^{i\omega_{kj}\xi} d\xi \right)\end{aligned}$$

On the right hand side, the first term is the initial value corresponding to the zeroth order. The second term is linear in the

electric field. The third and fourth terms are of second order contributing to the second order density matrix:

$$\sigma_{ij}^{(2)} = -\frac{1}{\hbar^2}\sum_k \int_0^t d\tau \left(\overrightarrow{p}_{ik} \cdot \overrightarrow{E} \left(\sigma_{ii}^0 - \sigma_{kk}^0\right) e^{i\omega_{kj}\tau} \overrightarrow{p}_{kj} \cdot \int_0^\tau \overrightarrow{E} e^{i\omega_{ik}\xi} d\xi \right)$$
$$+\frac{1}{\hbar^2}\sum_k \int_0^t d\tau \left(\overrightarrow{p}_{ik} \cdot \overrightarrow{E} \left(\sigma_{kk}^0 - \sigma_{jj}^0\right) e^{i\omega_{ik}\tau} \overrightarrow{p}_{kj} \cdot \int_0^\tau \overrightarrow{E} e^{i\omega_{kj}\xi} d\xi \right)$$

4.8 Third Order Density Matrix

By substituting the density matrix given to second order in the equation 4.61, we get the solution up to third order $\frac{d\sigma_{ij}}{dt} =$

$$\frac{1}{i\hbar}\sum_k \overrightarrow{p}_{kj} e^{i\omega_{kj}t} \cdot \overrightarrow{E} \cdot \left\{ \left[\sigma_{ii}^0 \delta_{ik} + \frac{1}{i\hbar}\left(\sigma_{ii}^0 - \sigma_{kk}^0\right) \overrightarrow{p}_{ik} \cdot \int_0^t \overrightarrow{E} e^{i\omega_{ik}\tau} d\tau \right] \right.$$

$$-\frac{1}{\hbar^2}\sum_\nu \left[\int_0^t d\tau \left(\overrightarrow{p}_{\nu k} \cdot \overrightarrow{E} \right) \left(\sigma_{ii}^0 - \sigma_{\nu\nu}^0\right) e^{i\omega_{\nu k}\tau} \overrightarrow{p}_{\nu k} \cdot \int_0^\tau \overrightarrow{E} e^{i\omega_{i\nu}\xi} d\xi \right]$$

$$\left. +\frac{1}{\hbar^2}\sum_\nu \left[\int_0^t d\tau \left(\overrightarrow{p}_{i\nu} \cdot \overrightarrow{E} \right) \left(\sigma_{\nu\nu}^0 - \sigma_{kk}^0\right) e^{i\omega_{i\nu}\tau} \overrightarrow{p}_{\nu k} \cdot \int_0^\tau \overrightarrow{E} e^{i\omega_{\nu k}\xi} d\xi \right] \right\}$$

$$-\frac{1}{i\hbar}\sum_k \overrightarrow{p}_{ik} e^{i\omega_{ik}t} \cdot \overrightarrow{E} \cdot \left\{ \left[\sigma_{jj}^0 \delta_{jk} + \frac{1}{i\hbar}\left(\sigma_{kk}^0 - \sigma_{jj}^0\right) \overrightarrow{p}_{kj} \cdot \int_0^t \overrightarrow{E} e^{i\omega_{kj}\tau} d\tau \right] \right.$$

$$-\frac{1}{\hbar^2}\sum_\mu \left[\int_0^t d\tau \left(\overrightarrow{p}_{k\mu} \cdot \overrightarrow{E} \right) \left(\sigma_{kk}^0 - \sigma_{\mu\mu}^0\right) e^{i\omega_{\mu j}\tau} \overrightarrow{p}_{\mu j} \cdot \int_0^\tau \overrightarrow{E} e^{i\omega_{k\mu}\xi} d\xi \right]$$

$$\left. +\frac{1}{\hbar^2}\sum_\mu \left[\int_0^t d\tau \left(\overrightarrow{p}_{k\mu} \cdot \overrightarrow{E} \right) \left(\sigma_{\mu\mu}^0 - \sigma_{jj}^0\right) e^{i\omega_{k\mu}\tau} \overrightarrow{p}_{\mu j} \cdot \int_0^\tau \overrightarrow{E} e^{i\omega_{\mu j}\xi} d\xi \right] \right\} \quad (4.70)$$

Integrating this with respect to time yields, besides the terms of the zeroth order, first order and second order the third order contribution to the density matrix given by $\sigma_{ij}^{(3)} =$

$$
\begin{aligned}
&-\frac{1}{i\hbar^3}\sum_k\sum_\mu\Bigg[\Bigg\{\int_0^t \vec{p}_{kj}\cdot\vec{E}e^{i\omega_{kj}\tau}\\
&\left(\int_0^\tau \vec{p}_{\mu k}\cdot\vec{E}\left(\sigma^0_{ii}-\sigma^0_{\mu\mu}\right)e^{i\omega_{\mu k}\xi}\int_0^\xi \vec{p}_{i\mu}\cdot\vec{E}e^{i\omega_{i\mu}\eta}d\eta d\xi\right.\\
&\left.-\int_0^\tau \vec{p}_{i\mu}\cdot\vec{E}\left(\sigma^0_{\mu\mu}-\sigma^0_{kk}\right)e^{i\omega_{i\mu}\xi}\int_0^\xi \vec{p}_{\mu k}\cdot\vec{E}e^{i\omega_{\mu k}\eta}d\eta d\xi\right)d\tau\Bigg\}\\
-&\Bigg\{\int_0^t \vec{p}_{ik}\cdot\vec{E}e^{i\omega_{ik}\tau}\\
&\left(\int_0^\tau \vec{p}_{\mu j}\cdot\vec{E}\left(\sigma^0_{kk}-\sigma^0_{\mu\mu}\right)e^{i\omega_{\mu j}\xi}\int_0^\xi \vec{p}_{k\mu}\cdot\vec{E}e^{i\omega_{k\mu}\eta}d\eta d\xi\right.\\
&\left.-\int_0^\tau \vec{p}_{k\mu}\cdot\vec{E}\left(\sigma^0_{\mu\mu}-\sigma^0_{jj}\right)e^{i\omega_{k\mu}\xi}\int_0^\xi \vec{p}_{\mu j}\cdot\vec{E}e^{i\omega_{\mu j}\eta}d\eta d\xi\right)d\tau\Bigg\}\Bigg]
\end{aligned}
$$

4.9 Double Integrals in the Expressions for Density Matrix

If the electric fields $\vec{E}$ appearing in the expressions for the density matrices given in the previous sections, are taken to be part of a travelling harmonic wave given by

$$\vec{E}=\hat{e}E\cos\left(\omega t-\vec{k}\cdot\vec{r}\right) \tag{4.71}$$

where $\hat{e}$ is the polarization unit vector giving the direction of the electric field vector, ω is the angular frequency of the wave, and $\vec{r}$ is the position vector in the medium. The resulting integrals are of the form given by

$$
\begin{aligned}
&\int_0^\tau d\eta e^{i\omega_{\nu\mu}\eta}\cos\left(\omega\eta-\vec{k}\cdot\vec{r}\right)\\
=&\int_0^\tau d\eta e^{i\omega_{\nu\mu}\eta}\frac{1}{2}\left(e^{i\left(\omega\eta-\vec{k}\cdot\vec{r}\right)}+e^{-i\left(\omega\eta-\vec{k}\cdot\vec{r}\right)}\right)\\
=&\int_0^\tau d\eta\frac{1}{2}\left(e^{i\left((\omega+\omega_{\nu\mu})\eta-\vec{k}\cdot\vec{r}\right)}+e^{-i\left((\omega-\omega_{\nu\mu})\eta-\vec{k}\cdot\vec{r}\right)}\right)
\end{aligned}
\tag{4.72}
$$

Carrying out the integration, we get

$$\begin{aligned}
&\frac{1}{2i}\left\{\left|\frac{e^{i\left((\omega+\omega_{\nu\mu})\eta-\vec{k}\cdot\vec{r}\right)}}{\omega+\omega_{\nu\mu}}\right|_0^\tau - \left|\frac{e^{-i\left((\omega-\omega_{\nu\mu})\eta-\vec{k}\cdot\vec{r}\right)}}{\omega-\omega_{\nu\mu}}\right|_0^\tau\right\} \\
= &\frac{1}{2i}\left\{\frac{e^{i\left((\omega+\omega_{\nu\mu})\tau-\vec{k}\cdot\vec{r}\right)}-e^{-i\vec{k}\cdot\vec{r}}}{\omega+\omega_{\nu\mu}} - \frac{e^{-i\left((\omega-\omega_{\nu\mu})\tau-\vec{k}\cdot\vec{r}\right)}-e^{i\vec{k}\cdot\vec{r}}}{\omega-\omega_{\nu\mu}}\right\} \\
= &\frac{1}{2i}\left\{\frac{e^{i((\omega+\omega_{\nu\mu})\tau)}-1}{\omega+\omega_{\nu\mu}}e^{-i\vec{k}\cdot\vec{r}} - \frac{e^{-i((\omega-\omega_{\nu\mu})\tau)}-1}{\omega-\omega_{\nu\mu}}e^{i\vec{k}\cdot\vec{r}}\right\} \\
= &\frac{1}{2}i\left\{\frac{1-e^{i((\omega+\omega_{\nu\mu})\tau)}}{\omega+\omega_{\nu\mu}}e^{-i\vec{k}\cdot\vec{r}} - \frac{1-e^{-i((\omega-\omega_{\nu\mu})\tau)}}{\omega-\omega_{\nu\mu}}e^{i\vec{k}\cdot\vec{r}}\right\} \qquad (4.73)
\end{aligned}$$

Now consider the double integral:

$$\int_0^t e^{i\omega_{rs}\tau}\cos\left(\omega\tau-\vec{k}\cdot\vec{r}\right)\left[\int_0^\tau d\eta e^{i\omega_{\nu\mu}\eta}\cos\left(\omega\eta-\vec{k}\cdot\vec{r}\right)\right]d\tau \qquad (4.74)$$

In view of the result for the single integral detailed above, the above double integral can be re-written

$$\begin{aligned}
&\int_0^t e^{i\omega_{rs}\tau}\cos\left(\omega\tau-\vec{k}\cdot\vec{r}\right) \\
&\frac{1}{2}i\left(\frac{\left(1-e^{i(\omega+\omega_{\nu\mu})\tau}\right)}{\omega+\omega_{\nu\mu}}e^{-i\vec{k}\cdot\vec{r}} - \frac{\left(1-e^{-i(\omega+\omega_{\nu\mu})\tau}\right)}{\omega-\omega_{\nu\mu}}e^{i\vec{k}\cdot\vec{r}}\right)d\tau \qquad (4.75)
\end{aligned}$$

Writing the cosine term in exponential form and combining it along with the first exponential factor with the bracketed pair of terms gives

$$\int_0^t \frac{d\tau}{4}\left(\frac{e^{i\left((2\omega+\omega_{\nu\mu}+\omega_{rs})\tau-2\vec{k}\cdot\vec{r}\right)}}{\omega+\omega_{\nu\mu}} - \frac{e^{-i\left((2\omega-\omega_{\nu\mu}-\omega_{rs})\tau-2\vec{k}\cdot\vec{r}\right)}}{\omega-\omega_{\nu\mu}}\right) \qquad (4.76)$$

After performing the indicated integration, we thus get the double integral simplified as

$$\begin{aligned}
&\frac{1}{4}e^{i(\omega_{\nu\mu}+\omega_{rs})\tau} \\
&\left(\frac{e^{i\left(2\omega\tau-2\vec{k}\cdot\vec{r}\right)}}{(\omega+\omega_{\nu\mu})(2\omega+\omega_{\nu\mu}+\omega_{rs})} - \frac{e^{-i\left(2\omega\tau-2\vec{k}\cdot\vec{r}\right)}}{(\omega-\omega_{\nu\mu})(2\omega-\omega_{\nu\mu}-\omega_{rs})}\right)
\end{aligned}$$

4.10 Second Harmonic Susceptibility

To derive the expression giving non-linear susceptibility corresponding to second harmonic generation, we need to consider the electric polarization $\vec{P}_{2\omega}$ at the angular frequency 2ω. Using the previously determined result for the expectation value of physical quantities, we have for the polarization of an ensemble of N atoms per unit volume,

$$\vec{P}_{2\omega} = N \langle \vec{p}_{2\omega} \rangle \tag{4.77}$$

Since the expectation value of $\vec{p}_{2\omega}$ is the trace of $(\rho \vec{p}_{2\omega})$,

$$\vec{P}_{2\omega} = N \sum_{ij} \rho_{ij} \vec{p}_{ji} \tag{4.78}$$

We already had developed the result for the σ_{ij} to second order in the electric field. From this result we should retain only those terms that have the time-dependence at the second harmonic angular frequency 2ω. Also we note that $\omega_{ij} = \omega_{i\mu} + \omega_{\mu j}$. Further we use $\rho_{ij} = \sigma_{ij} e^{-i\omega_{ij}t}$ to get $\rho_{ij} =$

$$\frac{E_0^2}{4\hbar^2} \sum_{\mu} p_{i\mu} p_{\mu j}$$
$$\left((\rho_{ii}^0 - \rho_{\mu\mu}^0) \left\{ \frac{e^{2i\left(\omega t - \vec{k}\cdot\vec{r}\right)}}{(\omega + \omega_{i\mu})(2\omega + \omega_{ij})} + \frac{e^{-2i\left(\omega t - \vec{k}\cdot\vec{r}\right)}}{(\omega - \omega_{i\mu})(2\omega - \omega_{ij})} \right\} \right.$$
$$\left. + (\rho_{jj}^0 - \rho_{\mu\mu}^0) \left\{ \frac{e^{2i\left(\omega t - \vec{k}\cdot\vec{r}\right)}}{(\omega + \omega_{\mu j})(2\omega + \omega_{ij})} + \frac{e^{-2i\left(\omega t - \vec{k}\cdot\vec{r}\right)}}{(\omega - \omega_{\mu j})(2\omega - \omega_{ij})} \right\} \right)$$

Using this result in the equation 4.78, we have

$$\vec{P}_{2\omega} = \frac{N E_{0\omega}^2}{4\hbar^2} \sum_{ij\mu} p_{i\mu} p_{\mu j} \vec{p}_{ji} S \tag{4.79}$$

where S is the summation given by

$$(\rho_{ii}^0 - \rho_{\mu\mu}^0) \left\{ \frac{e^{2i\left(\omega t - \vec{k}\cdot\vec{r}\right)}}{(\omega + \omega_{i\mu})(2\omega + \omega_{ij})} + \frac{e^{-2i\left(\omega t - \vec{k}\cdot\vec{r}\right)}}{(\omega - \omega_{i\mu})(2\omega - \omega_{ij})} \right\}$$
$$+ (\rho_{jj}^0 - \rho_{\mu\mu}^0) \left\{ \frac{e^{2i\left(\omega t - \vec{k}\cdot\vec{r}\right)}}{(\omega + \omega_{\mu j})(2\omega + \omega_{ij})} + \frac{e^{-2i\left(\omega t - \vec{k}\cdot\vec{r}\right)}}{(\omega - \omega_{\mu j})(2\omega - \omega_{ij})} \right\} \tag{4.80}$$

The above equation for S can be re-written, by interchanging i and j in the second terms of the two bracketed terms. And also noting that $\omega_{\mu j} = -\omega_{j\mu}$ and also that $p_{\mu k} = p^*_{k\mu}$, we rearrange the terms in the following way:

$$\begin{aligned}\overrightarrow{P}_{2\omega} = \frac{NE_{0\omega}^2}{4\hbar^2} \sum_{ij\mu} \left(\frac{\left(\rho^0_{ii} - \rho^0_{\mu\mu}\right)}{\left(\omega + \omega_{i\mu}\right)\left(2\omega + \omega_{ij}\right)} + \frac{\left(\rho^0_{jj} - \rho^0_{\mu\mu}\right)}{\left(\omega + \omega_{\mu j}\right)\left(2\omega + \omega_{ij}\right)} \right) \\ \left(\left(\widehat{e}_\omega \cdot \overrightarrow{p}_{\mu j}\right) \overrightarrow{p}_{ji} \left(\widehat{e}_\omega \cdot \overrightarrow{p}_{i\mu}\right) e^{2i\left(\omega t - \overrightarrow{k}\cdot\overrightarrow{r}\right)} \right. \\ \left. + \left\{ \left(\widehat{e}_\omega \cdot \overrightarrow{p}_{\mu j}\right) \overrightarrow{p}_{ji} \left(\widehat{e}_\omega \cdot \overrightarrow{p}_{i\mu}\right) \right\}^* e^{-2i\left(\omega t - \overrightarrow{k}\cdot\overrightarrow{r}\right)} \right) \end{aligned} \tag{4.81}$$

If we write the second harmonic polarization in the tensor notation, we have

$$\overrightarrow{P}_{2\omega} = Re\left(\overrightarrow{E}_\omega \cdot \chi_{2\omega} \cdot \overrightarrow{E}_\omega\right) \tag{4.82}$$

which means that the susceptibility tensor for the second harmonic polarization $\chi^{(2)}\left(-2\omega : \omega, \omega\right) =$ is given by

$$\frac{N}{2\hbar^2} \sum_{ij\mu} \left(\frac{\left(\rho^0_{ii} - \rho^0_{\mu\mu}\right)}{\left(\omega + \omega_{i\mu}\right)\left(2\omega + \omega_{ij}\right)} + \frac{\left(\rho^0_{jj} - \rho^0_{\mu\mu}\right)}{\left(\omega + \omega_{\mu j}\right)\left(2\omega + \omega_{ij}\right)} \right) \overrightarrow{p}_{\mu j} \overrightarrow{p}_{ji} \overrightarrow{p}_{i\mu} \tag{4.83}$$

The second harmonic polarization acts as a source to generate the electromagnetic wave at the angular frequency 2ω.

4.11 Relaxation Effects

The above treatment of the frequency dependence of the susceptibility tensors would be satisfactory if we are working in a range of frequencies far from the resonance regime. At resonance, the expressions for the density matrix elements and for the susceptibilities diverge. This is because, so far, we did not include the effects that lead to relaxation of the states or the damping factors. The relaxations due to radiative or non-radiative transitions are taken into account phenomenologically by adding the terms $\pm i\Gamma$ in each denominator appropriately. This is then expected to lead to realistic estimates of the susceptibilities: both real and imaginary. Thus the angular frequency term $\omega_{i\mu}$ is replaced by $\omega_{i\mu} + i\Gamma_{i\mu}$, ω_{ij} by $\omega_{ij} + i\Gamma_{ij}$ and $\omega_{\mu j}$ by $\omega_{\mu j} + i\Gamma_{\mu j}$.

4.12 Applications to Color Centers

4.12.1 Third Order Susceptibility

Adopting the methods outlined above, Krishnamurthy and Murti [1992] studied the third order non-linear optical susceptibility of F and F_A centers in crystalline KCl, corresponding to degenerate four wave mixing ($DFWM$) process. F center in an ionic crystal is an electron trapped at an anion vacancy. If one of the six nearest neighbors of the F center in a crystal such as KCl is occupied by a small monovalent impurity M^+ like Li^+ or Na^+ ,then the center is called F_A center.

Fig. 4.1 shows the atomistic models of the F and F_A centers.

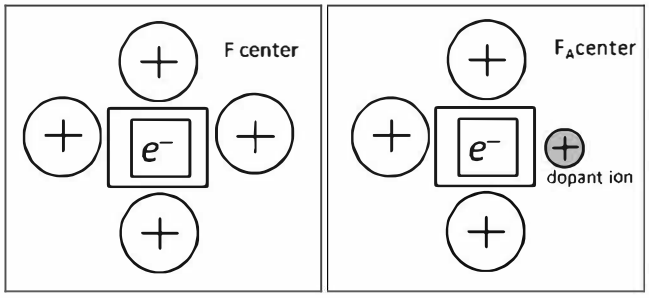


Figure 4.1: Atomistic model for color centers

Fig. 4.2 gives the well-known energy level schemes for these two types of centers.

Modelling the F center in a two-level scheme, they find for the third order non-resonant susceptibility (for field frequencies far from resonance) :

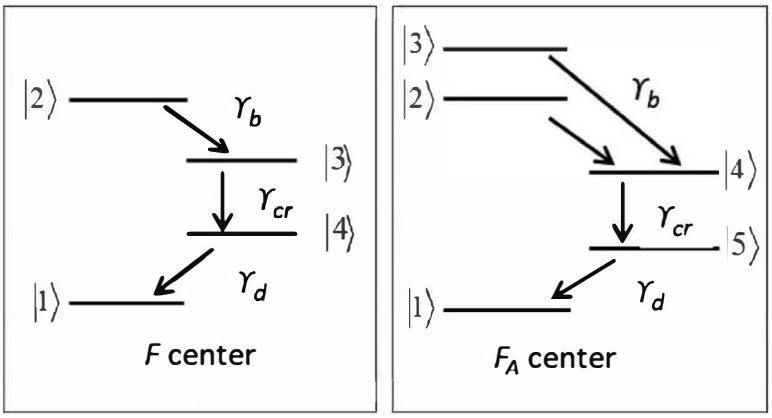


Figure 4.2: Energy level schemes for the color centers

$$\chi^{(3)}_{NR}(\omega:\omega,-\omega,\omega) = \frac{N_{12}}{\hbar^3}(\overrightarrow{p}_{12}\cdot\overrightarrow{e}_{\omega})^4 \frac{\omega_0}{(\omega_0^2-\omega^2)^2}\left(\frac{8\omega_0^2}{\omega_0^2-\omega^2}-1\right) \quad (4.84)$$

where ω_0 is the angular frequency given by $\omega_0 = (W_2 - W_1)/\hbar$. W_1 and W_2 being the energies of the two states $|1\rangle$ and $|2\rangle$. $N_{12} = N(\rho^0_{11} - \rho^0_{22})$

The real part of the resonant susceptibility is

$$\chi^{(3)}_{R}(\omega:\omega,-\omega,\omega) = \frac{N_{12}}{2\hbar^3}\frac{(\overrightarrow{p}_{12}\cdot\overrightarrow{e}_{\omega})^4\,\Gamma_{21}^2\delta\gamma_{eff}^{-1}}{(1+\delta^2)^2} \quad (4.85)$$

where δ is the departure from resonance (detuning) $\delta = \omega - \omega_0$. Γ_{21} is the dephasing time. γ_{eff} is the effective lifetime given by

$$\gamma_{eff}^{-1} = \gamma_b^{-1} + \eta\gamma_{cr}^{-1} + \gamma_d^{-1} \quad (4.86)$$

Note (Fig.2) that γ_b is the non-radiative relaxation time from the excited state $|2\rangle$ to the relaxed excited state $|3\rangle$ of the F center. γ_d is the corresponding time from the relaxed ground state $|4\rangle$ to

the ground state $|1\rangle$. η is the quantum efficiency of the radiative transition from $|3\rangle \Rightarrow |4\rangle$ with lifetime γ_{cr}.

The imaginary part of the susceptibility is given by

$$Im\chi^{(3)}(\omega:\omega,-\omega,\omega) = -\frac{N_{12}}{2\hbar^3}\frac{(\vec{p}_{12}\cdot\vec{e}_{\omega})^4}{(1+\delta^2)^2}\Gamma_{21}^2\gamma_{eff}^{-1} \tag{4.87}$$

The non-resonant third order susceptibility for the $DFWM$ process contributed by the F_A centers is given by

$$\chi_{NR}^{(3)}(\omega:\omega,-\omega,\omega) = -(\frac{N_{12}}{\hbar^3}(\vec{p}_{12}\cdot\hat{e})^4\frac{\omega_{21}}{(\omega_{21}^2-\omega^2)^2}\left(\frac{8\omega_{21}^2}{(\omega_{21}^2-\omega^2)}-1\right) \tag{4.88}$$

$$+\frac{N_{13}}{\hbar^3}(\vec{p}_{13}\cdot\hat{e})^4\frac{\omega_{31}}{(\omega_{31}^2-\omega^2)^2}\left(\frac{8\omega_{31}^2}{(\omega_{31}^2-\omega^2)}-1\right)$$

$$+\frac{N_{12}}{2\hbar^3}\omega_{31}\frac{(\vec{p}_{12}\cdot\hat{e})^2(\vec{p}_{13}\cdot\hat{e})^2}{(\omega_{21}^2-\omega^2)(\omega_{31}^2-\omega^2)}\left(\frac{8\omega_{21}^2}{(\omega_{21}^2-\omega^2)}-1\right)$$

$$+\frac{N_{13}}{\hbar^3}\omega_{21}\frac{(\vec{p}_{12}\cdot\hat{e})^2(\vec{p}_{13}\cdot\hat{e})^2}{2\hbar^3(\omega_{21}^2-\omega^2)(\omega_{31}^2-\omega^2)})\left(\frac{8\omega_{31}^2}{(\omega_{31}^2-\omega^2)}-1\right) \tag{4.89}$$

where $N_{13} = N(\rho_{11}^0 - \rho_{33}^0)$.

Similar studies were carried out by the same authors [Krishnamurthy and Murti, 1994] on the laser-active color centers F_2^+. The authors also explored the possible use of color centers for third harmonic generation.

4.12.2 Second Order Susceptibility

Extending the work of Krishnamurthy and Murti et al, Majles et al [1997] presented a detailed calculation of the second order susceptibility of the F_A centers for second harmonic generation. Even though the crystal itself has a center of symmetry precluding the possibility of second order nonlinearities, the F_A lacks a center of inversion symmetry and thus can provide such a nonlinearity and macroscopically it would be necessary to produce an alignment of these centers before realizing the nonlinearity. They calculated $\chi^{(2)}(-2\omega:\omega,\omega)$ of the F_A center in $KCl:Li$ crystals. They further derived the second order susceptibility of the F_A center in the optical parametric mixing process Majles et al [2001], calculating the values of $\chi^{(2)}(-\omega_3:\omega_1,\omega_2)$ and the dispersion of the real and

imaginary parts. Significant magnitudes of second order susceptibility emerged for both second harmonic generation as well as for parametric mixing in these crystal media.

4.13 Explorations

Note: You may assume the following relations while working out these explorations:

$$\left[\widetilde{a}, \widetilde{a}^{\dagger}\right] = 1, \ \widetilde{a}\,|n\rangle = \sqrt{n}\,|n-1\rangle \text{ and } \widetilde{a}^{\dagger}\,|n\rangle = \sqrt{n+1}\,|n-1\rangle$$

1. Consider an electromagnetic field represented by the normalized state vector $|\psi\rangle = a|0\rangle + b|1\rangle$ where $|0\rangle$ and $|1\rangle$ are the zero and one photon states respectively. Then

   a) Find the traces $Tr\,(\varrho)$ and $Tr\,(\varrho^2)$.

   b) Are they the same always? Justify.

   c) What is special about the state vector $|\psi\rangle$?

2. The Heisenberg's equation of motion for an operator $\widetilde{O}$ is given by the relation $i\hbar\frac{\partial \widetilde{O}}{\partial t} = [\widetilde{H}, \widetilde{O}]$.Consider the special case when $\widetilde{O}\,(\blacksquare) = \widetilde{a}\,(\blacksquare)$. Find the value of $\widetilde{O}\,(t)$ for $\widetilde{H} = \widetilde{a}^{\dagger}\widetilde{a}$.

3. Consider an operator $\widetilde{X} = \frac{\left(\widetilde{a}+\widetilde{a}^{\dagger}\right)}{\sqrt{2}}$.

   a) Find the expectation value $\left\langle \widetilde{X}\,(\blacksquare)\right\rangle$ for the state

   $$|\psi\rangle = a|1\rangle + b|2\rangle$$

   where $|a|^2 + |b|^2 = 1$.

   b) Find $\left\langle \widetilde{X}\,(t)\right\rangle$ for the same state $|\psi\rangle$, for $\widetilde{H} = \hbar\omega\widetilde{a}^{\dagger}\widetilde{a}$.

   c) Find $\left\langle \widetilde{X}\,(0)\right\rangle$ for the state $|\psi\,(t)\rangle$.

   Compare the expectation value with that of the previous question.

4. Consider two completely independent systems A and B. The system A consists of a single particle and system B consists of n particles. The particle in A can take n discrete states $|\psi_i\rangle$, for $i = 1, 2, ...n$. The j^{th} particle in system B can have

a time-independent state $|\psi_j\rangle$. Assume that both the systems can be represented as state vectors. Then

a) Find $\tilde{\rho}$ for the systems A and B separately. Is there any similarity between the two answers?

b) Write down the expression for the expectation value for any operator $\tilde{O}$ in both the cases.

5. Consider the density matrix $\tilde{\rho} = \sum_i P_i |\psi_i\rangle \langle\psi_i|$, the general form of the matrix where P_i is the weight factor. Find the traces $Tr(\varrho)$ and $Tr(\varrho^2)$ For this density matrix. Are they the same? What kind of a state is represented by this $\tilde{\rho}$?

Chapter 5

Nonlinear Wave Mixing Processes

"There are the rushing waves... mountains of molecules, each stupidly minding its own business...trillions apart... yet forming white surf in unison."

-Richard Feynman

The waves are important, so are the ways in which they mix.

Learning Objectives

- Recall of the basics of electromagnetic wave propagation in linear media
- Establishment of the conditions for optimal energy transfer in nonlinear media.
- Analysis of three wave mixing process and energy transfer resulting in second harmonic generation.
- Recognition of the need for phase matching and device schemes to achieve this

5.1 Introduction

Electromagnetic waves travel without interaction amongst themselves in a material with a linear optical response. There would be no energy exchange between the waves. On the other hand, if the material exhibits a significant optical nonlinearity, that would enable energy transfer between the waves. We refer to such energy transfer as a *wave mixing* process. Depending on the order of the nonlinearity, the mixing may involve three waves, four waves or more. Three wave mixing results in optical parametric amplification and second harmonic generation. Four wave mixing produces, among other things, third harmonic generation and optical phase conjugation. To set the stage for discussing these effects, we first review the basics of electromagnetism in linear dielectrics and then show how nonlinear polarization changes the propagation of the waves and provides coupling between them, ringing about this *wave mixing*.

5.2 Elements of Electromagnetism

Gauss' law of electrostatics relates the closed surface integral of the electric flux with the net charge q_{encl} enclosed in the volume bounded by the surface:

$$\oint_S \vec{E} \cdot \vec{dS} = \frac{q_{encl}}{\epsilon_0} \tag{5.1}$$

The left hand side is convertible into a volume integral according to the divergence theorem:

$$\oint_S \vec{E} \cdot \vec{dS} = \int_V \left(\vec{\nabla} \cdot \vec{E} \right) dV \tag{5.2}$$

The right hand side of Eq. 5.1 can also be written as a volume integral:

$$\frac{1}{\epsilon_0} q_{encl} = \frac{1}{\epsilon_0} \int_V \rho dV \tag{5.3}$$

where ρ is the volume charge density. This makes it possible to re-write Gauss' equation as

$$\int_V \left(\vec{\nabla} \cdot \vec{E} \right) dV = \int_V \frac{\rho}{\epsilon_0} dV \tag{5.4}$$

Being true for any volume, the integrands on either side of the above equation must therefore be equal:

$$\vec{\nabla} \cdot \vec{E} = \frac{\rho}{\epsilon_0} \tag{5.5}$$

In a polarized material, the charge density has two parts: (a) a free charge density ρ_f and (b) a bound charge density ρ_b. We can consider how the bound charge density is related to the polarization $\vec{P}$. To see this, let us write the potential at a point $\vec{r}$ due to a dipole $\vec{p}$ located at the point $\vec{r'}$:

$$V(\vec{r}) = \frac{1}{4\pi\epsilon_0} \frac{\vec{p} \cdot \hat{r}}{r^2} \tag{5.6}$$

where $\hat{r} = \frac{\vec{r} - \vec{r'}}{r}$, $r = \left| \vec{r} - \vec{r'} \right|$, defining the unit vector in the direction of the position vector of the field point relative to the source dipole. Now if there is a volume distribution of dipoles in a material, then the potential due to such a distribution is given by

$$V(\vec{r}) = \frac{1}{4\pi\epsilon_0} \int_v \frac{\vec{P}\left(\vec{r'}\right) \cdot \hat{r}}{r^2} dV' \tag{5.7}$$

because the dipole moment in the volume element dV' at $\vec{r'}$ is $\vec{P}\left(\vec{r'}\right) dV'$. Since $\vec{\nabla'}\left(\frac{1}{r}\right) = \frac{\hat{r}}{r^2}$ (the differentiation being with respect to the source position $\vec{r'}$), this can be written out as

$$V(\vec{r}) = \frac{1}{4\pi\epsilon_0} \int_v \vec{P} . \vec{\nabla'} \left(\frac{1}{r}\right) dV' \tag{5.8}$$

Now we have

$$\nabla' . \left(\frac{\vec{P}}{r}\right) = \vec{P} . \vec{\nabla'} \left(\frac{1}{r}\right) + \frac{1}{r} \vec{\nabla'} \cdot \vec{P} \tag{5.9}$$

Using this relation, we re-write Eq.4.8 as

$$V(\vec{r}) = \frac{1}{4\pi\epsilon_0} \left[\int_V \vec{\nabla'} \cdot \frac{\vec{P}}{r} dV' - \int_V \frac{1}{r} \left(\vec{\nabla'} \cdot \vec{P} \right) dV' \right] \tag{5.10}$$

Using the divergence theorem, this simplifies to

$$V(\vec{r}) = \frac{1}{4\pi\epsilon_0} \left[\oint_S \frac{1}{r} \vec{P} \cdot dS' - \int_V \frac{1}{r} \left(\vec{\nabla'} \cdot \vec{P} \right) dV' \right] \tag{5.11}$$

The first term on the right hand side of the above equation is the potential due to a surface charge of density

$$\sigma_b = \vec{P}.\hat{n} \tag{5.12}$$

The second term is the potential due to a volume charge of density

$$\rho_b = -\vec{\nabla} \cdot \vec{P} \tag{5.13}$$

with the result we may re-write Eq.5.11 as

$$V(\vec{r}) = \frac{1}{4\pi\epsilon_0} \oint_S \frac{\sigma_b}{r} dS + \frac{1}{4\pi\epsilon_0} \int_V \frac{\rho_b}{r} dV' \tag{5.14}$$

The total charge density is the sum of that due to the free charges ρ_f and that ρ_b due to the bound charges: $\rho = \rho_f + \rho_b$. Gauss law now becomes

$$\vec{\nabla} \cdot \vec{E} = \frac{\rho_f + \rho_b}{\epsilon_0} \tag{5.15}$$

Using the expression for the bound charge density given by Eq.5.13, this results in

$$\vec{\nabla} \cdot \left(\epsilon_0 \vec{E} + \vec{P}\right) = \rho_f \tag{5.16}$$

thereby leading to the concept of the electric displacement $\vec{D}$ defined by

$$\vec{D} = \epsilon_0 \vec{E} + \vec{P} \tag{5.17}$$

modifying the Gauss law for electric fields in the presence of the polarizable dielectrics to

$$\vec{\nabla} \cdot \vec{D} = \rho_f \tag{5.18}$$

For linear dielectrics, of course, we have

$$\vec{P} = \epsilon_0 \chi \vec{E} \tag{5.19}$$

$$\vec{D} = \epsilon_0 (1 + \chi) \vec{E} = \epsilon \vec{E} \tag{5.20}$$

$$\epsilon = \epsilon_r \epsilon_0 \tag{5.21}$$

$$\epsilon_r = 1 + \chi \tag{5.22}$$

defining the fundamental relationships between the dielectric permittivity ϵ, the relative permittivity ϵ_r and the susceptibility χ. Note while the relative permittivity and susceptibility are dimensionless, the permittivity has the same dimensions as the free space permittivity ϵ_0.

5.3 Travelling Electromagnetic Waves in Free Space

In free space devoid of any material, there is no charge. Maxwell's equations for the fields take the form

$$\vec{\nabla} \cdot \vec{E} = 0 \tag{5.23}$$

$$\vec{\nabla} \times \vec{E} = -\frac{\partial \vec{B}}{\partial t} \tag{5.24}$$

$$\vec{\nabla} \cdot \vec{B} = 0 \tag{5.25}$$

$$\vec{\nabla} \times \vec{B} = \mu_0 \epsilon_0 \frac{\partial \vec{E}}{\partial t} \tag{5.26}$$

We now wish to develop the differential equation for the travelling electric and magnetic fields. Toward this, we use the vector identity

$$\vec{\nabla} \times \left(\vec{\nabla} \times \vec{E} \right) = \vec{\nabla} \left(\vec{\nabla} \cdot \vec{E} \right) - \vec{\nabla}^2 \vec{E} \tag{5.27}$$

In view of the Eq.5.23, this becomes

$$\vec{\nabla} \times \left(\vec{\nabla} \times \vec{E} \right) = -\nabla^2 \vec{E} \tag{5.28}$$

Taking the curl of the right hand side of the Eq.4.20b, and making use of Eq.5.26, we get

$$\vec{\nabla} \times \left(-\frac{\partial \vec{B}}{\partial t} \right) = -\frac{\partial \left(\vec{\nabla} \times \vec{B} \right)}{\partial t} = -\mu_0 \epsilon_0 \frac{\partial^2 \vec{E}}{\partial t^2} \tag{5.29}$$

Thus sing Eq. 5.28 for the left hand side and Eq.5.29 for the right hand side, Eq.5.24 transforms to

$$\nabla^2 \vec{E} = \mu_0 \epsilon_0 \frac{\partial^2 \vec{E}}{\partial t^2} \tag{5.30}$$

In a similar way, we transform Eq.5.26 to give

$$\nabla^2 \vec{B} = \mu_0 \epsilon_0 \frac{\partial^2 \vec{B}}{\partial t^2} \tag{5.31}$$

These are the two wave equations for the electric and magnetic fields, propagating at the common wave velocity of magnitude

$$c = \frac{1}{\sqrt{\mu_0 \epsilon_0}} \tag{5.32}$$

As solutions of the wave equations for the electric and magnetic fields as given above, let us consider a monochromatic plane wave travelling in the $+X$ direction with the fields given by

$$\vec{E} = \vec{E_0} e^{i(\omega t - kx)} \tag{5.33}$$

$$\vec{B} = \vec{B_0} e^{i(\omega t - kx)} \tag{5.34}$$

where the field amplitudes $\vec{E_0}$ and $\vec{B_0}$ are complex and have no variation in the YZ plane. $\frac{\partial \vec{E}_0}{\partial y} = \frac{\partial \vec{E}_0}{\partial z} = 0$, $\frac{\partial \vec{B}_0}{\partial y} = \frac{\partial \vec{B}_0}{\partial z} = 0$. Since $\vec{\nabla} \cdot \vec{E} = 0$, $\frac{\partial E_x}{\partial x} = 0$, $\frac{\partial E_y}{\partial y} = 0$, $\frac{\partial E_z}{\partial z} = 0$ it follows that on differentiating partially with respect to x, $E_{0x} = 0$. Similar use of $\vec{\nabla} \cdot \vec{B} = 0$ leads to $B_{0x} = 0$, establishing the wave as purely transverse. Further, from Eq. 5.24, $B_0 = \frac{E_0}{c}$. Accordingly we write the travelling fields as

$$\vec{E}\,(\vec{r}, t) = \hat{e} E_0 e^{i\left(\omega t - \vec{k} \cdot \vec{r}\right)} \tag{5.35}$$

$$\vec{B}\,(\vec{r}, t) = \left(\vec{k} \times \hat{e}\right) \frac{E_0}{c} e^{i\left(\omega t - \vec{k} \cdot \vec{r}\right)} \tag{5.36}$$

Taking the real parts, the fields of the wave are given by

$$\vec{E}\,(\vec{r}, t) = \hat{e} E_0 \cos\left(\omega t - \vec{k} \cdot \vec{r}\right) \tag{5.37}$$

$$\vec{B}\,(\vec{r}, t) = \left(\vec{k} \times \hat{e}\right) \frac{E_0}{c} \cos\left(\omega t - \vec{k} \cdot \vec{r}\right) \tag{5.38}$$

5.3.1 Energy Density in the Travelling Wave

Per unit volume of space, the energy available in the combined electric and magnetic fields is given by

$$u = \frac{1}{2}\epsilon_0 E^2 + \frac{1}{2}\frac{B^2}{\mu_0} \tag{5.39}$$

Since $B = \frac{E}{c}$ and $\sqrt{\epsilon_0 \mu_0} = \frac{1}{c}$, the two energy densities are equal giving for the total energy density

$$u = \epsilon_0 E^2 \tag{5.40}$$

On using the real part of the electric field as given by Eq.5.37, we have

$$u = \epsilon_0 E_0^2 \cos^2(\omega t - kx) \tag{5.41}$$

Poynting vector $\vec{S}$ representing the energy transport defined by

$$\vec{S} = \frac{\left(\vec{E} \times \vec{B}\right)}{\mu_0} \tag{5.42}$$

becomes now

$$\vec{S} = \hat{i} c \epsilon_0 E_0^2 \cos^2(\omega t - kx) \tag{5.43}$$

or

$$\vec{S} = \hat{i} c u \tag{5.44}$$

The linear momentum density of the field (per unit volume) equals

$$\vec{p} = \frac{u}{c} \vec{i} \tag{5.45}$$

Averaging over one cycle of the wave ($\langle \cos^2(\omega t - kx) \rangle = 1/2$) these quantities are given by

$$\langle u \rangle = \frac{1}{2} \epsilon_0 E_0^2 \tag{5.46}$$

$$\left\langle \vec{S} \right\rangle = \frac{1}{2} c \epsilon_0 E_0^2 \hat{i} \tag{5.47}$$

$$\langle \vec{p} \rangle = \frac{1}{2c} \epsilon_0 E_0^2 \vec{i} \tag{5.48}$$

The intensity of the wave is given by

$$I = \langle S \rangle = \frac{1}{2} c \epsilon_0 E_0^2 \tag{5.49}$$

5.4 Propagation of Electromagnetic Waves in Linear Materials

If an electromagnetic wave is travelling in a material medium, the propagation is to be described differently. The Maxwell's equation undergo changes due to the effects of the applied fields in the material. The effects are represented macroscopically by the electric polarization $\vec{P}$ and the magnetization $\vec{M}$. We will consider only materials which are non-conducting, i.e. dielectric materials. With no net charge and no current, Maxwell's equations for the electric and magnetic fields in the material become

$$\vec{\nabla} \cdot \vec{D} = 0 \tag{5.50}$$

$$\vec{\nabla} \cdot \vec{B} = 0 \tag{5.51}$$

$$\vec{\nabla} \times \vec{E} = -\frac{\partial \vec{B}}{\partial t} \tag{5.52}$$

$$\vec{\nabla} \times \vec{H} = \frac{\partial \vec{D}}{\partial t} \tag{5.53}$$

For a linear material medium, we have

$$\vec{D} = \epsilon \vec{E} \tag{5.54}$$

$$\vec{H} = \frac{\vec{B}}{\mu} \tag{5.55}$$

If the material is homogeneous, with no variation of the electric permittivity ϵ and magnetic permeability μ with position, then the Maxwell's equations become

$$\vec{\nabla} \cdot \vec{E} = 0 \tag{5.56}$$

$$\vec{\nabla} \cdot \vec{B} = 0 \tag{5.57}$$

$$\vec{\nabla} \times \vec{E} = -\frac{\partial \vec{B}}{\partial t} \tag{5.58}$$

$$\vec{\nabla} \times \vec{B} = \mu\epsilon \frac{\partial \vec{E}}{\partial t} \tag{5.59}$$

Now let us take the curl of Eq.5.58 to give

$$\vec{\nabla} \times \vec{\nabla} \times \vec{E} = -\frac{\partial \left(\vec{\nabla} \times \vec{B} \right)}{\partial t} \tag{5.60}$$

In view of Eq.5.59, this gives

$$\vec{\nabla} \times \vec{\nabla} \times \vec{E} = -\frac{\partial}{\partial t} \mu\epsilon \frac{\partial \vec{E}}{\partial t} \tag{5.61}$$

Using the identity of Eq.5.27, and on making use of Eq.5.56, we get

$$\nabla^2 \vec{E} = \mu\epsilon \frac{\partial^2 \vec{E}}{\partial t^2} \tag{5.62}$$

This is the wave equation for the electric field propagating in a linear material characterized by the linear properties ϵ and μ. There

is also a similar equation for the magnetic field $\vec{B}$. The velocity of the waves has the magnitude given by

$$v = \frac{1}{\sqrt{\mu\epsilon}} \tag{5.63}$$

If, further the material is *non-magnetic* (i.e. non-ferromagnetic, non-antiferromagnetic, non-ferrimagnetic!), i.e. diamagnetic or paramagnetic, with μ close to μ_0, we have the wave speed given by

$$v = \frac{1}{\sqrt{\mu_0\epsilon_r\epsilon_0}} = \frac{c}{\sqrt{\epsilon_r}} \tag{5.64}$$

The refractive index n of the material defined by $n = \frac{c}{v}$ is thus equal to $\sqrt{\epsilon_r}$. The energy density, the Poynting vector and the intensity of the wave now are given by

$$u = \frac{1}{2}\epsilon E^2 + \frac{1}{2}\frac{B^2}{\mu} \tag{5.65}$$

$$\vec{S} = \frac{\left(\vec{E} \times \vec{B}\right)}{\mu} \tag{5.66}$$

$$I = \frac{1}{2}v\epsilon E_0^2 \tag{5.67}$$

5.5 Propagation of Electromagnetic Waves in Nonlinear Materials

5.5.1 The Wave Equation

We revert to the Maxwell's equations given by Eq. . Taking the curl of Eq.5.58, we have

$$\vec{\nabla} \times \left(\vec{\nabla} \times \vec{E}\right) = -\frac{\partial\left(\vec{\nabla} \times \vec{B}\right)}{\partial t} = -\frac{\partial\left(\vec{\nabla} \times \mu\vec{H}\right)}{\partial t} \tag{5.68}$$

Using Eq.5.59, this gives

$$\vec{\nabla} \times \left(\vec{\nabla} \times \vec{E}\right) = -\mu\frac{\partial^2\vec{D}}{\partial t^2} \tag{5.69}$$

or on using the earlier vector identity5.27, we have

$$\nabla^2\vec{E} = \mu\frac{\partial^2\vec{D}}{\partial t^2} \tag{5.70}$$

Recalling the definition of the displacement Eq.5.17
to get

$$\nabla^2 \vec{E} = \mu\epsilon_0 \frac{\partial^2 \vec{E}}{\partial t^2} + \mu \frac{\partial^2 \vec{P}}{\partial t^2} \tag{5.71}$$

Since our material now is nonlinear, we write the polarization $\vec{P}$ as a sum of the linear part $\overrightarrow{P^{(1)}}$ and the higher order nonlinear contributions $\overrightarrow{P^{(N)}}$:

$$\overrightarrow{P^{(N)}} = \overrightarrow{P^{(2)}} + \overrightarrow{P^{(3)}} + \overrightarrow{P^{(4)}} + ... \tag{5.72}$$

Thus Eq.5.71 is re-written as

$$\nabla^2 \vec{E} = \mu\epsilon_0 \frac{\partial^2 \vec{E}}{\partial t^2} + \mu \frac{\partial^2 \overrightarrow{P^{(1)}}}{\partial t^2} + \mu \frac{\partial^2 \overrightarrow{P^{(N)}}}{\partial t^2} \tag{5.73}$$

The first two terms on the right hand side of the above equation can be combined and brought to the left hand side as

$$\nabla^2 \vec{E} - \mu_0\epsilon \frac{\partial^2 \vec{E}}{\partial t^2} = \mu_0 \frac{\partial^2 \overrightarrow{P^{(N)}}}{\partial t^2} \tag{5.74}$$

This is the wave equation valid for nonlinear materials. Note that we changed μ to μ_0, as the materials we choose are nonmagnetic. This nonlinear wave equation differs from the linear wave equation in the occurrence of the term on the right hand arising from the nonlinear polarization $\overrightarrow{P^{(N)}}$. It is this term acting as "source" responsible for energy transfer between the coupled propagating waves.

5.5.2 Energy Transfer Rate

The rate at which work is done by an electric field $\vec{E}$ in creating the polarization $\vec{P}$ of a material is given by

$$\frac{dW}{dt} = \left\langle \vec{E} \cdot \frac{d\vec{P}}{dt} \right\rangle \tag{5.75}$$

where the averaging is over one cycle of the alternating electric field. The real parts of the electric field and polarization may be written as

$$\vec{E}\,(\vec{r}, t) = \frac{1}{2}\left[\vec{E}\,(\vec{r})\, e^{-i\omega t} + \vec{E}^{*}\,(\vec{r})\, e^{+i\omega t}\right] \tag{5.76}$$

$$\vec{P}(\vec{r},t) = \frac{1}{2}\left[\vec{P}(\vec{r})\,e^{-i\omega t} + \vec{P}^{*}(\vec{r})\,e^{+i\omega t}\right] \tag{5.77}$$

Note the amplitudes of the field and polarization are written as complex and position-dependent (which could come from the nonlinear wave coupling). The equation for the average power now becomes on use of the above two equations,

$$\frac{dW}{dt} = \frac{1}{4}\langle a + b + c + d\rangle \tag{5.78}$$

where the bracketed terms a, b, c, d are:

$$a = \vec{E}(\vec{r})\,e^{-i\omega t}\cdot(-i\omega)\,\vec{P}(\vec{r})\,e^{-i\omega t} \tag{5.79}$$

$$b = \vec{E}(\vec{r})\,e^{-i\omega t}\cdot(i\omega)\,\vec{P}^{*}(\vec{r})\,e^{+i\omega t} \tag{5.80}$$

$$c = \vec{E}^{*}(\vec{r})\,e^{+i\omega t}\cdot(-i\omega)\,\vec{P}(\vec{r})\,e^{-i\omega t} \tag{5.81}$$

$$d = \vec{E}^{*}(\vec{r})\,e^{+i\omega t}\cdot(+i\omega)\,\vec{P}^{*}(\vec{r})\,e^{+i\omega t} \tag{5.82}$$

Of the four terms on the right, two of them (the first and the last) have angular frequencies -2ω and 2ω. On averaging over a cycle these give vanishing contributions. The second term (b) and the third term (c) are the ones which need to be considered. Then

$$\frac{dW}{dt} = \frac{i\omega}{4}\left\langle \vec{E}\cdot\vec{P}^{*} - \vec{E}^{*}\cdot\vec{P}\right\rangle \tag{5.83}$$

In a linear material, the polarization has the same frequency as the electric field that creates it so that both the above terms give zero contribution. That is not however the case with a nonlinear material. We have learnt in an earlier chapter how to write the Fourier components of polarization of the n^{th} order due to a number of electric fields:

$$\vec{P}^{(n)}(\vec{r},\omega) = \epsilon_0\chi^{(n)}(-\omega;\omega_1,\omega_2,..,\omega_n)\,\hat{e}_1\hat{e}_2..\hat{e}_n E_1..E_n e^{-i\left(\vec{k}_1+..\vec{k}_n\right)\cdot\vec{r}} \tag{5.84}$$

where each electric field is given by

$$\vec{E}(\vec{r},\omega_i) = \hat{e}_i E_i e^{-i\hat{k}_i\cdot\vec{r}} \tag{5.85}$$

and the angular frequency ω of the polarization satisfies the photon energy conservation law:

$$\omega = \omega_1 + \omega_2 + ... + \omega_n \tag{5.86}$$

For effective energy transfer to occur over the non-linear material sample, the power which is proportional to $\left(\vec{E}\cdot\vec{P}^{*}-\vec{E}^{*}\cdot\vec{P}\right)$ should not be a varying function of position $\vec{r}$. In other words, the wave vector k should satisfy the linear momentum conservation condition:

$$\vec{k}-\left(\vec{k}_1+\vec{k}_2+..+\vec{k}_n\right)=0 \tag{5.87}$$

This condition is the well-known 'phase matching condition'.

5.6 Three Wave Mixing

Recall the wave equation Eq.5.74 for nonlinear materials

$$\nabla^2\vec{E}=\mu_0\epsilon\frac{\partial^2\vec{E}}{\partial t^2}+\mu_0\frac{\partial^2\overrightarrow{P^{(N)}}}{\partial t^2} \tag{5.88}$$

We will now consider how three plane monochromatic waves propagating along the X - axis in such a material interact. Let these waves be labelled $1,2,3$ have angular frequencies $\omega_1,\omega_2,\omega_3$ respectively and respective angular wave numbers k_1,k_2,k_3. Further we label their Cartesian components using suffixes i,j, and k. The equations of these waves are

$$E_{1i}(x,t)=\frac{1}{2}\left[E_{1i}(x)\,e^{i(\omega_1 t-k_1 x)}+c.c.\right] \tag{5.89}$$

$$E_{2j}(x,t)=\frac{1}{2}\left[E_{2k}(x)\,e^{i(\omega_2 t-k_2 x)}+c.c.\right] \tag{5.90}$$

$$E_{3k}(x,t)=\frac{1}{2}\left[E_{3j}(x)\,e^{i(\omega_3 t-k_3 x)}+c.c.\right] \tag{5.91}$$

where c.c. means the complex conjugate of the preceding term. Since the waves are all travelling in the $+X$ direction , the field Cartesian components i,j,k can only refer to either y or z components.

At this stage let us emphasize that the waves would be travelling without any interaction between them if the material were linear. Further, if the material is non-conducting, there would be no change in the field amplitudes with position x, as there is no current. On the other hand, if the material were a conducting material ($\sigma\neq 0$), there would be energy loss from the dissipation mechanisms even in a linear material. And the field amplitudes would decay exponentially as the wave travels forward. By taking only nonconducting

materials, we are avoiding the complication due to such linear energy changes with position.

The amplitudes of our waves do change with position because we have a nonlinear material and the nonlinear polarization couples the waves permitting energy transfer between them. To deduce the position dependence of the amplitudes, we proceed as follows. The Cartesian component i of the nonlinear polarization at the angular frequency $\omega_1 = \omega_3 - \omega_2$ is given by

$$P_i^{(\omega_1)}(x,t) = \epsilon_0 \chi_{ijk} E_{3j} E_{2k}^* e^{i\{(\omega_3-\omega_2)t-(k_3-k_2)x\}} + c.c. \tag{5.92}$$

Consider the first term of the nonlinear wave equation, $\nabla^2 E_{1i}(x,t)$. We may note that since the plane wave is travelling in the x direction, there would be no variation with the y and z directions: $\frac{\partial}{\partial y}E_{1i}(x,t) = \frac{\partial}{\partial z}E_{1i}(x,t) = 0$, with the result

$$\frac{\partial^2}{\partial x^2}E_{1i}(x,t) = \frac{\partial^2}{\partial x^2}\left[\frac{1}{2}E_{1i}(x)\, e^{i(\omega_1 t - k_1 x)} + c.c.\right] \tag{5.93}$$

or

$$\nabla^2 E_{1i} = \frac{1}{2}\left[\frac{\partial^2 E_{1i}}{\partial x^2} - k_1^2 E_{1i} - 2ik_1\frac{\partial E_{1i}}{\partial x}\right] e^{i(\omega_1 t - k_1 x)} + c.c. \tag{5.94}$$

5.6.1 An Approximation

As a simplifying approximation, we assert that the amplitude of the waves change at a rate such that the change in the gradient of the wave envelope with respect to x over one wavelength λ is negligible: $\left(\frac{\partial}{\partial x}\frac{\partial E}{\partial x}\right)\lambda \ll \frac{\partial E}{\partial x}$ or in terms of the angular wave number k, the approximation implies that

$$\frac{\partial^2 E_{1i}}{\partial x^2} \ll k_1 \frac{\partial E_{1i}}{\partial x} \tag{5.95}$$

Thus in Eq.5.94, we omit the $\frac{\partial^2 E_{1i}}{\partial x^2}$ term in comparison to the first derivative term. The nonlinear wave equation Eq.5.88 has the left hand side then given by

$$\nabla^2 \overrightarrow{E_{1i}} = -\frac{1}{2}\left[k_1^2 E_{1i} + 2ik_1\frac{\partial E_{1i}}{\partial x}\right] e^{i(\omega_1 t - k_1 x)} + c.c. \tag{5.96}$$

We turn to the terms on the right hand side of Eq.5.88: The first term is

$$\mu_0\epsilon_1\frac{\partial^2\overrightarrow{E}_{1i}}{\partial t^2} = \mu_0\epsilon_1\frac{\partial}{\partial t}\frac{1}{2}\left[i\omega_1 E_{1i}e^{i(\omega_1 t-k_1 x)} + c.c.\right] \tag{5.97}$$

$$= -\frac{1}{2}\left[\mu_0\epsilon_1\omega_1^2 E_{1i}e^{i(\omega_1 t-k_1 x)} + c.c.\right] \tag{5.98}$$

where ϵ_1 is the permittivity of the material at the angular frequency ω_1. Since the phase velocity of the wave 1 is given by $v_1 = \frac{1}{\sqrt{\mu_0\epsilon_1}}$ and $v_1 = \frac{\omega_1}{k_1}$, we have $\mu_0\epsilon_1\omega_1^2 = k_1^2$ and the above equation becomes

$$\mu_0\epsilon_1\frac{\partial^2\overrightarrow{E}_{1i}}{\partial t^2} = -\frac{1}{2}\left[k_1^2 E_{1i}e^{i(\omega_1 t-k_1 x)} + c.c\right] \tag{5.99}$$

This is just equal to the first term on the right hand side of Eq.5.96. Since these appear on either side of the nonlinear wave equation they cancel each other. Now what is left to be considered is the second term on right hand side of the wave equation Eq.5.88. Using Eq.5.92, we have

$$\mu_0\frac{\partial^2 P_{1i}}{\partial t^2} =$$

$$\mu_0\epsilon_0\chi_{ijk}E_{3j}(x)\,E_{2k}^*(x)\left\{i(\omega_3-\omega_2)\right\}^2 e^{i\{(\omega_3-\omega_2)t-(k_3-k_2)x\}} + c.c.$$

$$= -\mu_0\epsilon_0\omega_1^2\chi_{ijk}E_{3j}(x)\,E_{2k}^*(x)\,e^{i\{\omega_1 t-(k_3-k_2)x\}} + c.c. \tag{5.100}$$

wherein we have made use of the relation $\omega_3 - \omega_2 = \omega_1$. Now equating the two remaining terms on either side of the nonlinear wave equation, (i.e. we are omitting the first term $k_1^2 E_{1i}$ term of Eq.5.96 and the term given by Eq.5.97), we get

$$-ik_1\frac{\partial E_{1i}}{\partial x}e^{i(\omega_1 t-k_1 x)} + c.c. =$$

$$-\mu_0\epsilon_0\omega_1^2\chi_{ijk}E_{3j}(x)\,E_{2k}^*(x)\,e^{i\{\omega_1 t-(k_3-k_2)x\}} + c.c. \tag{5.101}$$

Or upon rearrangement and cancelling the common factor,

$$\frac{\partial E_{1i}}{\partial x} = \frac{\mu_0\epsilon_0\omega_1^2}{ik_1}\chi_{ijk}E_{3j}(x)\,E_{2k}^*(x)\,e^{-i(k_3-k_2-k_1)x} \tag{5.102}$$

Introducing the phase mismatch term $\Delta k = k_3 - k_2 - k_1$, and using the relation $\mu_0\epsilon_1\omega_1^2 = k_1^2$, the above equation becomes

$$\frac{\partial E_{1i}}{\partial x} = -i\omega_1\sqrt{\frac{\mu_0}{\epsilon_1}}\epsilon_0\chi_{ijk}E_{3j}(x)\,E_{2k}^*(x)\,e^{-i\Delta kx} \tag{5.103}$$

In a similar manner we derive the gradients of the fields for the other two waves, using the same approximations and the same mathematical manipulations:

$$\frac{\partial E_{2k}^*}{\partial x} = i\omega_2 \sqrt{\frac{\mu_0}{\epsilon_2}} \epsilon_0 \chi_{kij} E_{1i}(x) E_{3j}^*(x) e^{i\Delta k x} \tag{5.104}$$

$$\frac{\partial E_{3j}}{\partial x} = -i\omega_3 \sqrt{\frac{\mu_0}{\epsilon_3}} \epsilon_0 \chi_{jik} E_{1i}(x) E_{2k}(x) e^{i\Delta k x} \tag{5.105}$$

In arriving at the above equations, we used the relations $\omega_1 = \omega_3 - \omega_2$ in the equation for the wave 1, $-\omega_2 = \omega_1 - \omega_3$ in the equation for the wave 2 and $\omega_3 = \omega_1 + \omega_2$ in the equation for the wave 3.

5.7 Second Harmonic Generation

We are now ready to discuss second harmonic generation as a special case of the three wave mixing processes, with $\omega_1 = \omega_2 = \omega$ and $\omega_3 = 2\omega$. In order to deduce the growth of the second harmonic field, we need consider only one of the two fields given by Eq.?? and the Eq.5.105. The analysis becomes simpler if can make the assumption that the field amplitude of the fundamental wave suffers negligible depletion, i.e. $\frac{\partial E_{1i}}{\partial x} = 0$. This is an oversimplification in many a practical case but the analysis has instructive features and we will take up this case first and later remove this restriction by allowing for the depletion of the fundamental pump wave. Since this assumption means that the field amplitude $E_{1i}(x)$ remains constant not varying with position x, we need to integrate only the third equation for E_{3j}. Writing ω_3 as 2ω, this equation becomes

$$\frac{dE_{3j}}{dx} = -i2\omega \sqrt{\frac{\mu_0}{\epsilon_3}} \epsilon_0 \chi_{jik} E_{1i} E_{2k} e^{i\Delta k x} \tag{5.106}$$

We now wish to integrate the above equation from $x' = 0$ to $x' = x$. Remembering that the two fields E_1 and E_2 both belong to the fundamental frequency and so do not change with position, we have

$$\int dE_{3j} = -i2\omega \sqrt{\frac{\mu_0}{\epsilon_3}} \epsilon_0 \chi_{jik} E_{1i} E_{2k} \int_0^x e^{i\Delta k x'} dx' \tag{5.107}$$

Integration yields

$$E_{3j} = E_{3j}(0) - i2\omega \sqrt{\frac{\mu_0}{\epsilon_3}} \epsilon_0 \chi_{jik} E_{1i} E_{2k} \frac{e^{i\Delta k x'}}{i\Delta k} \Big|_0^x \tag{5.108}$$

If at the input end, $x' = 0$, there is zero second harmonic field, $E_{3j}(0) = 0$. To obtain the wave intensity, we need the square of the field amplitude:

$$E_{3j}(x) E_{3j}^{*}(x) = 4\omega^2 \frac{\mu_0}{\epsilon_3} \epsilon_0^2 \chi_{jik}^2 E_{1i}^2 E_{2k}^2 \left(\frac{e^{i\Delta kx} - 1}{i\Delta k}\right)\left(\frac{e^{-i\Delta kx} - 1}{-i\Delta k}\right) \tag{5.109}$$

$$E_{3j}^2(x) = 4\omega^2 \frac{\mu_0}{\epsilon_3} \epsilon_0^2 \chi_{jik}^2 E_{1i}^2 E_{2k}^2 x^2 \frac{\sin^2\left(\frac{\Delta kx}{2}\right)}{\left(\frac{\Delta kx}{2}\right)^2} \tag{5.110}$$

We can now write down the intensity of second harmonic wave as a function of position:

$$I_{2\omega} = \frac{1}{2}\sqrt{\frac{\epsilon_3}{\mu_0}} E_{2\omega}^2 \tag{5.111}$$

Eq.5.110 then gives

$$I_{2\omega} = 2\sqrt{\frac{\mu_0}{\epsilon_3}} \omega^2 \epsilon_0^2 \chi_{jik}^2 E_{1i}^2 E_{1k}^2 x^2 \frac{\sin^2\left(\frac{\Delta kx}{2}\right)}{\left(\frac{\Delta kx}{2}\right)^2} \tag{5.112}$$

To find what fraction of the energy of the incident wave is transferred to the harmonic wave, we need the intensity of the fundamental frequency wave, which is

$$I_{\omega} = \frac{1}{2}\sqrt{\frac{\epsilon_1}{\mu_0}} E_{1i} E_{1k}^{*} \tag{5.113}$$

so that the efficiency of the conversion under the approximation of no depletion of the pump wave, is given by

$$\frac{I_{2\omega}}{I_{\omega}} = 8\sqrt{\frac{\mu_0}{\epsilon_0}} \omega^2 \frac{\chi_{jik}^2}{n^3} I_{\omega} \frac{\sin^2\left(\frac{\Delta kx}{2}\right)}{\left(\frac{\Delta kx}{2}\right)^2} x^2 \tag{5.114}$$

We note that for a given length x of the crystal sample, the efficiency of conversion is proportional to χ^2, the square of the nonlinear susceptibility and to the intensity I_{ω} of the fundamental wave. Further, the efficiency oscillates as a function of the position x for $\Delta k \neq 0$. Maximum efficiency is realized if the phase matching condition $\Delta k = 0$ is satisfied. Since $\Delta k = k_3 - k_2 - k_1 = k_3 - 2k_1$, the phase matching condition may be phrased as

$$k_{2\omega} = 2k_{\omega} \tag{5.115}$$

which may be alternatively written as

$$\Delta k = \frac{2\omega}{c}\left(n_{2\omega} - n_{\omega}\right) \tag{5.116}$$

on using the relation $k_{2\omega} = \frac{2\omega}{v_{2\omega}} = \frac{2\omega c}{n_{2\omega}}$ for the harmonic and $k_{\omega} = \frac{\omega}{v_{\omega}} = \frac{\omega c}{n_{\omega}}$ for the fundamental frequency waves. The factor $f = \frac{\sin^2\left(\frac{\Delta k x}{2}\right)}{\left(\frac{\Delta k x}{2}\right)^2}$ has an oscillation period called the "coherence length" l_c defined by $l_c = \frac{2\pi}{\Delta k}$. Eq.5.116 then leads to the expression for the coherence length

$$l_c = \frac{\lambda}{n_{2\omega} - n_{\omega}} \tag{5.117}$$

What is this coherence length? We can see that when the phase matching condition is not satisfied, the length of the crystal over which we can realize the maximum cumulative energy transfer, is the spatial period of the oscillations arising due the factor f.

5.7.1 Phase Matching Schemes

Phase matching in second harmonic generation facilitates maximum energy transfer from the pump field to the harmonic field. Eq.5.115 tells us that the wave number of the harmonic wave must be double the wave number of the fundamental wave. ●r the wavelength of the second harmonic wave must be half the wavelength of the pump wave. Which is the case when the phase velocities are equal for these two waves. Accordingly the refractive indices for the two frequencies must also be equal:

$$n_{2\omega} = n_{\omega} \tag{5.118}$$

There are two schemes, denoted as Scheme I and Scheme II, possible for realizing the phase matching condition. First we detail Scheme I.

Scheme I

In this scheme, the optical anisotropy of uniaxial crystals is exploited. In a negative uniaxial crystal, like KH_2PO_4, the refractive index of the extraordinary ray is less than that of the ordinary ray at any wavelength for a given direction of travel. As may be expected, in normal dispersion, the refractive index (for both the rays) increases with increasing frequency. As a consequence, when both the fundamental and harmonic waves are of the same kind (either

ordinary or extraordinary), phase matching can not occur. However, if we launch one of the waves, say, the pump wave as an ordinary ray, and the second harmonic wave is extraordinary ray, then the refractive indices can be matched for a certain direction in the crystal, because the speed of the ordinary ray is isotropic whereas the extraordinary ray speed depends on the direction of travel in the crystal. Let θ be the angle made by the rays with the optical axis of the crystal. Then the refractive index of the extraordinary ray $n^e(\theta)$ depends on the angle θ according to the relation

$$\frac{1}{\{n^e(\theta)\}^2} = \frac{\cos^2\theta}{(n^0)^2} + \frac{\sin^2\theta}{(n^e)^2} \tag{5.119}$$

We can choose an angle θ_c, at which the refractive index $n^e_{2\omega}(\theta_c)$ of the extraordinary ray at the second harmonic frequency 2ω equals the refractive index $n^0_\omega(\theta)$ of the ordinary ray at the fundamental frequency ω. This means the angle θ_c should satisfy the equation

$$\frac{\cos^2\theta_c}{(n^0_{2\omega})^2} + \frac{\sin^2\theta_c}{(n^e_{2\omega})^2} = \frac{1}{\{n^0_\omega\}^2} \tag{5.120}$$

Solving for this phase matching angle, θ_c, we find that

$$\sin^2\theta_c = \frac{\frac{1}{(n^0_\omega)^2} - \frac{1}{(n^0_{2\omega})^2}}{\frac{1}{(n^e_{2\omega})^2} - \frac{1}{(n^0_{2\omega})^2}} \tag{5.121}$$

We illustrate this scheme by considering the fundamental wavelength $\lambda_1 = 1.00\ \mu$ so that the wavelength of the second harmonic is $\lambda_2 = 0.50\ \mu$. At these wavelengths, the refractive indices of KDP crystal are:

$\lambda_1(\omega) = 1.00\ \mu$: $\quad n^0_\omega = 1.496044,\ n^e_\omega = 1.460993$

$\lambda_2(2\omega) = 0.50\ \mu$: $\quad n^0_{2\omega} = 1.514928,\ n^e_{2\omega} = 1.472486$

Using these data in Eq.5.121, we get $\theta_c = 41.2^0$.

Scheme II

In an alternative method, phase matching is accomplished by choosing one of the input waves at the angular frequency ω as an ordinary ray and the other two as extraordinary rays. The frequency-doubled wave will be extraordinary. Now the phase matching condition ($\Delta k = k_3 - k_2 - k_1 = 0$) becomes

$$k^e_{3,2\omega} - k^o_{2,\omega} - k^e_{1,\omega} = 0 \tag{5.122}$$

Since the refractive index of the extraordinary ray depends on the direction of propagation, which makes an angle θ wit the optic axis of the crystal, this condition may be written as

$$k^{e}_{2\omega}(\theta) = k^{\bullet}_{2,\omega} + k^{e}_{1,\omega}(\theta) \tag{5.123}$$

With the relation $k = \frac{\omega n}{c}$, this becomes

$$\frac{2\omega}{c} n^{e}_{2\omega}(\theta) = \frac{\omega}{c} n^{o}_{\omega} + \frac{\omega}{c} n^{e}_{\omega}(\theta) \tag{5.124}$$

or

$$n^{e}_{2\omega}(\theta) = \frac{1}{2}\left[n^{o}_{\omega} + n^{e}_{\omega}(\theta)\right] \tag{5.125}$$

Substituting the expressions for the angle-dependence of the refractive indices in the above equation yields as the matching condition of *Scheme II as*

$$\left[\frac{\cos^2\theta_c}{\{n^{o}_{2\omega}\}^2} + \frac{\sin^2\theta_c}{\{n^{e}_{2\omega}\}^2}\right]^{-1/2} = \frac{1}{2}\left\{n^{o}_{\omega} + \left[\frac{\cos^2\theta_c}{\{n^{o}_{\omega}\}^2} + \frac{\sin^2\theta_c}{\{n^{e}_{\omega}\}^2}\right]\right\}^{-1/2} \tag{5.126}$$

5.7.2 Accurate Treatment of Second Harmonic Generation

We have solved the coupled equations describing three wave mixing under the approximation that the depletion of the pump wave is negligible. We shall now remove this unnecessary limitation and solve the equations more generally with the pump wave transferring appreciable amounts of energy to the harmonic wave.

In order to facilitate an easy handling of the equations, we introduce new field terms F_1, F_2, F_3 defined by

$$F_1 = \sqrt{\frac{n_1}{\omega_1}} E_1, F_2 = \sqrt{\frac{n_2}{\omega_2}} E_2, F_3 = \sqrt{\frac{n_3}{\omega_3}} E_3 \tag{5.127}$$

We recall that the intensity of a wave is the energy per unit area flowing per second. Therefore intensity is also equal to the photon flux multiplied by photon energy. Photon flux is the number of photons per unit area passing per second. As such, intensity is proportional to photon flux at a given frequency. Intensity being proportional to the square of the field amplitude $\left|\vec{E}\right|^2$, we see our new field variables are such that $F^2 \propto \frac{E^2}{\omega}$ and so are proportional to the photon flux!

In terms of these new variables F, we may re-write the coupled wave equations

$$\frac{dF_1}{dx} = -i\sqrt{\frac{\mu_0\omega_1\omega_2\omega_3}{n_1n_2n_3}}\epsilon_0\chi F_1^* F_3 e^{-i\Delta kx} \tag{5.128}$$

$$\frac{dF_2}{dx} = i\sqrt{\frac{\mu_0\omega_1\omega_2\omega_3}{n_1n_2n_3}}\epsilon_0\chi F_1 F_3 e^{i\Delta kx} \tag{5.129}$$

$$\frac{dF_3}{dx} = -i\sqrt{\frac{\mu_0\omega_1\omega_2\omega_3}{n_1n_2n_3}}\epsilon_0\chi F_1 F_2 e^{i\Delta kx} \tag{5.130}$$

Introducing the parameter

$$\alpha = \sqrt{\frac{\mu_0\omega_1\omega_2\omega_3}{n_1n_2n_3}}\epsilon_0\chi \tag{5.131}$$

the above equations may appear as

$$\frac{dF_1}{dx} = -i\alpha F_1^* F_3 e^{-i\Delta kx} \tag{5.132}$$

$$\frac{dF_2}{dx} = i\alpha F_1 F_3 e^{i\Delta kx} \tag{5.133}$$

$$\frac{dF_3}{dx} = -i\alpha F_1 F_2 e^{i\Delta kx} \tag{5.134}$$

For analyzing second harmonic generation, we know that we need to consider only the first and last of the above three equations. Further, if the phase matching condition is met, i.e. $\Delta k = 0$, then these equations become

$$\frac{dF_1}{dx} = -i\alpha F_1^* F_3 \tag{5.135}$$

$$\frac{dF_3}{dx} = -i\alpha F_1^2 \tag{5.136}$$

Let us choose the pump wave at the input end ($x = 0$) to be real. Then $F_1(0)$ and hence $F_1(x)$ become real giving

$$\frac{dF_1}{dx} = -i\alpha F_1 F_3 \tag{5.137}$$

$$\frac{dF_3}{dx} = -i\alpha F_1^2 \tag{5.138}$$

To obtain the solutions of these equations, we set $S_3 \equiv -iF_3$. The two above equations become then

$$\frac{dF_1}{dx} = \alpha F_1 S_3 \tag{5.139}$$

$$\frac{dS_3}{dx} = -\alpha F_1^2 \tag{5.140}$$

These are consistent with

$$\frac{d}{dx}\left(F_1^2 + S_3^2\right) = 0 \tag{5.141}$$

or

$$F_1^2 + S_3^2 = F_1^2(0) \tag{5.142}$$

since there is no harmonic field at the input end ($S_3^2(0) = 0$). This results in the equation

$$\frac{dS_3}{dx} = -\alpha\left(F_1^2(0) - S_3^2\right) \tag{5.143}$$

or

$$\frac{dS_3}{F_1^2(0) - S_3^2} = -\alpha dx \tag{5.144}$$

Integrating from $x = 0$, $S_3(0) = 0$, to $x = x$, $S_3(x)$, we have

$$\frac{1}{F_1(0)} \tanh^{-1}\left(\frac{S_3^2}{F_1^2(0)}\right) = -\alpha x \tag{5.145}$$

or

$$S_3(x) = F_1(0)\sqrt{\tanh\left(\alpha x F_1(0)\right)} \tag{5.146}$$

The conversion efficiency is thus given by

$$\frac{|S_3(x)|^2}{|F_1(0)|^2} = \tanh^2\left[\alpha F_1(0)\, x\right] \tag{5.147}$$

The maximum conversion efficiency (unity) is reached when the argument of the $\tanh^2$ function tends to infinity.

5.8 Explorations

1. The simplest experiment in nonlinear optics is perhaps focusing a high intensity laser beam from a Neodymium:YAG laser tightly using an appropriate lens as the beam propagates in air. Blue-violet splashes of light can be observed near the focal point. What could be happening here? (You will also hear some cracking sound, what is it due to, by the way?) The next simple experiment would be to focus the same beam to a sugar crystal when green flashes of light can be seen at appropriate orientations of the crystal. How is this phenomenon related to the earlier one? (*A word of caution: it is not advisable to bring in crystals of several faces with arbitrary orientation into the laser beam, for example, while trying out such an experiment. This can result in the laser beam getting reflected in several unexpected directions and it is likely that one of the reflected rays might get unto your eyes, damaging them instantaneously, without any warning*)

2. Obtain, from fundamental considerations, an expression for the rate at which work W is done by an electric field $\vec{E}$ of a monochromatic light wave of frequency ω in creating the polarization $\vec{P}$ in a material. Write down the real and imaginary part of the field as well as the polarization explicitly and show that this can be written as $\frac{dW}{dt} = \frac{i\omega}{4}\left\langle \vec{E}\cdot\vec{P}^{*} - \vec{E}^{*}\cdot\vec{P}\right\rangle$ here the averaging is done over a period of the electromagnetic wave.

3. Suggest how the second order susceptibility of a medium can be determined by measuring the intensities of the fundamental and the second harmonic light waves in a second harmonic generation experiment. What are the other parameters required for this calculation? Is there any way to arrive at a specific tensor component of the susceptibility involved, by this method?

4. What are the steps to be taken in order to obtain the best efficiency of power conversion in a second harmonic generation (SHG) experiment?

5. Following the method adopted in this chapter, arrive at an expression for the intensity at a frequency $\omega_3 = \omega_1 + \omega_2$ when monochromatic waves of two frequencies ω_1 and ω_2 interact in a second order nonlinear optical medium.

6. The process of difference frequency generation has certain features very different from those of SHG and the general case of sum frequency generation. Consider the process of *optical parametric oscillation* in which a strong *pump wave* at frequency ω_p mixes with a *signal wave* of frequency ω_s , resulting in the generation of an *idler* wave of frequency $\omega_i = \omega_p - \omega_s$. Write out the individual wave forms and obtain an expression for the nonlinear polarization at the frequency ω_i . Substitute this in the nonlinear wave equation and show (using a treatment similar to that in the case of SHG worked out in the text) that the intensity of the idler increases as $\sinh^2(gx)$ where g is some gain factor which contains the corresponding $\chi^{(2)}$ and x is the path length in the nonlinear medium along the direction of beam propagation. What is the physical significance of this result? Compare the expression for intensity with that obtained in the previous problem on sum-frequency-generation.

7. Consider a second harmonic generation process when the fundamental wave at 1.00 μ passing through a crystal with the difference between the ordinary and extra ordinary refractive indices $n^{2\omega} - n^{\omega} = 0.01$.What would be the coherence length involved? What should the coherence length if it is desired to increase the intensity at the second harmonic wavelength by a factor of 1000?

8. What is the relation between refractive index and the angle of propagation of light in a positive uniaxial crystal? Depict this in a diagram. Draw such diagrams for both ordinary and extraordinary rays corresponding to both fundamental and the second harmonic waves in the case of second harmonic generation. Hence show geometrically how phase matching is possible by angle tuning.

9. Consider a laser beam of wavelength $\lambda = 1\mu$ incident on a medium with a reasonably large second order susceptibility. Given that the values of the *ordinary* and *extra-ordinary* refractive indices of the medium at the fundamental and the

second harmonic are given respectively as $n_{\omega}^{O} = 1.496044$, $n_{\omega}^{e} = 1.460993$, $n_{2\omega}^{O} = 1.514928$ and $n_{2\omega}^{e} = 1.472486$, find the angle for phase matching.

10. A significant technological advance of the past decade is the realization of tunable solid state lasers such as the Ti:Sapphire laser. Look up references such as how a Ti: Sapphire laser works. What are optical parametric oscillators and why are relevant here? What is their significance in science and technology?

11. We have seen that second order nonlinear optical processes do not occur in a medium with inversion symmetry. This is based on the dipole approximation in light-matter interaction, which you learn in electromagnetic theory. If this symmetry can be broken somehow, SHG would be possible even in such media. Suggest some possible approaches to make this possible.

Chapter 6

Optical Phase Conjugation and Bistability

"Beauty is Truth's smile when she beholds her own face in a perfect mirror".

Rabindranath Tagore

There is a lot to reflect upon, when we talk about mirrors.

Learning Objectives

- Identification of the aspect of time reversal involved in the phenomenon of phase conjugation.
- Design of an experimental setup for demonstrating optical phase conjugation.
- Explanation of the applications of optical phase conjugation.
- Identification of the technique of distortion-healing of wavefronts.
- Analysis of photonic switching using a nonlinear Fabry-Perot etalon.

6.1 Optical Phase Conjugation

Wave mixing phenomena based on third order nonlinearity are quite diverse compared to those involving second order nonlinearity. Second order phenomena are exhibited only by crystals lacking center of symmetry whereas third order phenomena are not inhibited by any symmetry constraint and can, in principle, be exhibited by almost any material, in any physical form if it has sufficiently strong third order nonlinearity. Apart from third harmonic generation, several other phenomena such as optical phase conjugation, bistability and self focussing are governed by the third order optical nonlinearity. Optical phase conjugation [Stepanov et al, 1971, Icoerdman, 1970, Zel'Dovich et al 1972, Shkunov and Zel'Dovich, 1985] is a peculiar kind of four-wave mixing process of immense fundamental interest as well as application potential [Pepper, 1986]. What makes it very interesting is the prospect of achieving time reversal (in some sense), as phase conjugation in quantum mechanics is equivalent to time reversal. Let us examine what this implies and how this comes about.

6.1.1 Phase Conjugation as Time Reversal

There exist several pointers that remind us in daily life that time moves only forwards and thus we have some sort of awareness of the 'arrow of time', a phrase often used to denote the fact that cause always precedes its effect. One of the arrows of time is supposed to be the increasing entropy. We can always tell when a movie is being run backwards because then the events go in a manner that we are not familiar within normal daily life. This is because we are surrounded by complicated systems with a very large number of degrees of freedom, often undergoing irreversible processes and thus entropy keeps increasing. This does not happen in a reversible process and then this arrow can not exist. Further, it is the loss of energy which actually implies its degradation into a non-available form that leads to irreversibility. These two aspects, namely the large number of degrees of freedom and the loss of energy make time reversal difficult in a complicated thermodynamic system. However, in a simple optical system with transparent components, for example, a system consisting of a beam passing through a glass slab, the laws of

physics do not change if the direction of the beam is reversed. In some sense, the system permits a time reversal or possesses a time reversal symmetry. This involves quite a few degrees of freedom to describe and has a very small loss of energy. Thus one might expect time reversal to be a feasible proposition in optical system.

We shall try to understand how optical phase conjugation is realized and in what sense it can be described as time reversal. Optical phase conjugation is an important topic discussed in all books on nonlinear optics and several papers including reviews are available on this subject [for example, Yariv, 1978, Zel'Dovich 1978, Giuliano, April 1981, Hellwarth, 1977, Pepper, 1982, He and Liu, 2000, Pepper, 1982, He, 2002, Gu, 2003]. Hence the intention here is to provide a clear conceptual understanding to the basic ideas and not to provide a comprehensive coverage on all aspects of phase conjugation.

We have basically two different kinds of operators in quantum mechanics– those involving the imaginary number i and those which do not involve i.

Consider the magnitude of an electric field $\vec{E}(x,t)$ of a plane sinusoidal electromagnetic wave travelling in the $+\widehat{e}_x$ direction, given by

$$E(x,t) = A\exp i(-kx - \omega t) \tag{6.1}$$

where A is the real amplitude, k is the angular wave number and ω the angular frequency of the wave. Assuming negligible loss in amplitude, the phase conjugated wave can be represented as

$$E_{conj}(x,t) = A\exp[-i(-kx - \omega t)], \tag{6.2}$$

if it were to propagate in the reverse direction.Or,

$$E_{conj}(x,t) = A\exp[i(kx + \omega t)] \tag{6.3}$$

which may be expressed as

$$E_{conj}\,(x,t) = A\exp i\{kx - \omega(-t)\}. \tag{6.4}$$

Now this is equivalent to $E(x,-t)$, time-reversed replica of the original wave, traveling in the opposite direction ($-\widehat{e}_x$ direction). Thus

the effect of phase conjugation would be equivalent to time reversal. The conjugated wave is a time-reversed replica of the incident wave, traveling in the opposite direction.

6.1.2 Phase Conjugation through Four-Wave-Mixing

Optical phase conjugation (OPC) can be understood on the basis of the theory of wave mixing outlined in an earlier chapter, where three-wave-mixing was described. The treatment can be extended to the interaction of the three input beams through nonlinear wave mixing. Here we have a case of four-wave-mixing, where three input waves propagate in a medium, leading to the generation of a fourth wave. For the sake of simplicity, we consider the case of degenerate four wave mixing (DFWM) where the four waves involved have the same optical frequency.

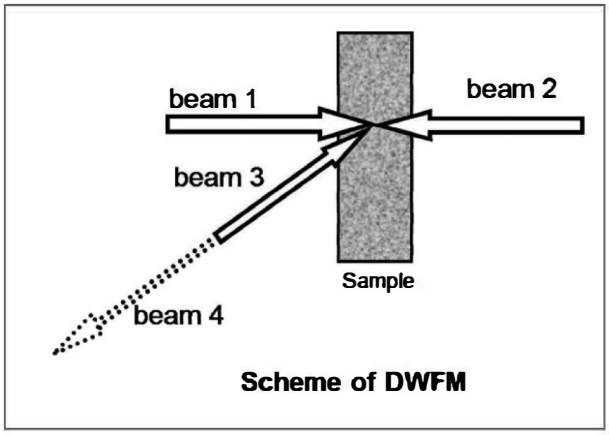


Figure 6.1: A scheme for optical phase conjugation through DFWM

Consider a geometry where two of the three waves mixing in a medium are counter propagating, as depicted in figure 6.1. The waves are then described by

$$E_{1j} = A_{1j}(z)e^{i(\omega t - k_1 z)} \tag{6.5}$$

$$E_{2k} = A_{2k}(z)e^{i(\omega t + k_2 z)} \tag{6.6}$$

$$E_{3l} = A_{3l}(z)e^{i(\omega t - k_3 z)} \tag{6.7}$$

where j, k and l are the Cartesian components of the electric vectors of the three input light waves of the same frequency ω. Here k_1, k_2 and k_3 are the magnitudes of the wave vectors of the three input waves with amplitudes $A_{1j}(z)$, $A_{2k}(z)$ and $A_{3l}(z)$ respectively, where the space-dependence arises from the wave mixing process. The induced polarization, of the third order, is given by

$$P_i^{(3)}(z,t) = \frac{3}{4}\varepsilon_0 \chi_{ijkl}^{(3)} A_{1j}(z) A_{2k}(z) A_{3l}^*(z) e^{i(\omega+\omega-\omega)t-(+k_1-k_2+k_3)z} \tag{6.8}$$

This polarization $P_i^{(3)}$generates a new field, $E_4(z,t)$ with the same frequency ω and wave vector the fourth wave (i.e. the output) $k_4 = k_1 + k_2 - k_3$ according to the phase matching condition corresponding to the maximum exchange of energy between the induced polarization in the medium and the radiation field outside the medium. Further, this also implies that the output beam would emerge in a direction exactly opposite to that of the probe beam (beam 3), provided the two pump beams, beam 1 and beam 2 are counter propagating, in accordance with the principle of conservation of momentum. The output field $E_4(z,t)$ satisfies the wave equation

$$\nabla^2 \vec{E}(\vec{r}, t) - \mu_0 \varepsilon \frac{\partial^2 \vec{E}(\vec{r}\ \ t)}{\partial t^2} = \mu_0 \frac{\partial^2 \vec{P}^{(3)}(\vec{r}\ \ t)}{\partial t^2} \tag{6.9}$$

The slowly varying envelope approximation (SWEA), discussed in an earlier chapter, helps us to proceed with a simplified model without much loss of generality at this stage. According to this approximation, the variation in the overall wave envelope $A(z)$ during propagation in the medium through the distance of a wavelength is not much so that the second derivative of $A(z)$ can be neglected in comparison with the product of $\left|\vec{k}\right|$ and the second derivative of $A(z)$ with respect to z, the distance along the line of propagation. i.e.

$$\left|\frac{\partial^2}{\partial z^2} A(z)\right| = \left|\vec{k}\right| \frac{\partial}{\partial z} |A(z)| \tag{6.10}$$

This would imply

$$ik_3 \frac{\partial A_{3l}}{\partial z} = \varepsilon_0 \mu_0 \omega^2 \chi^{(3)}_{ijkl} A_{1j}(z) A_{2k}(z) A^*_{4m}(z) e^{[-i\delta kx]} \tag{6.11}$$

where

$$\delta k = -k_1 - k_2 + k_3 + k_4 \tag{6.12}$$

and

$$ik_3 \frac{\partial A_{4m}}{\partial z} = \varepsilon_0 \mu_0 \omega^2 \chi^{(3)}_{ijkl} A_{1j}(z) A_{2k}(z) A^*_{3l}(z) e^{[i\delta kx]} \tag{6.13}$$

The fourth beam resulting from phase conjugation would then be

$$E_{4m} = A_{4m}(z) e^{i(\omega t - k_4 z)} \tag{6.14}$$

Assuming negligible pump depletion,

$$\frac{\partial A_3}{\partial z} = -i\Gamma A^*_4 \tag{6.15}$$

and

$$\frac{\partial A_4}{\partial z} = i\Gamma A^*_3 \tag{6.16}$$

where

$$\Gamma = \frac{\omega}{2} \left(\frac{\mu}{\epsilon}\right)^{\frac{1}{2}} A_1 A_2, \tag{6.17}$$

is the coupling parameter. The solution is

$$A_{3x} = -i \frac{|\Gamma| \sin(|\Gamma| x)}{\Gamma \cos(|\Gamma| L)} A_4(z) + \frac{\cos(|\Gamma| x[x - L])}{\cos(|\Gamma| L)} A_3(0) \tag{6.18}$$

Now if we design the two input beams, beam 1 and beam 2, to be counter propagating, $k_1 + k_2 = 0$ and hence $k_3 = k_4$ under the condition of phase matching which implies maximum energy transfer between the induced nonlinear polarization within the medium and the field radiated out of the medium. Thus the output beam, beam 4, would propagate in a direction exactly opposite to that of beam 3. The two input beams 1 and 2 are designed to be intense and are denoted as pump beams whereas beam 3 is weaker and is denoted as a *probe* beam. This beam is made to be incident in the medium at a very small angle with the direction of propagation of beam 1 so that the assumption that it propagates along the z-direction is satisfied approximately.

6.1.3 Practical Realization

The process of phase conjugation can be realized through different experimental methods such as degenerate four wave mixing (DWFM) and Brillouin scattering. The former involves interaction between three input waves of the same wavelength inside the experimental medium, as depicted in figure 5.1. Laser beams designated as 1, 2 and 3 in the figure are made to interact simultaneously with the sample which results in the generation of the phase conjugate beam, designated as beam 4, which comes out of the sample. There are different possible geometrical arrangements by which the scheme of DFWM shown in figure 6.1 can be realized in a laboratory and one such experimental set up is shown in figure 6.2 . First of all, it is convenient to derive all the three input beams from a single laser source, which can be done in the case of degenerate four wave mixing. The beam from the laser L is sent through a beam splitter BS which splits the beam into a strong pump beam (beam 1) and a weaker probe beam (beam 3). The pump beam is made to pass through the experimental specimen under study in the form of a transparent film. A plane mirror M kept behind the sample and close to it reflects the beam back into the sample and counter propagates in the sample as the second pump beam (beam 2).

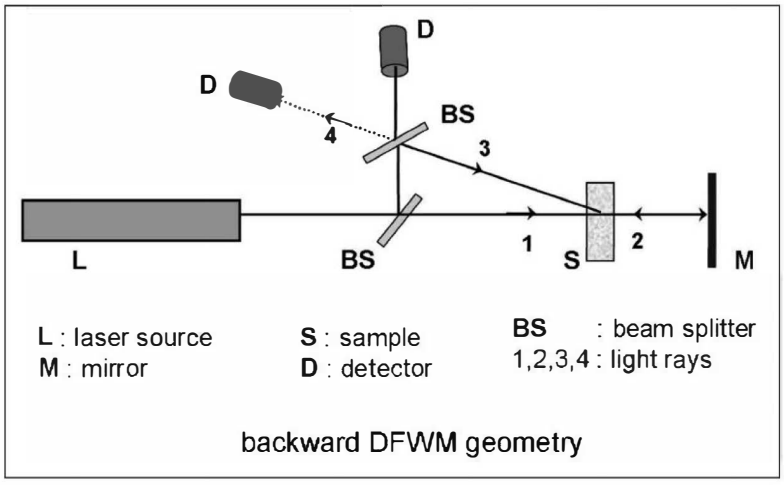


Figure 6.2: Experimental set up for OPC through DWFM

The probe beam, (beam 3), is deflected by a partial mirror so that it passes through the sample. The geometry of the three beams

passing through is designed to have maximum spatial overlap of the three beams within the sample. Further, it is also important to have the maximum temporal overlap of the three input beams occurring within the sample in the case of pulsed laser excitation. The interaction of the three beams results in the generation of a fourth beam (beam 4), which comes out from the region of overlap in a direction exactly opposite to that of the probe beam. This is expected as beam 1 and beam 2 are counter propagating in this geometry and hence phase matching implies that beam 3 and beam 4 also are counter propagating. This set up is suitable for a sample that absorbs weakly at the wavelength used so that beam 2 can be a pump beam of sufficient intensity. The intensities of the pump, probe and phase conjugate beams are measured using appropriately placed optical detectors.

The third order susceptibility can be calculated by a measurement of the intensities of the input and output beams (Caro and Grower 1982). Phase conjugate reflectivity is defined as the ratio

$$R = \left| \frac{A_4(0)}{A_3(0)^*} \right|^2 \tag{6.19}$$

which is used is to estimate the third order susceptibility

$$\chi^{(3)} = \frac{2c^2 n^2 \epsilon_0 \alpha}{3\omega e^{-\alpha L'}(1 - e^{-\alpha L})} \frac{R^{(1/2)}}{I_1}. \tag{6.20}$$

This is applicable for low reflectivities, ~10%. Here c is the speed of light, $L' = \frac{L}{\cos\theta}$ is the interaction length when the sample has a length L along the beam direction and the angle between the input beam 1 and the probe beam is θ . α is the absorption coefficient and I_1 is the intensity of beam 1.

There are certain important considerations for the success of this experiment.

a) It is important for the three interacting beams to have optimal interaction both spatially as well as temporarily. For this, all the three beams must be made to fall on the same spot within the sample. Also, in the case of pulsed lasers, the pulses must be times so that all the three pulses arrive at the spot at the same time and stay for the same duration; at least they should overlap well in time.

b) The optical density of the sample at the wavelength of excitation must be small so that the second beam 2 (which is obtained by reflecting the first beam after its passage through the sample once), also has sufficient intensity.

c) The angle between the pump beam (beam 1) and the probe beam must be optimal. It would be difficult to make this angle very close to zero in view of the finite size of the optical components used. On the other hand, a large angle would shorten the effective interaction length within the sample.

d) It is important to ensure that the beam being observed as the fourth beam is actually the phase conjugate beam and not some beam scattered or reflected from one of the several components being used. This can be tested by noting that this beam disappears when any one of the three incident beams is blocked. It can also be tested for the distortion-healing property of the phase conjugate beam, to be detailed in the next section.

6.1.4 Peculiar Properties of the Phase Conjugate Beam

What makes the phenomenon of phase conjugation exciting is the fact that output beam generated by four wave mixing (beam 4) is a time-reversed replica of the input beam (beam 3, the probe beam). In order to understand this clearly, let us consider the entire experimental set up for phase conjugation as a 'black box' and designate it as PCM, the phase conjugate mirror. Beams 3 and 4 described above would then be the input and the output for this black box (PCM, the special mirror) respectively. Such a mirror has some exotic properties much unlike the ordinary mirror. Beam 3, the input beam for PCM and it is considered to 'get *reflected*' as beam 4 from this special mirror. Now we are in a position to compare the process of reflection from an ordinary mirror with the process of phase conjugation and discuss how beam 4 is different from the output we get when beam 3 is reflected from an ordinary mirror.

When a beam traveling along the positive $z-$ direction gets reflected from a plane mirror kept in the $xy-$plane, the two components k_x and k_y of $\vec{k}$ are unchanged and only the component k_z is

reversed in sign. However, in the case of '*reflection*' from a phase conjugate mirror, the vector of the input wave $\vec{k}_3$ is reversed in direction and hence all the three Cartesian components of $\vec{k_3}$ change sign and hence the output wave vector $\vec{k_4} = -\vec{k_3}$. This implies that the beam traces itself back exactly rather than getting reflected in a direction determined by the law of reflection. This is the essential difference between *reflection* in linear optics and *nonlinear reflection* in nonlinear optics (Fig. 6.3). A diverging beam will thus emerge as a converging beam after phase conjugation whereas it diverges further in the case of ordinary reflection (in accordance with the laws of reflection. It is as if the PCM sends the beam back to its source and in this sense the process amounts to a time *reversal.*

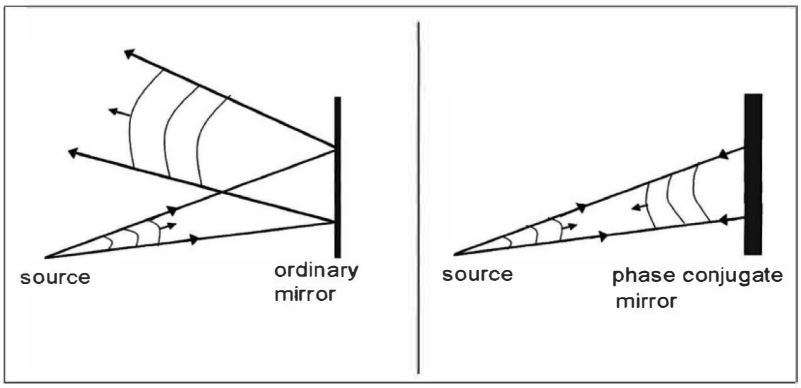


Figure 6.3: Comparison of linear and nonlinear reflection

The time reversal aspect is usually explained on the basis a comparison of reflection of a phase-distorted beam from an ordinary plane mirror and a PCM. Consider beam 3 of a phase conjugation setup as the input beam for a phase conjugate mirror. This incident beam can be described by

$$E_{in}(z,t) = A_0 \exp i(kz) \exp(-i\omega t) \tag{6.21}$$

where A_0 is the amplitude and the other symbols have their usual meaning. Now this beam encounters a phase distorter on its way to the mirror. Consider the distortion to be equivalent to a phase change by ϕ. Then the incident beam gets modified as

$$E_d(z,t) = A_0 \exp i(kz + \phi) \exp(-i\omega t) \tag{6.22}$$

On reflection from the mirror, this becomes

$$E_{ref}(z,t) = A_0 \exp i(-kz + \phi) \exp(-i\omega t) \tag{6.23}$$

assuming no change in amplitude. When this passes through the distorter again in its return path, it becomes

$$E_{out}(z,t) = A_0 \exp i(-kz + 2\phi) \exp(-i\omega t), \tag{6.24}$$

a highly distorted beam with the phase aberration doubled.

Now consider the same event except for the fact that the reflection occurs from a PCM rather than an ordinary plane mirror. The incident beam passes through the distorter on its way to the PCM. Now this beam encounters a phase distorter and gets modified, as in the earlier case, as

$$E_d(z,t) = A_0(z) \exp i(kz + \phi) \exp -(i\omega t) \tag{6.25}$$

On reflection from the PCM, this becomes the phase conjugate beam

$$E_{pc}(z,t) = A_0(z) \exp -i(kz + \phi) \exp(i\omega t) \tag{6.26}$$

assuming no change in amplitude. When this passes through the distorter again in its return path, it becomes

$$E_{out}(z,t) = A_0(z) \exp(-ikz) \exp(i\omega t) = E_{in}(-z,-t) \tag{6.27}$$

which can be interpreted as a time reversed replica of the input beam traveling in the opposite direction (with the distortion annulled completely). It may be emphasized again that PCM shown in Fig. 5.4, usually shown in literature [such as He, 2002] is not actually any mirror in the normal sense of the word, but the whole setup for phase conjugation. The input and output beams are beam 3 and beam 4 of this setup and the other beams or the other parts of the setup are not shown explicitly in Fig. 6.4; these are included in the black box called PCM .

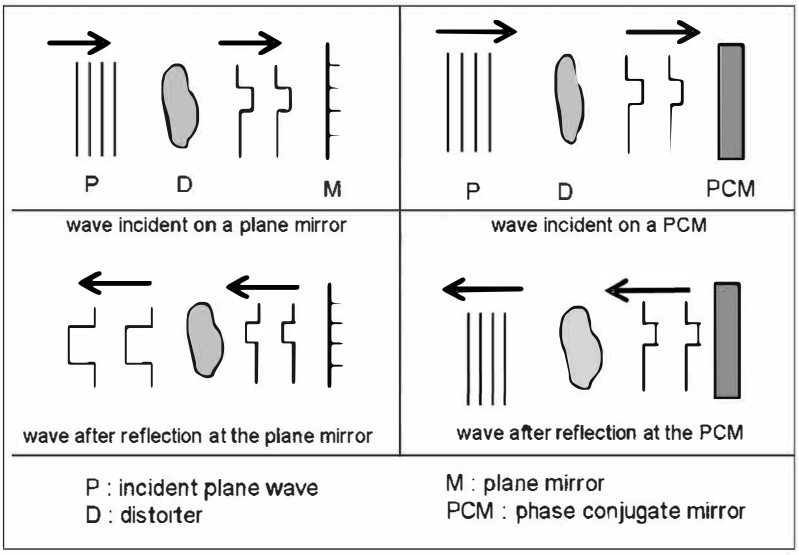


Figure 6.4: Time reversal in phase conjugaion

6.1.5 The Grating Picture

A convenient way of visualizing the phenomenon of optical phase conjugation is using the concept of dynamic grating formation [Jain and Lynd, 1983, Roussignol, 1987]. We can think of three different kinds of gratings being formed in the volume of interaction where the three input beams interact with one another. Two of these form a grating which can be considered to diffract the third beam. The intensity grating gets converted into a refractive index grating as the refractive index depends on the intensity in the nonlinear regime in a material with sufficiently large third order nonlinearity. The nonlinear polarization $\vec{P}_{NL}$ can be written in terms of the interacting electric fields

$$\vec{P}_{NL} = A(\vec{E}_1.\vec{E^*}_3)\vec{E}_2 + B(\vec{E}_2.\vec{E^*}_3)\vec{E}_1 + C(\vec{E}_1.\vec{E}_2)\vec{E_3}^* \quad (6.28)$$

where A, B and C are constants of appropriate dimensions. The three terms correspond to three kinds of gratings with the terms in the brackets representing the fields that form the grating. The first of these contributions (term 1) is from beam 2, which gets diffracted off from the grating formed by beams 1 and 3 (fig. 6.5a). Similarly, the second term represents the diffraction of beam 1 by the Bragg

grating formed by beams 2 and 3 (fig. 6.5b). The third one denotes the diffraction of beam 3 from the temporal grating (rather than a spatial grating) formed by beams 1 and 2. The first grating, with a grating vector $\left(\vec{k}_1 - \vec{k}_3\right)$ has a shorter period than that of the second grating, with grating vector $\left(\vec{k}_2 - \vec{k}_3\right)$ While the first two are spatial gratings with no time dependence, the third one has no spatial modulations and oscillates at a frequency 2ω.This grating is formed by the beams 1 and 2, the two pump beams and it diffracts beam 2, resulting in the formation of beam 4.

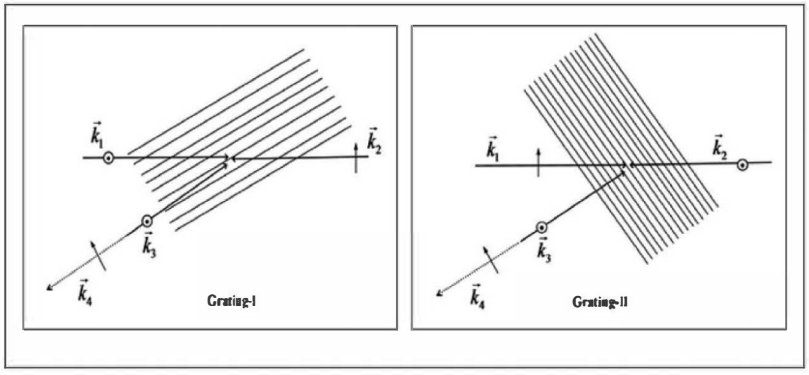


Figure 6.5: Two possible types of spatial *gratings* in phase conjugation

6.1.6 Applications of Phase Conjugation

Phase conjugation permits the restoration of the original wave fronts by the inherent property of error-correction and distortion healing through wave front reversal. This suggests the obvious use of the process of phase conjugation for annulling wave aberrations caused by distortions during propagation. The distorted beam can be 'reflected' off a PCM and sent throughout the medium once again to annul the aberrations (Pepper, 1986, He 2000, 2002). Typically, a double-pass geometry is used where the distorted beam is reflected by a PCM and sent back through the distorter thereby rendering distortion-healing. Correction of wave front aberrations is an important issue in adaptive optics. The conventional method of correction involves manipulating the shapes of optical components in accordance with the nature of the aberration, which is very difficult and

aberration-specific whereas wave front correction by phase conjugation offers *in situ* compensation for dynamic distortions. This is important in the imaging of distant objects, self-targeting of radiation in laser-induced thermonuclear fusion, communications, photolithography and pulse-shape restoration where even a small distortion in an amplified beam can lead to serious consequences. Optical phase conjugation offers a dynamic aberration-correction. Phase conjugation can also be used to characterize the optical nonlinearity in media by measuring their third order optical susceptibility and has been successfully used for a variety of materials ranging from bulk materials and engineered polymers, to semiconductor nano materials(Jain and Lynd, 1983, Roussignol et al, 1987, Vijaya et al, 1990, 1992, Nandakumar et al 2000, John Kiran et al 2007). Several novel types of applications continue to be demonstrated successfully over the years. These include high brightness lasers, target aiming systems, light propagation through turbid media, ultra-high bit rate fiber optic transmission, optical data storage and processing, contrast enhancing microscopy and nonlinear photonic crystals [Ehrke et al, 1999, Merker et al 2000, Hirooka et al 1998, Cui and Yang 2010, Lu at al 2011, Pegard et al 2011]

6.2 Optical Bistability and Photonic Switching

There is a class of nonlinear optical phenomena which can be described as arising due to the dependence of refractive index on the intensity of the incident light. These include optical bistability leading to the design of photonic switching and self effects such as self phase modulation and which could be useful in pulse shaping applications. We shall take up optical bistability in this chapter and self effects in the next one.

6.2.1 Refractive Index at High Intensities : An Overview

The refractive index of an optical material is the ratio of the speed of light in vacuum to that in the material in a given direction. It is a dimensionless quantity which depends on the frequency of the light wave involved in the interaction. Though this quantity may be independent of the intensity of light at the normal levels of intensities, measurable changes occur at high intensities of illumination. This is understood on the basis of the nonlinear interaction of the

medium with light of high intensity and is characterized in terms of the third order nonlinear optical susceptibility of the medium, as will be shown in this chapter. This intensity dependence of the refractive index leads to a variety of optical processes with ample scope for innovative applications while being of immense conceptual interest. Basically, this introduces a nonlinear phase as the beam propagates in the medium, resulting in self phase modulation, and self focusing and optical bistability. These influence the nature of wave propagation in many different ways and hence a proper understanding of these effects offers possibilities of controlling the parameters of beam propagation in specific practical applications such as optical communication and switching.

Consider an isotropic optical medium with $\chi^{(2)} = 0$. This is in fact true for most of the materials except for non-centrosymmetric crystals. In such media, the displacement vector $\vec{D}$ is related to the field $\vec{E}$ by

$$\vec{D} = \epsilon \vec{E} = \epsilon_0 \vec{E} + \vec{P} \tag{6.29}$$

In the case of a nonlinear optical medium, the polarization has an additional (nonlinear) part and is given by

$$\vec{P} = \vec{P}^{l} + \vec{P}^{nl} \tag{6.30}$$

$$\vec{P}^{l} = \epsilon_0 \chi^{(1)} \vec{P} \tag{6.31}$$

$$\vec{P}^{nl} = \epsilon_0 \chi^{(3)} \vec{E}.\vec{E}.\vec{E}. \tag{6.32}$$

Thus we get

$$\epsilon \vec{E} = \epsilon_0 \vec{E}\{1 + \chi^{(1)} + \chi^{(3)} \vec{E}.\vec{E}\} \tag{6.33}$$

The linear dielectric constant ϵ is related to the refractive index n by the relation $\epsilon = \epsilon_r n^2$ where $\epsilon_r = \frac{\epsilon}{\epsilon_0}$ is the relative dielectric constant. (It may be noted that refractive index also depends on the frequency of incident electromagnetic radiation as contributions from atomic, electronic and dipolar mechanisms of polarization are different at different frequencies and this relationship holds only at optical frequencies where only electronic contributions are significant.)

Rewriting the terms,

$$\epsilon_r = n^2 = \{1 + \chi^{(1)} + \chi^{(3)} \vec{E}.\vec{E}\} \tag{6.34}$$

Thus

$$n = \left(1+\chi^{(1)}\right)^{1/2}\left[1+\frac{\chi^{(3)}E^2}{1+\chi^{(1)}}\right]^{1/2} \tag{6.35}$$

$$n = \left(1+\chi^{(1)}\right)^{1/2}+\frac{\chi^{(3)}E^2}{2\left(1+\chi^{(1)}\right)^{1/2}} \tag{6.36}$$

$$n = n_0 + n_2 I \tag{6.37}$$

Here binomial expansion is used for the quantity under square bracket, in view of the fact that the second term in bracket has a magnitude much less than unity. Intensity is usually defined in terms of the square of the amplitude of the electric field of the electromagnetic wave as $I = \epsilon_0 \upsilon E^2$, where υ is the speed of light in the medium. The linear refractive index is given by $n_0 = \left(1+\chi^{(1)}\right)^{1/2}$, and the intensity dependence of refractive index can be described by n_2, the nonlinear refraction coefficient, which is given by

$$n_2 = \frac{\chi^{(3)}}{2\upsilon n_0 \epsilon_0} = \frac{\chi^{(3)}}{2c\epsilon_0} \tag{6.38}$$

where c denotes the speed of light in vacuum [Hecht, 2001] .

Thus it is clear that the refractive index actually depends on the incident intensity in view of the term, $n_2 I$. Often n_2 itself is termed as nonlinear index in literature though strictly the refractive index is $n_2 I$. This term is $n_2 I$ is generally much smaller than the linear refractive index, n_0, often by a few orders of magnitude. It may not be noted that the relation between I and E^2 is not given in the same manner in literature and hence the definition of n_2 will vary accordingly. Also, the term *intensity*, as defined here, is being replaced by *irradiance* in recent literature.

Now let us examine how the dependence of the refractive index on intensity leads to optical switching. The output state of the switching device depends on the present state of the device. The device can switch to a 'high' state from a 'low' state and vice versa. Optical processes also lead to multi stability where the number of stable states need not be just two, thus providing scope for new possible kinds of logic in addition to binary logic. It is interesting to examine how this is brought about by nonlinear interaction of light with matter.

6.2.2 Fabry-Pérot Etalon

We start with a description of light transmission through a Fabry-Pérot (FP) etalon, following the treatment given in most standard text books on Optics. The etalon consists of two semi silvered glass plates (i.e. partial mirrors) separated by a thin layer of an optical medium of refractive index n. The medium outside the etalon is taken to be air, with refractive index unity. Let t and t' denote the transmission coefficients of the two plates and r and r' denote the corresponding reflection coefficients respectively. Let L be the separation between the mirrors. Consider a monochromatic plane light wave of amplitude A_i and wavelength λ incident on the first mirror at a small nonzero angle of incidence. A part $A_i t$ (marked in the figure as path 1) gets transmitted into the medium through the first partial mirror. Assuming that the medium does not absorb at this wavelength, this waves reaches the other partial mirror and gets partly reflected back into the medium (path 2) and partly transmitted out of the medium(marked in the figure by A_1). The fraction reflected would be $A_i tr'$ and the fraction transmitted would be $A_i tt'$. Thus the first wave that would come out of the system will have an amplitude $A_1 = A_i tt'$. The back-reflected part, along path 2, gets reflected by the first mirror along path 3 with an amplitude $A_i trr'$ and partly emerges out of the second partial mirror with an amplitude $A_2 = A_i tt'rr'$. A part of the wave also gets reflected back into the medium from the second mirror, with an amplitude from $A_i tr^2 r'$ and this processes continues till the intensity of the beam dies out to negligible levels. Following up the path of the beams getting multiply reflected within the etalon and emerging out of the second partial mirror of the etalon, it is easy to see that the m^{th} beam that emerges out of the etalon (Fig. 6.6) will have an amplitude of

$$A_m = A_i tt'(r')^{(2m-2)} \tag{6.39}$$

We have to also note the fact that any single round trip of the beam within the cavity involves a phase shift of

$$\delta = \frac{2\pi}{\lambda}\{2nL\cos\theta'\} \tag{6.40}$$

where θ' is the angle of refraction within the medium. Incorporating the phase shift, the amplitude of the m^{th} emerging beam

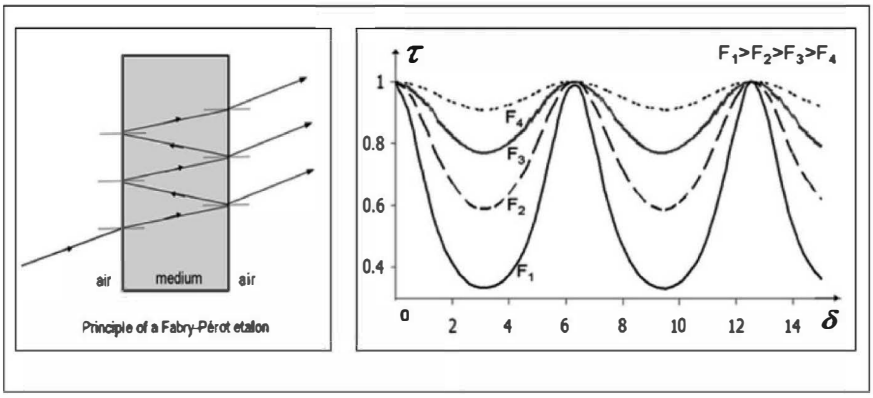


Figure 6.6: FP etalon and its fringe pattern

should be written as

$$A_m = A_i tt'(r')^{(2m-2)}\ e^{i(m-1)\delta} \tag{6.41}$$

The net amplitude of the output beam A_O is obtained by a summation of the amplitudes of all the m emerging beams, i.e. $A_O = \sum A_m$. The summation of the infinite series leads to the expression

$$A_O = \frac{TA_i}{(1 - Re^{i\delta})} \tag{6.42}$$

$$T = tt' \tag{6.43}$$

$$R = r'^2. \tag{6.44}$$

Now the transmitted intensity I_O is proportional to $A_O A_O^*$.and the input intensity I_i is proportional to $A_i A_i^*$. The nett transmittance Transmittance τ, given by the ratio of the output intensity to the input intensity, is then

$$\tau = \frac{T^2}{(1 - Re^{i\delta})^2} \tag{6.45}$$

$$\tau = \frac{(1-R)^2}{(1 + R^2 - 2R\cos\delta)} \tag{6.46}$$

$$\tau = \frac{1}{\left\{1 + F\sin^2\left(\frac{\delta}{2}\right)\right\}}, \tag{6.47}$$

noting that $T = 1 - R$ and defining $F = \frac{4R}{(1-R)^2}$

The plot of transmittance as a function of the round trip phase shift δ is shown in Fig 5.7 . This is a curve with maxima at $\delta = 2m\pi$ where $m = 0, 1, 2.....$ Further, the value of F determines the sharpness of contrast of the fringes observed in the output of the etalon. The maximum transmittance $\tau_{\max} = 1$ and τ falls to half this value at $\sin(\delta/2) = 1/\sqrt{F}$. The full width at half maximum for the peaks can be seen to be $4/\sqrt{F}$. Often, a finesse factor $\Im$ is defined as

$$\Im = \frac{\pi}{2}\sqrt{F}. \tag{6.48}$$

The performance of the etalon is governed by its finesse factor, which in turn depends on the reflectivity of the cavity mirrors.

6.2.3 Photonic Switching in a Nonlinear Fabry-Pėrot Etalon

The discussion above is purely within the domain of linear optics. Now, let us examine how increasing the intensity would affect the performance of an etalon whose medium between the mirrors has a sufficiently large value of $\chi^{(3)}$ (and hence n_2) [Gibbs, 1985, Smith, 1986]. First, we examine graphically how the transmittance varies with increasing input intensity. At large enough intensities, the refractive index depends on the intensity, as shown earlier. Thus we can describe refractive index is that of the nonlinear medium within the cavity by

$$n = n_0 + n_2 I_C \tag{6.49}$$

where I_C is the intensity within the cavity of the etalon. Thus

$$\delta = \frac{2\pi}{\lambda}\{2nL\cos\theta'\} \tag{6.50}$$

$$\delta = \frac{4\pi}{\lambda}nL \tag{6.51}$$

for normal incidence. Now introducing nonlinearity,

$$\delta = \frac{4\pi}{\lambda}Ln_0 + \frac{4\pi}{\lambda}Ln_2 I_C \tag{6.52}$$

and hence

$$I_c = \frac{1}{n_2}\left(n_0 - \frac{\delta\lambda}{4\pi L}\right) \tag{6.53}$$

Now, I_C is the sum of two contributions, I_C^+ and I_C^- , from the forward propagating and the backward propagating beams within the cavity, where

$$I_C^+ = \frac{I_O}{(1-R)} \tag{6.54}$$

$$I_O = (1-R)\, I_C^+ \tag{6.55}$$

whereas

$$I_C^- = RI_C^+ = \frac{RI_O}{(1-R)} \tag{6.56}$$

Now we have

$$I_C = I_C^+ + I_C^- = \frac{(1+R)}{(1-R)} I_O \tag{6.57}$$

which gives

$$\tau = \frac{I_O}{I_i} \tag{6.58}$$

$$\tau = \frac{I_C}{I_i}\frac{(1-R)}{(1+R)} \tag{6.59}$$

$$\tau = \frac{1}{I_i n_2}\frac{(1-R)}{(1+R)}\left\{ n_0 - \frac{\delta\lambda}{4\pi L} \right\} \tag{6.60}$$

This shows that a plot of τ as a function of δ will be linear with a slope determined by the inverse of the input optical intensity I_i. In the case of the etalon with a linear medium, we had obtained the plot as shown in Fig. 6.6 b. Now we plot these together in Fig. 6.7 (the plot of τ versus δ shown here is only an indicative sketch and not based on actual calculations) and look for the common points, i.e. the points at which the straight line meets the curve. The slope of the line (plot of τ versus δ in the nonlinear case) decreases with increasing input intensity and a few such lines (dotted/dashed) are shown.

Something very interesting happens as the intensity increases. We examine how the point of intersection (of the straight line with the curve) moves as the intensity is increased slowly. For initial values of I_i close to I_1 (in the figure), such that $I_1 < I_2$, the point of intersection does not move much and thus the value of τ changes only little. There are two points of intersection when the intensity equals I_2 , one corresponding to *low* transmittance and the other corresponding to *high* transmittance. Thus there are two values

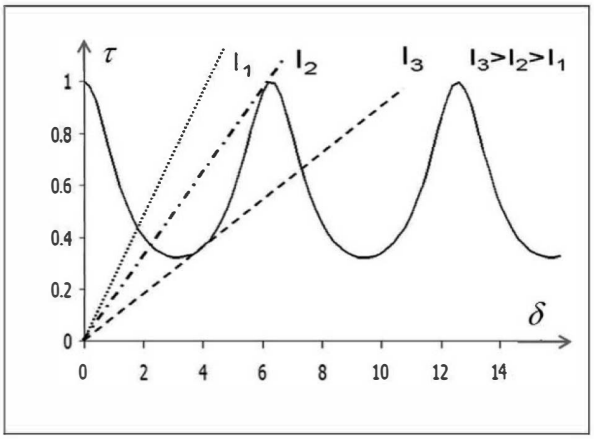


Figure 6.7: Transmittance of an FP etalon with a nonlinear medium as a function of RTPS

of τ corresponding to any value of I_i in the region of intensities $I_2 < I_3$, denoting the possibility of two separate stable states of a given input state of the device for this range of intensities. Now if the intensity increases a little above I_3, the next point of intersection occurs at a larger value of intensity and hence there is an increase in intensity. If the intensity were to decrease at this point, the transmittance remains at high values till I_i becomes equal to I_2 „On further decrease from I_2, the transmittance falls abruptly to a much lower value as the next point of intersection is where the line corresponding to I_2 „goes tangential to the curve.

There are two important conclusions that we arrive at from the analysis of the nonlinear etalon. One is the existence of a region of two separate values for the same input and the other one is the fact that the transmittance goes through a different set of values when we decrease the input intensity compared to the case when the intensity is increased. Thus the device exhibits bistability and hysteresis. It should be noted that the extent of abruptness of the change in transmittance or the sharpness of the hysteresis are governed by the width of the peaks of the Airy function, which is governed by the finesse factor $\mathfrak{F}$ of the device. Another important factor is the slope of the line corresponding to a given intensity I_i, which depends on the reflectivity of the mirrors, the linear as well as the nonlinear refractive indices of the medium, the length of the

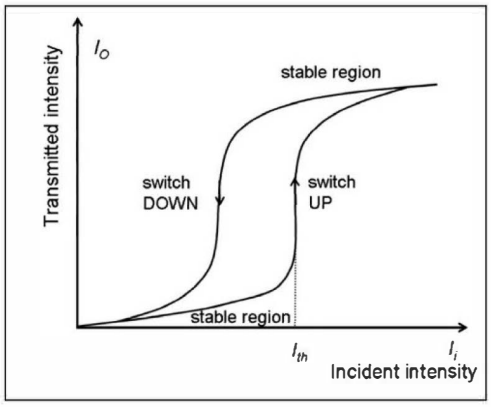


Figure 6.8: Optical bistability

cavity and the wavelength of operation. Attempts have been made to design all optical devices based on optical bistability. The figure also implies the possibility of multi-stability at high input intensities as there could be more than two points of intersection of the line with the curve.

The physical basis of the bistable behavior can be understood as follows. The phase change introduced by a round trip passage is given by

$$\delta = \frac{4\pi}{\lambda} L n_0 + \frac{4\pi}{\lambda} L n_2 I_C \tag{6.61}$$

Let the initial intensity be almost zero initially. Then I_C is almost zero. Let the cavity be tuned by an angle θ off resonance. Then

$$\frac{4\pi L}{\lambda} n_0 = 2m\pi - \theta \tag{6.62}$$

where m is an integer. As the input intensity increases gradually, I_C also increases and δ begins to approach the resonance value corresponding to $2m\pi$. At the threshold value $I_i = I_{th}$, there is a cumulative or runaway effect. As δ increases, there is a photon buildup in the cavity and I_C increases; this in turn increases δ even further. This leads to a switching of I_O from a *low* to a *high* state. This corresponds to $\delta \gtrsim 2m\pi$, which implies a negative feedback, essential for stability. Due to this negative feedback, the runaway effect becomes controlled and the photon density within the cavity is less than the maximum value. On decreasing I_i, the value of I_O continues to be as the value of I_C is large enough and keeps δ close

to $2m\pi$. The output I_O decreases abruptly to a low value only when

$$\frac{4\pi L}{\lambda} n_2 I_C - \theta = 0. \tag{6.63}$$

An etalon is frequency-tuned by adjusting the length of the medium in the case of linear optics. Instead, it is possible to keep the length fixed and tune it by varying the input intensity refractive index varies as $n = n_0 + n_2 I_C$ and this is what is happening in the nonlinear etalon. The area of the hysteresis loop (Fig.6 .8) can be altered by changing the parameters of operation and a variety of devices such as switches, memory elements, latches etc. based on bistability and multi-stability can be designed. Bistability has applications in optical computing and photonic switching and a lot of work was done towards realizing this phenomenon in a variety of materials and designing nonlinear optical devices based on bistability. There is a revival of interest in photonic devices based on bistability and switching in recent years as interesting processes in nano materials and photonic crystals give rise to an unexplored potential in optical bistability and photonic switching. [Soljacic´, et al, (2002); Haret et al, 2009; Mabuchi, 2011; Pernice et al, 2010; Chen, and Matsuo, 2011]

6.3 Explorations

1. Write down the equation of a plane wave in the exponential notation, with the real and imaginary parts and complex conjugate written out explicitly. Now take a complex conjugate of this wave and show that it is time-reversed.

2. Sketch diagrams to show how the following types of beams get 'reflected' from a 'phase conjugate mirror', drawing the corresponding wave fronts as well as the ray diagrams:

   a) a parallel beam at normal incidence.

   b) a parallel beam incident at any other angle.

   c) a converging beam.

   d) a diverging beam.

3. Sketch, in the same plot, the variation of the amplitudes of the probe beam and the signal beam in a degenerate four wave mixing (DWFM) as a function of the distance of propagation.

4. How does the intensity of the observed phase conjugate signal vary with (a) the linear optical absorption coefficient of the medium and (b) angle between the pump beam and the probe beam, in a DFWM experiment with back-refection geometry? Sketch the appropriate plots.

5. The experimental set-up for the realization of DWFM given in text is suitable for a sample that does not absorb much at the wavelength of operation. Suggest a geometry for the phase conjugate experiment for samples which do not satisfy this criterion.

6. What information can be obtained if the DWFM experiment is carried out using a short single pulse as the probe beam and the growth of the phase conjugate signal is studied as a function of time?

7. A medium of refractive index 2.3 is used in the form of a thin slice of thickness 0.1 mm in an optical phase conjugation experiment in the back-reflection geometry. The second harmonic of an Nd:yag laser with a repetition rate of 10 pps, a pulsewidth of 9 ns and a pulse energy of 0.2 mJ is used for excitation. The optical absorption coefficient of the medium at this wavelength has a value 20 cm^{-1}.Estimate the reflectivity of the phase conjugate mirror obtained in this experiment.

Chapter 7

Self Focusing, Phase Modulation and Pulse Shaping

"Who are You?" ... "I know who I was when I got up this morning, but I think I must have changed (shape) several times since then"

Lewis Carroll (from Alice in Wonderland)

The focus is on how to face the changing shapes and what to make out of it.

Learning Objectives

- Quantification of the the effect of intensity of the incident light on the refractive index of a medium.
- Analysis of the phenomena of self focusing and self trapping of light.
- Utilization of self focusing to characterize a medium by measuring the nonlinear refractive index.
- Assessment of the role of dispersion and nonlinearity in pulse shaping.
- Formulation of design criteria for soliton propagation in optical media

7.1 Self Focusing of Light

7.1.1 The Concept of Self Focusing

One of the many interesting phenomena resulting from the interaction of intense light with matter is the self focusing effect exhibited by materials with large third order nonlinear optical susceptibility, which can be thought of as a direct consequence of the dependence of refractive index on intensity. This causes a beam of light to get focussed to a point in a nonlinear optical medium without the help of any external optical component such as a lens or a mirror. It is convenient to describe this effect in terms of an intensity-dependent refractive index. Self focusing can lead to possible damage of optical media due to the increased intensity within the medium as an extremely narrow beam of high intensity light passes through the medium as a result of self focusing. On the other hand, this can be used to obtain an extremely narrow pencil of intense light in media that can withstand such intensities. It can also be used in compensating for the natural beam divergence due to diffraction and thus obtaining trains of optical pulses that maintain their shape, with obvious application in optical communication.

On the other hand, the change in the beam profile due to focussing effects can be used to characterize the optical material by a measurement of the real and imaginary parts of the third order optical susceptibility. Self focusing leads to an intensity modulation of the beam along its path and can lead to nonlinear absorption of light by the media which can be used in a variety of applications [Boyd, 2009].

Consider a monochromatic beam of light, with a Gaussian cross section traveling through a medium such as air, with a negligible value of n_2 and entering another transparent medium with a reasonably significant value of n_2. The corresponding wave front is plane parallel while in air, but starts getting distorted as the beam begins to propagate in the medium. The intensity modulation across the beam leads to a corresponding modulation in the refractive index due to the intensity-dependent contribution. The intensity and hence the refractive index are larger at the center of the beam than at the periphery and hence the speed is less at the center. Thus the plane wave front bends as shown in the figure, leading to focusing in a medium with $n_2 > 0$. The idea of self focusing is depicted in Fig. 7.1, schematically.

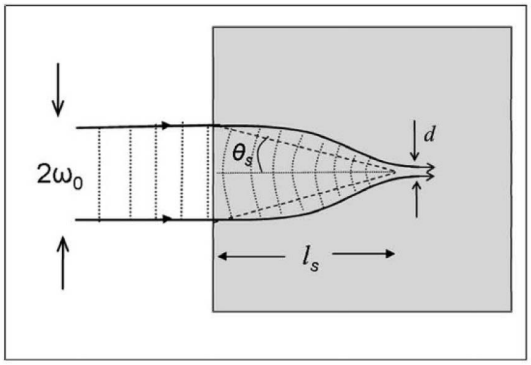


Figure 7.1: Self focusing of a beam of Gaussian profile

Distortion of the wave fronts inside the nonlinear medium is also shown in the figure. The parameters that describe self focusing are (i) ω_0, the beam radius before it enters the nonlinear medium, (ii) θ_s, the angle of self focusing (as defined in figure 7.1) (iii) d , the minimum beam diameter on self focusing within a medium of linear refractive index n_0 and (iv) the nonlinear refractive index $n_2 I$ where I is the intensity of the beam [Boyd, 2008.] The angle θ_s is given by

$$\theta_s = \sqrt{\frac{2n_2 I}{n_0}} \tag{7.1}$$

and the distance l_s at which the beam focusses is given by

$$l_s = \frac{\omega_0}{\theta_s} = \omega_0 \sqrt{\frac{n_0}{2n_2 I}} \tag{7.2}$$

Thus the extent of beam convergence due to self focusing expressed by θ_s, is directly proportional to the square root of the nonlinear refractive index. The corresponding *focal length* l_s is inversely proportional to it. It may also be noted that some materials have a negative value for n_2 which leads to a self-defocusing effect and a divergence of the beam instead of self focusing.

7.1.2 Self Trapping and Spatial Solitons

What happens when the beam continues to pass through the medium beyond focus is governed by an interplay of linear and nonlinear optical effects. While self focusing leads to a reduction in the beam

diameter while traveling in a nonlinear medium, the beam also tends to spread transversely due to linear optical diffraction. The resulting angular spread θ_d for a beam of diameter d is given by

$$\theta_d = \frac{0.61\lambda_0}{n_0 d} \tag{7.3}$$

where λ_0 is the wavelength of the light in vacuum. It is interesting to look for conditions under which this beam divergence due to diffraction can be compensated exactly by the beam convergence effect due to self focusing. On equating θ_s given by Eq.7.1 , with θ_d as given by Eq.7.3, we see that

$$I_{cr} = \frac{(0.61)^2\ \lambda_0^2}{2n_0 n_2 d^2} \tag{7.4}$$

When this compensation occurs, the resulting beam can maintain its profile unchanged for large distances within the medium and is said to be self-trapped, as if the beam has generated its own waveguide. Such beams are also termed as spatial solitons [Trillo and Torruellas 2010; Reinisch 1998].

Beams of intensity less than this critical vale tend to diverge eventually whereas large intensities $I \gg I_{cr}$ lead to beam filamentation where the beam is split up into several narrow beams, each with an intensity corresponding to I_{cr} . This is normally expressed in terms of the power of the beam $P = \frac{\pi}{4}d^2 I$ and the critical power is given by

$$P_{cr} = \frac{\pi}{4}d^2 I_{cr} \tag{7.5}$$

$$P_{cr} = \frac{\pi(0.61)^2\ \lambda_0^2}{8n_0 n_2} \tag{7.6}$$

$$P_{cr} \approx \frac{\lambda_0^2}{8n_0 n_2}. \tag{7.7}$$

Self focusing causes the beam intensity to be concentrated into one or more very narrow pencils and hence may lead to dielectric breakdown or other damage. Since the change of shape originates from the intensity-dependence of the refractive index and hence provides a method to measure the nonlinear refractive index.

7.1.3 The z-scan Experiment

There are several practical applications based on self focusing, mainly on pulse shaping and related aspects. This phenomenon can also be used as a tool to characterize optical nonlinearity by measuring the nonlinear refractive index. The real as well as imaginary parts of the third order susceptibility can be obtained by a method originally devised by Sheik Bahae et al. [1989,1990]. A detailed treatment on this technique is provided by Sutherland [2003].

The method consists of moving the experimental specimen, a nonlinear medium, through a region of modulated intensity and observing the corresponding changes in the beam profile. A block diagram of the basic set up for this experiment is shown in Fig.7.2.

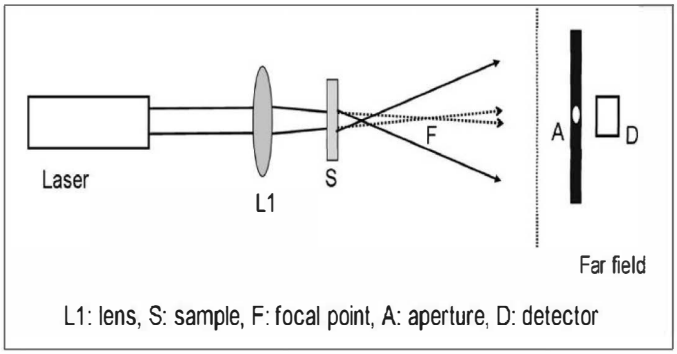


Figure 7.2: Experimental setup for closed z scan

A laser beam of Gaussian cross section is passed through a convex lens *L1* which creates an intensity modulation along the direction of propagation, taken to be the $z-$ direction. The sample in the form of a thin film or slice or liquid in a thin cuvette is then moved along the beam direction, thus exposing it to a continuously varying laser intensity as it moves. Since the nonlinear medium acts as a lens due to self focusing effect, the situation is similar to that when a thin lens is moved along the beam direction, through the focal length of the lens L1. The sample thus alters the focusing effect on the beam caused by the convex lens and this alteration depends on the instantaneous position of the sample, i.e., where it is located with reference to the lens, during its movement along the

beam direction. The beam profile at any cross sectional plane of the beam also changes accordingly. If a screen is kept at the far field, the profile on it can be seen to alter its diameter as the sample is moved.

When the sample is close to the lens, there is not much change in the profile compared to that before placing the sample. However, the profile starts changing when the sample starts moving along the beam. The sample tends to focus the already focussed beam to a point closer to the lens, reducing the effective focal length initially. This causes an increase in the cross sectional area initially on the screen kept at the far field. However, the profile gets back to the original one (without the sample) as the sample reaches the focal point F of the lens $L1$. This is because one lens cannot alter the beam profile modified by another lens when it is placed exactly at the focus of the other lens, in the thin lens approximation. The sample is moved further away from the focal point of the lens where the original beam starts diverging. This causes a profile change in a manner opposite to what happened when the sample was approaching the focal point. Eventually, the sample moves far enough from the lens so that the profile gets back to the original size and shape. Thus the profile on the screen at far field diverges first, then converges to a diameter shorter than the original value and then diverges again, finally attaining the original shape (that in the absence of the sample) as the sample moves along the beam. The sample was assumed to be self focusing (i.e. $n_2 > 0$) for the description given above. The profile variation which would occur if the medium were to have a negative value of n_2 will be opposite to what was described, with a pre focal maximum and a post-focal minimum.

A few schemes have been proposed for making quantitative measurements in this experiment. The original proposal by Sheik Bahae was to keep a small aperture in the far field and to measure the variation of intensity of light transmitted through the aperture as the sample moves through the beam direction. A typical plot of the transmitted intensity as a function of the distance moved, in the case of a sample with a positive value of n_2, is given in figure 7.3.

The corresponding plot for a sample with negative value of n_2 will have a pre-focal peak followed by a post-focal valley. Such a plot is a *signature* of nonlinear refraction and it is quite easy to see

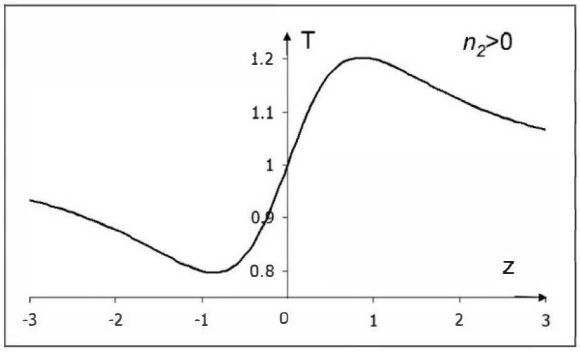


Figure 7.3: Typical trace of the z scan experiment

from the plot whether the sign of nonlinearity is positive or negative. The transmitted intensity is normalized to have a value unity when the sample is at the focal point, taken as the origin ($z = 0$). The difference in the ordinate values of the maximum and the minium (i.e. the peak-to-valley height) is an indirect measure of the amount of nonlinear refraction.

This description assumes pure nonlinear refraction to occur. This type of experiment which employs an aperture is called 'closed z-scan'. If the sample also exhibits nonlinear absorption, the shape of the z-scan plot would be distorted bringing in an asymmetry between the peak and the valley. Such samples can be analyzed by a modification of the techniques called the 'open z-scan' technique and is taken up in a subsequent section.

7.1.4 Analysis of the z- scan Trace

The method of analysis of the z-scan method was presented originally by Sheik Bahae et al [1989, 1990] and summarized here. The laser beam used in the experimental set up shown above, assumed to be of Gaussian cross section, travels through air along the $+z$ direction and is focused by the lens $L1$ kept at a fixed position. The magnitude of the electric field is given by

$$|E(r,z,t)| = |E_0(t)| \frac{\omega_0}{\omega(z)} \exp\left[-\frac{r^2}{\omega^2(z)}\right] \quad . \tag{7.8}$$

where

$$\omega^2(z) = \omega_0^2\left(1 + \frac{z^2}{z_R^2}\right) \tag{7.9}$$

$\omega(z)$ is the radius of the beam at any point z along the path of propagation and

$$z_R = \frac{\pi\omega_0^2}{\lambda} \tag{7.10}$$

is the Raleigh range of the beam, λ is the wavelength of light used. The beam is focussed using a lens $L1$, as described in the previous section and the focal point is taken as the origin, $z = 0$. The magnitude of the electric field at the origin is given by E_0. The experiment is normally done under the thin sample approximation. The thickness of the sample along the z- direction is assumed small so that the beam diameter does not alter due to linear or nonlinear diffraction during the beam propagation within the sample. The sample thickness L along the beam direction should be smaller than z_R, the Raleigh range for this to be valid.

The nonlinear phase shift introduced by the sample is given by

$$\Delta\Phi(z,t) = \frac{\Delta\Phi_0(t)}{\left\{1 + \left(\frac{z}{z_R}\right)^2\right\}} \tag{7.11}$$

where

$$\Delta\Phi_0(t) = \left(\frac{2\pi}{\lambda}\right) n_2 I_0(t) L_{eff} \tag{7.12}$$

is the on-axis phase shift at the focus, $I_0(t)$ is the on-axis irradiance at focus and $L_{eff} = \left(1 - e^{-\alpha L}\right)/\alpha$, α being the optical absorption coefficient at λ, the wavelength of the laser. The experimental data points resulting from the closed z-scan experiment can be fitted with a model described by Sheik Bahae to obtain the nonlinear refractive index accurately. However, it is possible to obtain a value of n_2 to $\pm 3\%$ accuracy more readily by a measurement of the quantity $\Delta T_{p-v} = T_p - T_v$, the difference between normalized transmittance values at the peak (T_p) and the valley (T_v) of the z- scan trace. In terms of the on-axis phase shift $\Delta\Phi_0$ we have

$$\Delta T_{p-v} \approx 0.405\left(1 - S^{0.25}\right)|\Delta\Phi_0| \tag{7.13}$$

for the case where $|\Delta\Phi_0| \leq \pi$ where S is the linear aperture transmittance given by

$$\left\{1 - \exp\left(-2r_a^2/\omega_a^2\right)\right\}, \tag{7.14}$$

r_a and ω_a being the beam aperture radius and the beam radius at the aperture respectively. The approximate value of n_2 can be calculated from the time-averaged value $\langle\Delta\Phi_0\rangle$, the averaging being done over the excitation pulse duration. The details of such a calculation in the case of a Gaussian beam are given in the paper cited.

As mentioned earlier, the typical shape shown in figure 7.3 arises from nonlinear refraction alone and is exhibited only in the case of samples with no nonlinear optical absorption at the wavelength used. However, nonlinear absorption occurs at relatively higher intensities in many samples and this leads to a very different shape of the plot. The actual value of intensity required for nonlinear absorption to occur depends on the magnitude of the imaginary part of the third order susceptibility of the sample in use. Nonlinearity in such samples is studied using a variant of the z-scan technique knows as the 'open z- scan"

7.1.5 Measurement of Nonlinear Optical Absorption

Linear optical absorption by a medium is described in terms of the optical absorption coefficient $\alpha(\lambda)$ which determines how the intensity $I(0)$ of a monochromatic beam of wavelength λ is attenuated to $I(z)$ on traveling through a distance z in the medium. These quantities are related through the well known relation

$$I(z) = I(0)e^{-\alpha(\lambda)z} \tag{7.15}$$

Thus the transmittance is given by

$$\ln\left\{\frac{I(z)}{I(0)}\right\} = -\alpha z. \tag{7.16}$$

Nonlinear absorption can occur when a high intensity laser beam is made to interact with matter, in which case the variation of intensity with distance traversed within the medium is described by

$$\ln\left\{\frac{I(z)}{I(0)}\right\} = -\alpha z - \beta z I \tag{7.17}$$

where β is the nonlinear absorption coefficient. The magnitude of β is such that the βI is negligible in comparison with α for most materials at low intensities.

The z-scan technique is employed in a modified configuration for the measurement of β . This scheme is similar to the 'closed scan' except for the fact that there is no aperture to curtail the beam profile and the entire cross section of the beam is collected for intensity measurement, using one more lens to collect the light, if required. A schematic diagram of this set up is shown in Fig 7.4. This is called the 'open aperture z-scan' method. Here again, the sample is moved through the beam direction, across the focal point F of the lens $L1$. Since this path is intensity-modulated due to the focusing action of the lens $L1$, the sample experiences the highest intensity when it is at the focal point and much smaller intensities when far away, on either side of it.

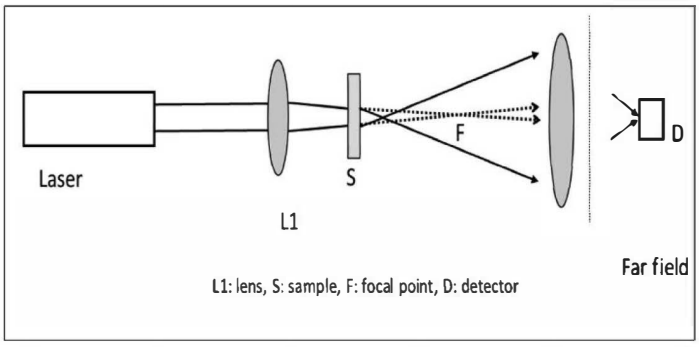


Figure 7.4: Experimental set up for open z-scan

Thus nonlinear absorption is expected to be maximum when the sample is at the focal point. The total fluence of the beam transmitted by the sample is measured by an optical detector and plotted against the instantaneous position of the sample. The plot would be a line parallel to the z-axis (abscissae) in the absence of any nonlinear absorption as the sample position is not relevant for linear optical absorption. A typical plot of the transmitted intensity as a function of the distance moved (with the focal point as the origin) would look like Fig. 7.5b or 7.5c, depending on the mechanism involved, as explained in the coming section. The data points can be

fitted to models incorporating the different mechanisms responsible for nonlinear absorption.

7.1.6 Mechanisms of Nonlinear Absorption

Nonlinear absorption can occur due to a variety of processes when a medium is exposed to large optical intensity. Multi photon absorption as well as reverse saturable absorption can occur in the case of several media such as semiconductors. For example, the most predominant mechanism in the case of metallic nano particles is saturable absorption .

Consider a two-level system with energies E_1 and E_2 such that $E_2 > E_1$ where E_1 denotes the ground state of the system. Let N_1 and N_2 be the number of species (atoms/molecules) in levels E_1 and E_2 respectively. A photon of frequency υ and energy $E = \hbar\upsilon = \{E_2 - E_1\}$ can be absorbed by atoms/molecules in the lower energy level. However, suppose the number of photons incident simultaneously on this system is just equal to the number of atoms/molecules in the lower energy state, the entire absorbing species could be excited to the higher level at unity quantum yield, making the lower level momentarily empty. If one more photon of the same energy is incident after this, there is no more atom/molecule to absorb this and hence the photon passes through, leading to a case of 'induced transparency'. Thus the material which was opaque to a smaller number of photons has now become transparent when a large number of photons are incident. This is called *saturable absorption* (SA). The spatial rate of decay of the intensity of a beam (of initial intensity I_0) is given by

$$\frac{dI}{dz} = \frac{\alpha I}{1 + I/I_0} \tag{7.18}$$

where α is the linear absorption coefficient at a wavelength λ.

There are a few points to be noted at this stage. Normally the ground state is well populated at room temperature and the numbers of species in the two levels in thermal equilibrium are related by $N_2 = N_1 \exp\{-(E_2 - E_1)/k_B T\}$ at temperature T where k_B is the Boltzmann's constant. So a very large number of photons, of the order of the Avogadro number, would be required to interact with the medium simultaneously at a time to enable saturation of absorption. This is not easy to achieve with light sources of ordinary intensities and a pulsed laser which delivers a large number of

photons in a very short span of time would be required. Also, the absorbing species excited by the pulse does not stay at E_2 for a long time; there is finite life time associated with the level. Thus saturation is transient. The excited species gets de-excited and undergo a transition back to the ground state, emitting the excess energy as a photon.

Another interesting possibility for an atom excited to the first excited state by the incident laser beam is that there could be transitions to further higher states, in the case of a multi-level system with appropriate energy levels. Thus the upper level can be momentarily depleted, leading to further absorption and a corresponding decrease in transition. This is known as *reverse saturable absorption* (RSA). Typical plots of transmittance as a function of the sample position in an open z-scan experiment corresponding to these situations are depicted in Fig.7.5a and 7.5b respectively. As these effects are transient, the duration of the pulse and the lifetimes of the levels involved play a crucial role in determining which mechanism can occur in a given material for a given pulse width of excitation. The other possible process that leads to nonlinear absorption is multi photon absorption (MPA) excited by a beam of high intensity. In a two level system with energies E_1 and E_2, a photon of energy

$$h\upsilon = \left(\frac{1}{2}\right)\{E_2 - E_1\} \tag{7.19}$$

interacts with this system. This photon is not capable of exciting a transition between the levels as it has only half the energy required. However, a two photon process could occur in which two photons of the same energy interact simultaneously with the given energy level system and the transition to level E_2 becomes possible. Similarly, many-photon transitions could occur at still higher optical intensities. Occurrence of nonlinear absorption processes produce deviations in the shape of the closed z–scan trace. A suppression of the peak and/or the valley is such a possible distortion. So, both closed and open $z-$ scan traces are recorded for samples with nonlinear absorption and the closed scan trace is divided point-by-point by the open scan trace to obtain the trace corresponding to pure refractive $z-$ scan trace.

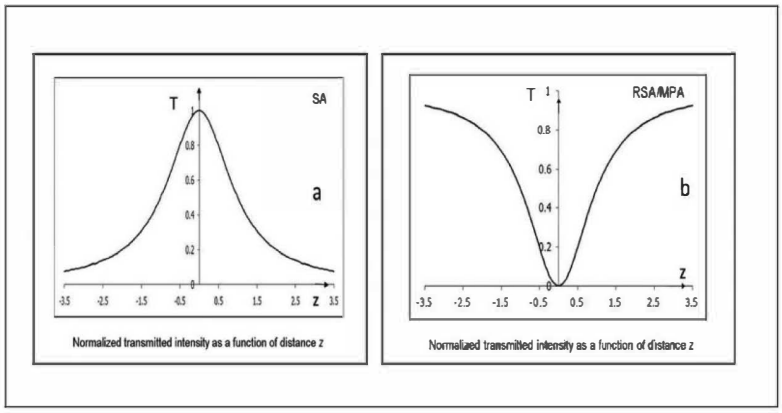


Figure 7.5: Typical open scan traces for SA and RSA/MPA

7.2 Self Phase Modulation (SPM)

The concept of phase plays is significant in linear as well as nonlinear optics. Thus a light beam traveling a distance z through a medium of refractive index n acquires an extra phase of $\Phi_0 = knz$ where k is the magnitude of the wave vector, numerically equal to $2\pi/\lambda$. A simple way to introduce the nonlinear phase shift $\Delta\Phi$ is to replace n by $n(I) = n_0 + n_2 I$. Thus

$$\Phi = \Phi_0 + \Delta\Phi = kn_0 z + kn_2 Iz \tag{7.20}$$

The nonlinear phase shift $\Delta\Phi$ can be written as

$$\Delta\Phi_0 = kzn_2 \frac{P}{A} \tag{7.21}$$

where P is the power of the beam and A is its area of cross section. Thus the nonlinear phase shift becomes considerable in the case of optical fibers where media of large lengths with small cross sections are used. This has resulted in the development of a new area of research to fiber optics, namely, nonlinear fiber optics [Agrawal 2008; Guo 2010] where the influence of optical nonlinearity is analyzed and even utilized in the design of efficient communication systems. The optical power required for a phase shift of $\Delta\Phi_0 = \pi$ is given by

$$P_\pi = \frac{A\pi}{kn_2 z} = \frac{A\lambda}{2n_2 z} \tag{7.22}$$

on substituting $k = \frac{2\pi}{\lambda}$. If the angular frequency is denoted by ω_0, the instantaneous phase Φ for a path length Δz at any time t is given by

$$\Phi(t) = \omega_0 t - k\,(n_0 + n_2 I)\,\Delta z. \tag{7.23}$$

The effective angular frequency is then given by

$$\omega_i = \frac{d\Phi}{dt} = \omega_0 - k n_2 \Delta z \frac{dI}{dt} \tag{7.24}$$

It may be noted that the instantaneous frequency ω_i would be the same as the central frequncy ω_0 if the nonlinear refarctive index were negligble. In this case, the pulse would hae the same value for the instantaneous frequency throughout its duration, as shown in figure 7.6.

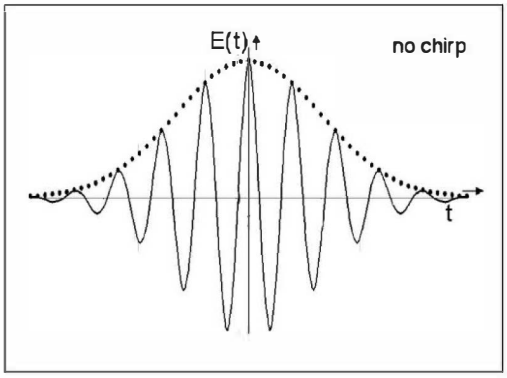


Figure 7.6: Unchirped pulse

However, ω_i differs from ω_0 the contribution due to the nonlinear phase shift $\Delta\Phi_0$ in the case of an optical pulse and the magnitude and sign of the frequency shift $\Delta\omega$ from the central value ω_0 are governed by the time-dependence of intensity $I(t)$. This instantaneous variation of frequency with time is known as a *chirp*. Fig. 7.7 shows how chirping occurs to a pulse propagating in a nonlinear medium with $n_2 > 0$.

The sign of the nonlinear phase shift depends on the sign of the rate of variation of intensity, $\frac{dI}{dt}$. When this quantity is negative, the frequency shift $\Delta\omega = -k n_2 \Delta z \frac{dI}{dt}$ is positive and $\omega_i = \omega_0 + \Delta\omega$. Thus the trailing edge of the pulse is *blue*-shifted. For the leading edge, $\frac{dI}{dt} > 0$ and $\omega_i = \omega_0 - \Delta\omega$,there is a *red*-shift.

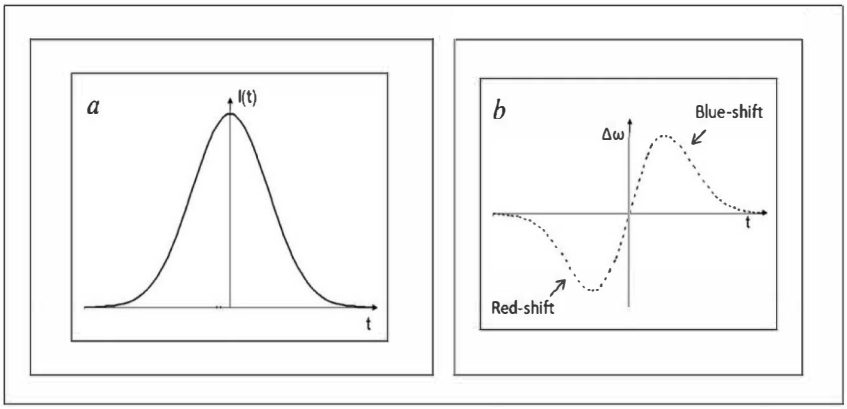


Figure 7.7: The origin of chirp

Thus the leading edge of the pulse is redshifted while the trailing edge of is blueshifted and chirping leads to a spectral broadening, which can be studied by analyzing the spectral content of the pulse by Fourier transform techniques. This is called a positive chirp as the instantaneous frequency increases with time. A comparison between an unchirped pulse, a negatively chirped pulse and a positively chirped pulse is provided in Fig. 7.7.

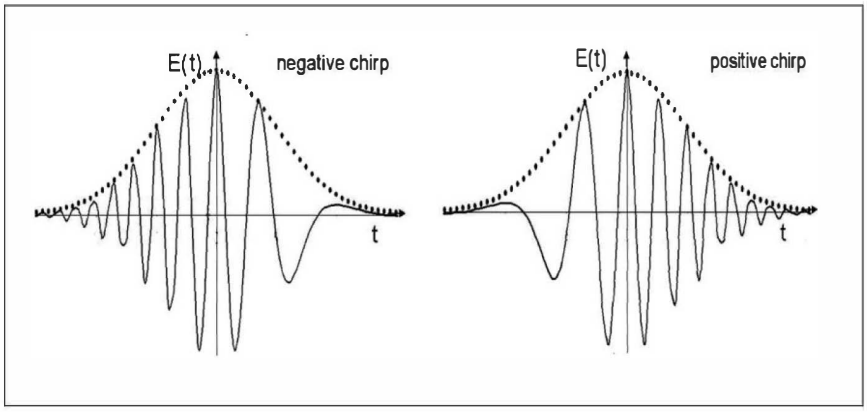


Figure 7.8: Chirping of pulses

7.3 Pulse Shaping and Optical Soliton Propagation

SPM can be considered to be the temporal equivalent of self focusing. This is because SPM is a result of the time-dependent variation in refractive index by a laser pulse of intensity $I(t)$ while self focusing, arises from the spatial variation of the refractive index across the beam profile $I(x, y)$ of a laser beam, continuous or pulsed. Thus self focusing can lead to spatial trapping of a pulse while SPM can result in changes in the temporal shape of the pulse.

In an analogous manner, SPM effects in the nonlinear medium of propagation can be utilized in temporal pulse shaping. Let us first consider pulse propagation in a linear optical medium, with $n_2 = 0$. The pulse undergoes group velocity dispersion (GVD) which causes different frequencies associated with the pulse to travel with different speeds. Thus different time delays are experienced by the spectral components and this leads to a continuos change in the pulse shape, leading to a dispersion of the pulse. Dispersion effects are described in terms of the wavelength-dependence of the wave vector , given by

$$k(\omega) = k_0 + (\omega - \omega_0) k_1 + \frac{1}{2}(\omega - \omega_0)^2 k_2 + \ldots, \text{ with } k_n = \left(\frac{d^n k}{d\omega^n}\right)_{\omega=\omega_0} \tag{7.25}$$

for $n = 1, 2...$ Further, the group velocity v_g of the pulse is known to be given by

$$\frac{1}{v_g} = \left(\frac{dk}{d\omega}\right)_{\omega=\omega_0} = k_1 \tag{7.26}$$

and

$$-\frac{1}{v_g^2}\frac{dv_g}{d\omega} = \left(\frac{d^2k}{d\omega^2}\right)_{\omega=\omega_0} = k_2 \tag{7.27}$$

Further, the coefficient k_2 can be positive or negative for a given material depending on the wavelength used. If $k_2 < 0$, GVD is described as anomalous and $\frac{dv_g}{d\omega} > 0$. (For example, this happens in the case of silica for wavelengths greater than 1.27μ). This means that in such a case, v_g increases with frequency and decreases with wavelength. Thus shorter wavelength will have a larger group velocity than that for longer wavelengths. It is as if the blue part of the spectrum travels faster to 'catch up' with the red part, which gets slower. the net effect of this is a pulse shortening.

7.3.1 Solitary Waves and Optical Solitons

Now if this happens in a medium with $n_2 > 0$ we also have the chirping effect due to SPM described in the previous section. This is an effect opposite to frequency chirping due to anomalous GVD described earlier. If these effects can be made to balance each other exactly [Yuri et al, 2003], the pulse travels for long distances without any decay in its temporal profile and is said to be a *temporal soliton.* Solitary waves are single peaks moving in isolation, maintaining their shape and velocity in a medium for very long distances. The first observation of a solitary wave by John Scott Russel while traveling along a canal in a boat is an interesting incident [Russel, 1844] which triggered a lot of theoretical and practical interest in the propagation of such waves in a variety of media [http://www.ma.hw.ac.uk/solitons]. The name *soliton* was used later, on realizing that certain kinds of solitary waves can pass through each other without undergoing any change in shape and retaining their individual identity. Though this is common in linear optics as a consequence of the principle of superposition, such a behavior in nonlinear systems is rather rare. A very good introduction to the subject is presented by Kajzara and Reinisch [1998].

The propagation of solitary waves in shallow water due to an exact balance between nonlinearity and dispersion effects is described by the Kortweg and de Vrie (KdV) equation [Korteweg, and de Vries, G. (1895)], in a partial differential equation of the form

$$\frac{\partial u}{\partial t} + 6u\frac{\partial u}{\partial x} + \frac{\partial^3 u}{\partial x^3} = 0 \tag{7.28}$$

where the disturbance u moves essentially along one direction, such as in the case of a shallow water wave. A delicate balance between these two effects of linear dispersion and nonlinearity leads to a stable solitary wave solution u_s of this equation, of the form

$$u_s(x,t) = \frac{\upsilon}{2}\sec h^2\left\{\frac{\sqrt{\upsilon}}{2}(x - \upsilon t + \delta)\right\} \tag{7.29}$$

where υ is the speed of the wave and δ is a constant of integration. [Miwa et al, 2000] This wave has an amplitude proportional to υ and and a width inversely proportional to $\sqrt{\upsilon}$.

The compensation of pulse spreading effects using nonlinearity is an interesting possibility from the point of view of optical communications. Optical nonlinearity was initially considered by

communication engineers as a factor that affects the pulse propagation adversely . However, the recent trend is to recognize that it is unavoidable and how best it can be made use of in pulse propagation and this has renewed the interest in optical solitons in fiber optical communications because basically optical fibers are nonlinear dispersive media, in general. An intense optical pulse with a pulse envelope function $A(z,t)$ with speed v and angular frequency ω traveling through a fiber is described by the nonlinear Schrodinger equation |Boyd, 2008|

$$\frac{\partial A}{\partial z} + \frac{1}{2} i k_2 \frac{\partial^2 A}{\partial \tau^2} - i\gamma |A|^2 A = 0 \tag{7.30}$$

where

$$\tau = t - \frac{z}{v_g} \tag{7.31}$$

$$\gamma = \frac{n_0 n_2 \omega_0}{2\pi} \tag{7.32}$$

The second term of this differential equation represents the changes in the pulse shape due to group velocity dispersion and the third term describes changes due to SPM. If the propagation happens in a nonlinear medium with anomalous dispersion, the chirping effects due to SPM and anomalous dispersion can be balanced to a large extent to yield a solitary wave solution of the form

$$A_s(z,\tau) = A_0 \text{ sech } \left(\frac{\tau}{\tau_0}\right) e^{i\kappa z} \tag{7.33}$$

where the pulse amplitude A_0 is related to the pulse width τ_0 by $|A_0|^2 = \frac{-k_2}{\gamma \tau_0^2}$ and $\kappa = \frac{1}{2}\gamma |A_0|^2$. This represents a pulse maintaining its shape during propagation over large distances. This equation provides a better physical insight into the nature of the solutions more readily if we reformulate it. First we understand the important length scales involved in the problem, which are the *dispersion length* L_D and the nonlinear length L_{NL}, defined by the equations

$$L_D = \frac{\tau_0^2}{|k_2|} \tag{7.34}$$

$$L_{NL} = \frac{1}{\gamma P_0} \tag{7.35}$$

where P_0 is the soliton peak power. The ratio $N = \frac{L_D}{L_{NL}}$ is called the soliton order. Then the NL Schröedinger equation can be written as

$$i\frac{\partial u}{\partial \xi} + \frac{1}{2}\frac{\partial^2 u}{\partial T^2} + |u|^2 u = 0 \tag{7.36}$$

where u is a suitably normalized amplitude, $\xi = \frac{z}{L_D}$ and $T = \frac{\tau}{\tau_0}$ [Agrawal, 2008, Boyd 2008]. The parameter N helps us to analyze the relative strengths of pulse shape modifications due to anomalous dispersion and self phase phase modulation and it determines whether the pulse compression effect or the pulse elongation effect would dominate. Obviously, for $N = 1$, we have a soliton solution.

It will be very interesting if a pulse can be a temporal as well as a spatial soliton simultaneously. The name *light bullet* has been used to describe such spatiotemporal solitons [Minardi, 2010] There is also interest in the behavior of solitons in new media such as photonic crystals [Joannopolous, 2008] These aspects of nonlinear optical pulse shaping are of intrinsic scientific interest in view of the possibility of enhanced light-matter interaction and hold promise for powerful applications in information processing systems and communications [Ferreira, 2011; Suhara and, Masatoshi Fujimura 2010, Kivshar and Agrawal 2003].

7.4 Explorations

1. The phenomenon of self focusing can lead to damage of the medium through dielectric breakdown as the beam narrows down in its path through the medium. What are the parameters that decide the fate of the medium as well as that of the propagating beam within the medium? Consider a specimen of glass with a linear refractive index of 1.50 and nonlinear coefficient n_2 of $1.0 \times 10^{-20} MW^{-1}$. Estimate the '*focal length*' due to self focusing in this medium glass if Gaussian laser beam of diameter 1cm, wavelength 500 nm, pulse width 10 ns at 10 pps and energy per pulse 25 mJ is allowed to pass through it, neglecting linear absorption. Would this happen without dielectric breakdown in this case, which is expected at fields of the order of $10^{-20} Vm^{-1}$?

2. Would self focusing occur if the incoming plane wave has a uniform intensity across its profile? Discuss what happens if the intensity profile is (a) *doughnut* and (b) *top hat.*

3. Sketch the variation of the transmittance as a function of input intensity for (a) a typical saturable absorber and (b) a typical reverse saturable absorber. Suggest practical device applications for materials belonging to both of these types.

4. Simulate the propagation of a pulse in a medium using any appropriate mathematical/graphical software that can visualize pulse propagation. Sketch the time evolution of a pulse if its height is proportional to its speed. Compare the results with that when the height is independent of the speed.

5. Show that the normalized transmittance for an open z scan experiment can be expresses as $T_{OA} = 1 - \alpha_2 I_0 L_{eff}/2^{3/2}$ if two-photon absorptions happens to be the major mechanism leading to nonlinear absorption , where α_2 is the TPA coefficient, I_0 is the intensity at focus and L_{eff} is the effective length of the medium in the z-direction. Hence calculate the TPA absorption coefficient of a material used in an open scan experiment performed at 532 nm using 1kHz pulses of 10 ns duration and average power 1 mW, with a beam waist of 20 μm if the transmittance is found to be 0.7 at z=0.

6. Sketch the variation in transmittance in the previous example as a function of z using $I\,(z) = \frac{I_0}{1+(z/z_0)^2}$ where $z_0 = \frac{\pi\omega_0^2}{\lambda}$.

7. The differential transmittance between the peak and the valley of the pure refractive z scan trace for a sample is found to be $\Delta T_{p-v} = 0.40$. If the material has a linear trasmittance of 60% and the aperture used in the closed z scan experiment has a transmittance of 30 %, deduce the nonlinear refractive index of the material if the peak intensity and the wavelength of the laser source is $10GW/cm^2$ and 532 nm respectively.

8. The trace of a typical z-scan obtained in an experiment may be somewhat different from what you expect ideally based on considerations of self focusing effect alone, as the detector faithfully records all variations on intensity irrespective of the reasons for it. For example, diffraction can occur if there is some tiny spec of dirt or bubble on the cuvette or in the sample inside. SPM can lead to spatial ring patterns of intensity variation. Existence of nonlinear absorption and thermal lens effect can lead to asymmetry in the peak-valley structure, as mentioned in the text. liquid sample. Suggest

ways of avoiding/incorporating corrections for such effects in a typical z-scan experiment to obtain a *pure refractive scan.*

9. Find the value of the critical power to be carried by a beam of light at 500 nm for undergoing self-trapping in a medium of linear refractive index 1.7000 and nonlinear coefficient $n_2 = 3 \times 10^{-16} m^1 W^{-1}$. What would happen if the power were to increase beyond this value?

10. Consider self focusing of 10 ns pulses at a repetition rate of 10 pps from a Q-switched laser at a wavelength of 500 nm in a medium with $n_2 = 1.60$. Find the pulse energy required to focus a beam of initial diameter of 100 μm within a path length of 1 cm.

11. What kind of chirping do you expect when a pulse travels through a medium of negative n_2? What would happen to the pulse the medium also has a positive GVD?

12. The concept of a soliton is very interesting as well as useful. The idea of compensating for the effect of one physical process on pulse propagation exactly by the effect of by another process is quite fascinating. A lot of research has gone into the mathematical aspects of obtaining soliton solutions for nonlinear differential equations [Porsezian, 2010]. On the other hand, a lot of work has been done in exploring the scope of soliton propagation in fiber optic communications [Agrawal, 2010 and 2012]. You can take the help of popular mathematical software to explore the influence of designing systems with different values of L_D and L_N and visualize soliton propagation. This may help to arrive at design parameters for practical systems based on realistic materials available.

Chapter 8

Mechanisms and Materials

"There is no object so foul that intense light will not make it beautiful".

Ralph Waldo Emerson

The wide variety of possible mechanisms in different materials, natural and artificial, is quite amazing.

Learning Objectives

- Assessment of the role of different physical processes that lead to optical nonlinearity.
- Distinguish between the mechanisms involved in these processes
- Comparison of the nature and magnitude of nonlinearity arising from the mechanisms.
- Identification of the upcoming frontiers in the design of novel Photonic materials.

8.1 Introduction

In this chapter, we learn about materials which exhibit optical nonlinearities and the underlying fundamental processes that lead to nonlinearity. The response of a dispersive dielectric to an incident electromagnetic wave is described in terms of the dielectric constant of the medium, which is a complex quantity. The real part of dielectric constant governs its dispersive behavior and the imaginary part is responsible for optical absorption in the medium. An interesting consequence of the fact that the electric field in a material at any given instant is determined by the polarization which occurred at all preceding times is that the real and imaginary parts of the dielectric constant are related to each other. The equations governing the relation between the processes of dispersion and absorption are known as Kramers-Kronig relations and are discussed in standard textbooks on solid state physics [Kittel, 2004; Ashcroft and Mermin, 1976]. The scope of these relations extend also to nonlinear optical absorption as well as dispersion. The changes in nonlinear absorption due to optical excitation processes are normally limited to a range of frequencies and hence can be measured more easily than changes in dispersion and hence the relation between absorption and dispersion becomes very useful [Hutchings et al, 1992; Peiponen et al, 2010; Lucarini et al, 2005]. A variety of physical mechanisms can lead to absorption, excitation and dispersion processes in different materials. Thus a systematic analysis of the known types of nonlinear materials and the underlying dominant mechanisms of light-matter interaction in these materials is a very important frontier area of research.

It is convenient to classify materials according to their physical state: single crystals, polycrystals, noncrystalline materials, liquids and gases. We have seen in previous chapters that certain non-linearities can be exhibited only by single crystals. It is also possible to distinguish nonlinear optical materials as per their well-known standard classification: inorganic materials, organic materials, polymers, semiconductors, and liquid crystals. Another classification may be based on the physical / atomistic mechanism of the nonlinearity. Space limitation does not permit us to make a comprehensive account of all these aspects. We therefore give an instructive perspective of some of the relevant features in this chapter.

8.2 Mechanisms of Nonlinearity

There are a number of distinct fundamental processes that could lead to observed optical non-linearities in materials. We summarize these and then give a brief account of each to follow. Of course all these mechanisms do not operate in all materials and some are specific to some type of materials while some have a universal character. Experimental investigations can disclose which mechanism operates in a given material and for a given nonlinear optical process. The various mechanisms are:

- Anharmonicity of potential
- Thermal mechanism
- Orientational mechanism
- Inelastic photon scattering
- Photorefractivity
- Saturable absorption
- Band gap distortion
- Band gap filling
- Band non-parabolicity
- Delocalization

8.2.1 Anharmonicity of Potential

The classical equation of motion for the displacement ξ from the equilibrium position (potential minimum) for the forced oscillations of a damped anharmonic oscillator having the charge e and mass m, subject to a harmonic electric field E is

$$m\frac{d^2\xi}{dt^2} = -k_1\xi - k_2\xi^2 - k_3\xi^3 - \gamma\frac{d\xi}{dt} + eE_0\frac{1}{2}\left(e^{i\omega t} + e^{-i\omega t}\right) \quad (8.1)$$

where $-k_1\xi$ is the linear restoring force, $-k_2\xi^2$ and $-k_3\xi^3$ are the anharmonic force terms, $-\gamma\frac{d\xi}{dt}$ is a damping force, the last being

the electric force. E_0 is the amplitude of the applied electric field, having the angular frequency ω. Assuming solutions of the form

$$\xi = \frac{1}{2}\left(x_1 e^{i\omega t} + x_2 e^{i2\omega t} + x_3 e^{i3\omega t} + c.c.\right) \tag{8.2}$$

Substituting this in the equation of motion and equating coefficients of the same frequency on either side, and assuming that $\frac{k_2}{m}x_2 \ll \left[\left(\frac{k_1}{m} - \omega^2\right)^2 + \left(\frac{\gamma}{m}\right)^2\omega^2\right]^{\frac{1}{2}}$,

$$x_1 = \frac{eE_0}{m}\left(\frac{1}{\frac{k_1}{m} - \omega^2 + i\omega\frac{\gamma}{m}}\right) \tag{8.3}$$

The linear susceptibility corresponds to the polarization at the angular frequency ω. This polarization is given by $P^{(\omega)} = Nex_1$, given by

$$P^{(\omega)} = \frac{Ne^2}{m}\left(\frac{1}{\frac{k_1}{m} - \omega^2 + i\omega\frac{\gamma}{m}}\right) \tag{8.4}$$

Equating this with

$$P^{(\omega)} = \epsilon_0\frac{1}{2}\left(\chi_\omega^{(1)}E_0 e^{i\omega t} + c.c.\right) \tag{8.5}$$

we have the susceptibility given by

$$\chi_\omega^{(1)} = \frac{Ne^2}{m\epsilon_0}\left(\frac{1}{\frac{k_1}{m} - \omega^2 + i\omega\frac{\gamma}{m}}\right) \tag{8.6}$$

Proceeding in the same way, we solve for the second order displacement amplitude x_2. The solution is

$$x_2 = \frac{k_2 e^2 E_0^2}{2m^3}\left[\frac{1}{\left(\frac{k_1}{m} - \omega^2 + i\omega\frac{\gamma}{m}\right)^2}\right]\left[\frac{1}{\frac{k_1}{m} - 4\omega^2 + 2i\omega\frac{\gamma}{m}}\right] \tag{8.7}$$

This leads to the second order optical susceptibility

$$\chi_\omega^{(2)} = \frac{-\gamma N e^3}{\epsilon_0 m^3}\left[\frac{1}{\left(\frac{k_1}{m} - \omega^2 + i\omega\frac{\gamma}{m}\right)^2}\right]\left[\frac{1}{\frac{k_1}{m} - 4\omega^2 + 2i\omega\frac{\gamma}{m}}\right] \tag{8.8}$$

Now it can be seen that there is an inherent relationship between the second order and the first order susceptibilities, given by

$$\chi^{(2\omega)} = \frac{k_2\epsilon_0^2}{2N^2e^3}\left(\chi_\omega^{(1)}\right)^2\left(\chi_{2\omega}^{(1)}\right) \tag{8.9}$$

A similar calculation for the third order susceptibility leads us to the relation

$$\chi^{(3)}(\omega;\omega,\omega,-\omega) = \frac{k_3}{2N^3e^4}\left(\chi^{(1)}_{\omega}\right)^4 \tag{8.10}$$

for centrosymmetric materials. [Jamroz 1980]. And the relation for non-centrosymmetric materials is

$$\chi^{(3)}(\omega;\omega,\omega,-\omega) = \frac{k_2^2}{N^4e^6}\left(\chi^{(1)}_{\omega}\right)^5 \tag{8.11}$$

These relations are known as Miller's rules [Miller, 1964; Garrett and Robinson, 1966].

8.2.2 Thermal Mechanism

When an incident electromagnetic wave is absorbed by the nonlinear material, de-excitation (return of the material from the electronic excited state to the ground state) could occur via exchange of energy with the surrounding heat bath of lattice phonons. This results in a local change in temperature which in turn produces a change in the mass density ρ and hence in the dielectric permittivity ϵ. In semiconductors this could also result in a local change in the band gap E_g. Both effects lead to a net change in the permittivity given by

$$\delta\epsilon = \frac{\partial\epsilon}{\partial T}\delta T + \frac{\partial\epsilon}{\partial\rho}\delta\rho \tag{8.12}$$

The temperature change is governed by the standard thermal diffusion equation which has parameters such as heat capacity C_p and diffusivity D. The explicit dependence of the permittivity on temperature usually is not significant. In order for the thermal mechanism to be effective two conditions are to be met: (1) Enough time must elapse for the non-radiative energy to be off-loaded at the grating maxima enabling the build up of the density change $\delta\rho$. The minimum time needed for thermal expansion to obtain is of the order of $\frac{\Lambda}{2v_s}$ where Λ is the spatial grating wavelength and v_s is the speed of sound in the material. (2) A second conflicting aspect is the fact that heat may conduct away from the grating maxima resulting in a blurring of the nonlinearity effect. The blurring time may be estimated as $\frac{\Lambda^2}{4\pi^2 D}$. With pulsed lasers having pulse duration

τ_p, therefore, we may state the condition to be satisfied for thermal mechanism to be operative as

$$\frac{\Lambda}{2v_s} \leq \tau_p \leq \frac{\Lambda^2}{4\pi^2 D} \tag{8.13}$$

In semiconductors, the other possible process is through the change in the band gap with temperature following the de-excitation.. The change in the refractive index δn as a consequence may be written as

$$\delta n = \delta T \frac{\partial n}{\partial E_g} \frac{\partial E_g}{\partial T} \tag{8.14}$$

It is a fact that thermal nonlinearities could have large magnitudes but also large response times.

8.2.3 Orientational Mechanism

This mechanism works in materials having molecules with anisotropic polarizabilities. We may consider liquid CS_2 as a prototype of this class of materials. The principal electronic polarizabilities of CS_2 are α_{33}, $\alpha_{11} = \alpha_{22}$. α_{33} is nearly three times larger than the other components. The potential energy of such a molecule in an electric field is given by

$$U = -\frac{1}{4}\alpha_{ij} E_i E_j \tag{8.15}$$

This energy is a minimum when the molecule has its axis parallel to the electric field direction. The degree of orientation of the molecule under an electric field depends on the temperature T according to the magnitude of the quantity $(\alpha_{33} - \alpha_{11}) \frac{|E|^2}{k_B T}$, where k_B is the Boltzmann constant. Partial orientation of the molecules causes change in the permittivity according to the equation

$$\delta\epsilon_{ij} = \frac{3}{8}\epsilon_z \left[E_i E_j^* + E_i^* E_j - \frac{2}{3}\left(\vec{E} \cdot \vec{E}^*\right) \delta_{ij} \right] \tag{8.16}$$

where ϵ_z is a constant of the material. Any anisotropic molecule in liquids or gases can give rise to this effect and the relaxation time is of the order of 10^{-10} s to 10^{-12} s.

8.2.4 Inelastic Photon Scattering

There occur many processes in which, following the illumination, the atoms of the material end up in an eigen state different from the initial state, as a consequence of the nonlinear interaction of the relevant waves. In such cases, the energy is not conserved among the interacting photons but one has to include the change in the internal energy of the atoms. Stimulated Brillouin scattering and Stimulated Raman scattering are examples of this class.

8.2.5 Photorefractivity

This is an important mechanism which has been used often in optical amplification applications. The photorefractive crystals have been seen to provide high phase conjugate reflectivities. The basic photorefractive effect consists of a change in the refractive index tensor due to second order interaction with light waves [Yariv, 1989]. This is essentially the linear electro-optic effect phenomenologically depicted by the relation

$$\Delta\left(\frac{1}{n^2}\right)_{ij} = r_{ijk}E_k \tag{8.17}$$

wherein six refractive index components are written as functions of the electric field components. With the condensed notation we have introduced in an earlier chapter, we may write out the matrix equation as

$$\begin{pmatrix} \delta\left(\frac{1}{n^2}\right)_1 \\ \delta\left(\frac{1}{n^2}\right)_2 \\ \delta\left(\frac{1}{n^2}\right)_3 \\ \delta\left(\frac{1}{n^2}\right)_4 \\ \delta\left(\frac{1}{n^2}\right)_5 \\ \delta\left(\frac{1}{n^2}\right)_6 \end{pmatrix} = \begin{pmatrix} r_{11} & r_{12} & r_{13} \\ r_{21} & r_{22} & r_{23} \\ r_{31} & r_{32} & r_{33} \\ r_{41} & r_{42} & r_{43} \\ r_{51} & r_{52} & r_{53} \\ r_{61} & r_{62} & r_{63} \end{pmatrix} \begin{pmatrix} E_1 \\ E_2 \\ E_3 \end{pmatrix} \tag{8.18}$$

A number of photorefractive crystalline materials have been investigated. These include $BaTiO_3$, $Bi_{12}SiO_{20}$ (BSO), $KTa_{1-x}Nb_xO_3$ (KTN), $LiNbO_3$, $LiTaO_3$, $Bi_{12}GeO_{20}$ (BGO), $KNbO_3$.

The popular photorefractive crystal, $BaTiO_3$ belongs to the point group C_{4v} $(4mm)$ and crystal symmetry effects leads us to give 3 independent components of the r tensor: $r_{13} = r_{23}$, r_{33}, $r_{42} = r_{51}$. The values of these components are for $BaTiO_3$, $r_{13} = 8 \times 10^{-12}$ $m\ V^{-1}$, $r_{33} = 28 \times 10^{-12}$ $m\ V^{-1}$, $r_{42} = r_{51} = 820 \times 10^{-12}$ $m\ V^{-1}$. Note r_{42} and r_{51} are the strongest. And $r_{13} \equiv r_{xxz}$, $r_{42} \equiv r_{yzy}$, $r_{51} \equiv r_{zxx}$. Therefore, these strong components do not contribute to the effect if the electric field is along the Z direction ([001] direction of the crystal). Therefore one should orient the crystal such that the grating vector is away from the c axis ([001]).

Photorefractive materials are most sensitive for optical phase conjugation. The sensitivity is comparable to that of photographic emulsions. Laser beams of low power (μW)are used to realize high reflectivities of the order of 100%.

The effect operates as follows:

(1) Light causes charges to migrate and separate in the crystal.

(2) Charge separation produces strong electrostatic fields.

(3) This static light-induced electric field produces large changes in the refractive index via linear electro-optic effect (Pockels' effect).

The photorefractive index change depends on the relative intensity of the interacting beams in the steady state. The writing times depend on the intensity and the magnitude of changes δn are independent of the intensity. The effect is spatially nonlocal in that δn is maximum not where the intensity of the beams is greatest. Charges existing in defect states play a significant role.

Let us now consider the details of the phase conjugate four wave mixing in a photorefractive crystal. The geometry of the wave mixing in the crystal is shown in Fig. 8.1 [Feinberg and Hellwarth 1980]

The reference write beam is 1, the image writing beam is 2, 3 is the read beam and 4 is the conjugate beam. The grating vector $\vec{k}$ makes a non-zero angle θ with the Z axis so that we can reap a significant contribution from the large components of the r tensor

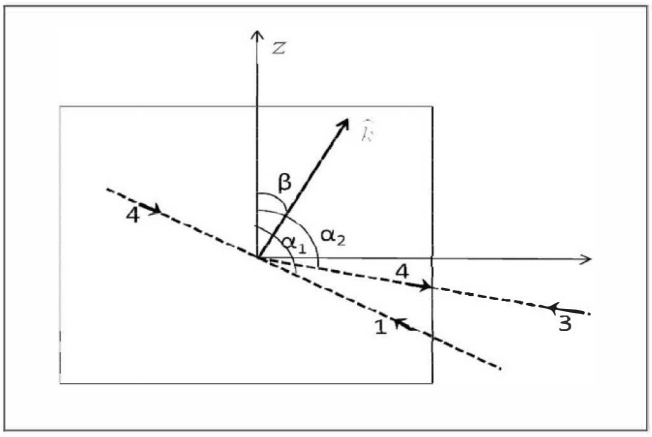


Figure 8.1: Beam geometry in OPC in a photorefractive crystal

of the crystal. Fig. 8.2 depicts the wave vectors of the interacting beams in reference to the grating.

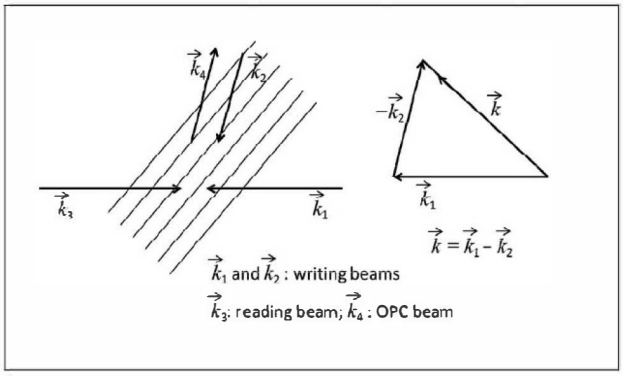


Figure 8.2: The grating picture for OPC in a photorefractive rystal

The periodic intensity pattern in the grating is given by

$$I(\vec{r}) = I_0 \left(1 + m \cos \vec{k} \cdot \vec{r}\right) \tag{8.19}$$

where $\vec{k} = \vec{k}_1 - \vec{k}_2$, is the grating vector. $I_0 = I_1 + I_2$, the sum of the intensities of the two writing beams. m is the modulation index given by

$$m = \frac{2\vec{E}_1 \cdot \vec{E}_2^*}{I_0} \tag{8.20}$$

and the magnitude of the grating vector is equal to $\left|\vec{k}\right| = 2k_1 \sin\theta$, where θ is the angle between the two vectors $\vec{k}_1$ and $\vec{k}_2$, as shown in Fig. 8.2.

Initially there is a uniform charge density N. With the illumination, charges migrate, there being an equal number of the mobile and immobile charges. The migrating charges move from regions of high intensity to regions of low intensity. Eventually, a steady state periodic pattern of grating is formed with the spatial periodicity characterized by the vector $\vec{k}$. A steady state electric field $\vec{E}$ is produced which is given by

$$\vec{E}\,(\vec{r}) = Re\left(E\hat{k}e^{i\vec{k}\cdot\vec{r}}\right) \tag{8.21}$$

The field is directed parallel to the grating vector. The electric field is given by

$$\vec{E}(\vec{r}) = -\frac{k_B T}{q} m \frac{\vec{k}}{\left(1 + \frac{|\vec{k}|}{s}\right)} \sin\left(\vec{k}\cdot\vec{r}\right) \tag{8.22}$$

where $s = \sqrt{\frac{Nq^2}{\epsilon_r \epsilon_0 k_B T}}$.

We can see that the intensity has a uniform constant value I_0 on which is superposed a periodic spatial wave $\cos\left(\vec{k}\cdot\vec{r}\right)$. This gives rise to a periodic charge distribution described by $-\cos\left(\vec{k}\cdot\vec{r}\right)$, which then gives an electric field which varies as $-\sin\left(\vec{k}\cdot\vec{r}\right)$ and a consequent refractive variation of $\sin\left(\vec{k}\cdot\vec{r}\right)$. The constant uniform intensity tends to randomize the charge distribution, while the relative intensity gives rise to the periodic component.. The steady state distribution depends on these two opposing effects.

8.2.6 Saturable Absorption

There are many kinds of electronic transitions that can contribute to this mechanism. Fundamentally, this mechanism depends on the fact the populations of electronic levels depend on the light intensity especially for levels with long life-times. Because these changes can be quite large, susceptibilities of higher order such as fifth order

can play a significant role. The intensity dependence of the state populations lead to the absorption coefficient α depending on the light intensity (I) , which is phenomenologically written as

$$\alpha(\omega, I) = \frac{\alpha_0(\omega)}{\left(1 + \frac{I}{I_{sat}}\right)^{\frac{1}{2}}} \tag{8.23}$$

Correspondingly the intensity-dependent susceptibility may be written as

$$\chi(\omega, I) = \frac{\chi_0(\omega)}{\left(1 + \frac{I}{I_{sat}}\right)^{\frac{1}{2}}} \tag{8.24}$$

where I_{sat} is the saturation intensity. This may be expanded in powers of intensity I for $\frac{I}{I_{sat}} \prec\prec 1$, leading to susceptibilities of various orders.

In semiconductor materials, there are several electronic transitions that exhibit saturable absorption and hence possible candidates under this category. These are (i) valence band to valence band transitions (ii) conduction band to conduction band transitions (iii) exciton transitions and (iv) impurity transitions. The first two types involve free carrier transitions in heavily doped extrinsic semiconductors.

8.2.7 Band Gap Distortion (Franz-Keldysh Effect)

Under illumination with a sufficiently strong electromagnetic wave, the band gap is smeared and the effective band gap E_g is reduced. The effect due to a DC electric field was discovered by Keldysh[1958] and Franz [1958]. This effect involves a change in the dielectric permittivity. Van Vechten and Aspnes [1969] calculated the third order susceptibility due to this effect using a two-band model, giving an expression for $\chi^{(3)}$ as

$$\chi^{(3)}(\omega) = \frac{1}{32}\frac{e^4 C_0^2 h}{2\pi m^2}\sqrt{m^*}E_g^{-\frac{9}{2}} \tag{8.25}$$

8.2.8 Band Filling Mechanism

This is alternatively known as band blocking mechanism or Burstein-Moss effect. In this mechanism, valence band to conduction band

transitions generate free carrier plasma. There results a loss of states or blocking of these states which causes the refractive index to be modified according to the equation

$$\Delta n = \frac{2\pi N e^2}{n m^* \omega^2} \frac{\omega_g^2}{\omega_g^2 - \omega^2} \tag{8.26}$$

where $\omega_g = \frac{2\pi E_g}{h}$, E_g being the band gap. Large third order susceptibilities can result from this mechanism especially in small band gap semiconductors. For example, in $InSb$ which has the band gap of 0.235 eV, $\chi^{(3)} \approx 10^{-9}\ m^2\ V^{-2}$. In $Hg_{0.78}Cd_{0.22}$ with a band gap of 0.14 eV, $\chi^{(3)} \approx 10^{-10}\ m^2\ V^{-2}$.

8.2.9 Non-parabolicity of Bands

The conduction bands especially in small band gap materials exhibit significant deviations from parabolic shape. The resulting nonlinear carrier motion and energy relaxation present important nonlinear effects in response to driving dielectric fields. The effective mass of the electron m_e^* becomes significantly dependent on the energy (or linear momentum p). For example, Kane's model for band structure of $InSb$ is given by (for the conduction band edge E_c)

$$E_c = \frac{p^2}{2m} + \frac{E_g}{2} + \left(\frac{E_g^2}{4} + E_g \frac{p^2}{2m_e^*} \right)^{\frac{1}{2}} \tag{8.27}$$

Under the assumption that $\frac{p^2}{2m_e^*} \ll E_g$ and $m_e^* \ll m$, the effective mass and drift speed of the carrier are given by

$$m^*(p) \simeq m_e^* \left(1 + \frac{p^2}{2m_e^* E_g} \right) \tag{8.28}$$

$$\vec{v}(p) = \frac{\partial E_c}{\partial p} = \frac{\vec{p}}{m_e^* \left(1 + \frac{p^2}{2m_e^* E_g} \right)^{\frac{1}{2}}} \tag{8.29}$$

With nondegenerate frequencies, the equation of motion for the linear momentum is

$$\frac{d\vec{p}}{dt} + \frac{\vec{p}}{T_{2m}} = e\vec{E} = \frac{1}{2} e \left[\vec{E}_1 e^{i\omega_1 t} + \vec{E}_2 e^{i\omega_2 t} + c.c. \right] \tag{8.30}$$

which has the solution for the linear momentum

$$\vec{p} = \frac{e\vec{E}_1}{2\left(i\omega_1 + \frac{1}{T_{2m}}\right)} + \frac{e\vec{E}_1}{2\left(i\omega_1 + \frac{1}{T_{2m}}\right)} + c.c. \tag{8.31}$$

In most cases, the relaxation term can be neglected and the solution can be used to give, after expansion, expressions for the nonlinear susceptibilities. The third order susceptibility is, for example, given by

$$\chi^{(3)} = \frac{Ne^4}{4\left(m_e^*\right)^2 E_g \omega_1^2 \omega_2 \omega_3} \tag{8.32}$$

8.2.10 Delocalization of Electrons

We have learned in an early chapter that large sizes of electron distributions tend to give large linear polarizability and in the spirit of Miller's rules, large non-linearities also may be expected. Thus electrons delocalized over an extended spatial region do give rise to large nonlinear responses. This is most prominently seen in the π electrons of polymeric organic materials. The delocalization essentially decreases the binding of the electrons at the same time enhancing their linear as well as non-linear optical responses.

A conjugated polymer chain having alternating σ and π bonds is schematically represented in Fig. 8.3.

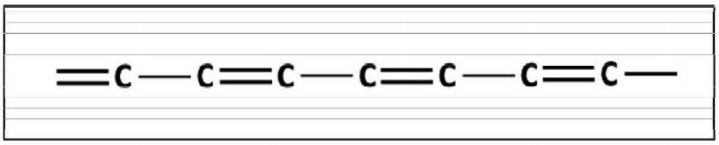


Figure 8.3: A conjugate polymer chain

Using a quasi-free electron model moving in a one-dimensional potential well, Rustagi and Flytzanis [1984] deduced the linear polarizability (α) and hyper-polarizability (γ) of such a chain as dependent on the chain length L as

$$\alpha = \frac{8L^3}{3a_0\pi^2 N} \tag{8.33}$$

$$\gamma = \frac{256L^5}{45a_0^3e^2\pi^6N^5} \tag{8.34}$$

where a_0 is the first Bohr radius, and N is the number of electrons per unit length of the polymer chain. The linear polarizability increases with the chain length fast as $\propto L^3$ but the higher order polarizability increases even faster at the rate $\propto L^5$. Experimental investigations support these theoretical predictions.

Because of the advantages offered by organic substances, many studies had been performed on organic polymeric materials [references of others as well as our lab research findings to be given here]. Possibility of making waveguides by the method of Langmuir-Blodgett films, and molecular engineering make these materials attractive candidates for nonlinear-optical device applications.

Some aspects of the molecular engineering toward developing materials yielding large magnitudes of second order optical susceptibilities have been identified. These involve

- non centrosymmetric moieties spatially arranged
- design of non-centric NLO organic moieties with large β values
- incorporating these moieties into optically transparent polymers
- fabrication of polymers for orientational control

The needed characteristics for obtaining large β values in molecules are: (i) highly delocalized electronic distribution (ii) large electronic dipole moment. To realize the second feature, it is suggested that one should have electron donor and electron acceptor substituents to be placed at opposite ends of the molecule. Amines, methylene, etc. are electron-donors. Halogens, nitro, cyano, etc. are acceptor units. [De Martino et al 1988]. They illustrated these points with the material para-nitroaniline (PNA) having the following structure (Fig. 8.4).

This has a measured value of $\beta = 5.7 \times 10^{-30}\ esu$. The effect of increasing the conjugation length, adding effective donor acceptor entities and maintaining planarity helped enhancing the nonlinear

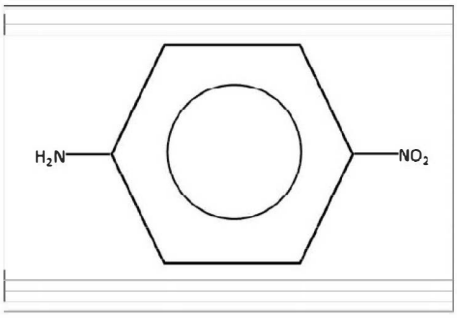


Figure 8.4: Structure of PNA

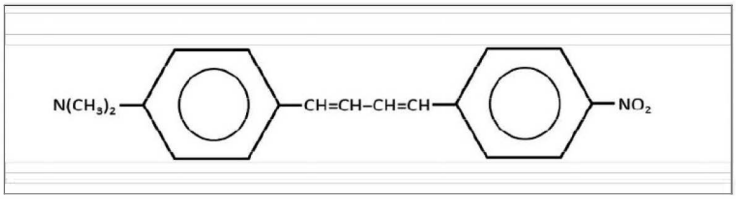


Figure 8.5: Molecular engineering with PNA

polarizability to the value $\beta = 111 \times 10^{-30}$ *esu*. The engineered structure looks as in Fig. 8.5.

Polymers offer a large scope for structure modification, which can be utilized to engineer materials with large and fast optical nonlinearity. The structures of certain polymers such as polyphenyl acetylene (PPA) have well-spread electron clouds resulting in large values of linear as well as nonlinear susceptibility. Structure of such polymers can be modified easily by doping with other materials and/or attaching appropriate side groups to the main chain. Some of these variations are known to enhance the nonlinearity of the basic polymer by way of extending the spatial spread of electrons and hence enlarging the linear as well as nonlinear susceptibilities [Vijaya et al, 1993; Martino et al, 1988]

A second example is that of structure variation studies in porphyrins, phthalocyanines etc which also has yielded interesting results [Unnikrishnan, et al, 2002;Venkatram, et al, 2008]. Porphyrins allow for incorporation of various ligands and different core metal ions, which alter the susceptibilities dramatically. Incorporation of

porphyrins into solid polymer membranes is found to enhance nonlinearity, besides stabilizing the materials against photodegradation and providing a convenient solid matrix . Composites of optical materials with different kinds of mechanisms and several other materials in solid, liquid and film state appear to hold promise from the device application point of view [Chemla, 1980; Chemla and Zyss, 1987; Gupta et al, 2011, 2012].

8.3 A Perspective on Newer Materials and Processes

We have come across several classes of nonlinear optical materials in the process of surveying the physical mechanisms of nonlinearity in the previous section. These include semiconductors, polymers, inorganic crystals and liquid crystals, which are being used widely as conventional materials for applications in nonlinear optics. The most important limitation in the technology of nonlinear optics has been the non-availability of ideal materials for exploiting the potential of nonlinear optical processes to their fullest extent. This is known as the *materials bottleneck*. It turns out that most of the available materials do not meet the simultaneous requirements of large as well as fast nonlinearity required for the practical devices. Thus recent research has focused on design and development of artificial materials with fast as well as large nonlinearity. The emerging candidate materials from this perspective are modified/functionalized molecular materials, low dimensional materials and photonic band gap materials.

8.3.1 Low Dimensional Materials

One of the key approaches to obtaining nonlinear optical materials with acceptable values of figure-of-merit is that of *Quantum Engineering* of semiconductor nanostructures. Mechanisms of nonlinearity in a variety of low dimensional materials such as semiconductor quantum dots, quantum wells, quantum wires, nanohybrids and composites, functionalized carbon nanotubes, graphene hybrids is being studied in this context. Quantum wells are made by confining electrons to a plane, in quasi-two-dimensional structures. This can be achieved by placing a thin layer of a semiconductor material sandwiched between two layers of an insulating material (or even some other semiconductor a larger value of the bandgap). Thus the

electrons in the middle layer experience a potential when they try to move in a direction perpendicular to the plane while they are free to move within the plane. These are now being used in several devices. Electrons can be confined further to one dimension by embedding a semiconductor wire or a conducting polymer chain in a material of larger band gap.

Quantum dots are quasi zero dimensional materials formed by embedding tiny crystalline islands of semiconductors or a metals (called nanoclusters) in an insulating host such as glass or a polymer matrix. The surrounding material provides the confining potential while also holding the material in place. These are practical realizations of *particle in a box* whose optical properties depend on the particle size. Several techniques of obtaining such monosize clusters have been perfected by materials scientists. However, a major problem with free standing nanoclusters disperse in solutions is the lack of stability in view of the fact that individual quantum dots to cluster together, become heavier and get precipitated eventually, often within a few hours after preparation. The techniques used to prevent this include the use of a capping agent or a shell over the quantum dot or embedding them in appropriate insulating host media. Other techniques are ion-implantation, monolayer building and molecular beam epitaxy also are being used widely to produce strongly confined quantum dots. Embedding semiconductor quantum dots in appropriate transparent insulating media such as Nafion ionomer |Nandakumar et al, 2002| has been shown to hold promise in obtaining highly stable quantum dots in a format convenient for optical measurements. Quantum confinement alters the electronic structure of the semiconductor and hence influences the linear and nonlinear optical properties. The band gap is modified by the increased oscillator strength of exciton transitions and hence there is an effective blueshift of the absorption edge with decreasing cluster size. This results in an alteration of the effective band gap, which is also termed as *Bandgap Engineering*. Recent studies indicate that strong quantum confinement results in considerable increase in the nonlinear susceptibilities.

Understanding Quantum Confinement

An approach to understanding quantum confinement effects in semiconductor quantum dots is to consider the behavior of Mott-Wannier (MW) excitons in these systems |Kittel, 2004; Woggon, 1997|. These

are well understood systems in the bulk [Ibach and Luth, 1991]. This exciton is an electron-hole pair, which can be represented by a simple hydrogen-like picture, with energy levels E_n proportional to n^2, $(n = 1, 2, 3...)$ with a Bohr model radius

$$R^{(n)} = (1/2)(\varepsilon_r/m')n^2$$

where ϵ_r is the relative dielectric constant of the material, m' is the reduced mass of the electron and hole effective masses in units of the electron rest mass. The MW exciton is weakly bound and can have a spatial extent of a few lattice spacings. The effects of confinement start showing up when the size R becomes comparable to or less than the exciton Bohr radius. In this case, it is as if the electron gets trapped in a quantum jail [Murti et al, 1999].

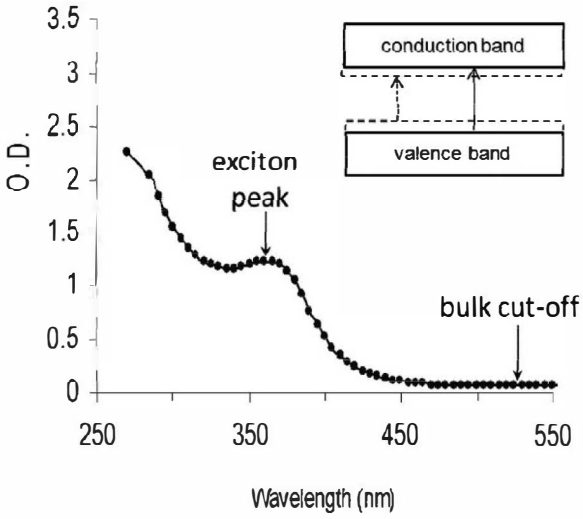


Figure 8.6: Optical absorption spectrum of nanocrystalline CdS. The inset shows the band picture

Let us apply the principles of quantum mechanics to the dot embedded in a dielectric medium. For spherical dots of radius R, the exciton Hamiltonian H can be written, to the first approximation, as

$$H = \frac{h^2}{8\pi^2 m_e^*}\nabla_e^2 - \frac{h^2}{8\pi^2 m_h^*}\nabla_h^2 + V_C + V_e(r_c) + V_h(r_h)$$

The first and second terms are the kinetic energies of the electron and hole, V_C is the Coulomb energy between the electron and the hole. $V_i(r_i)$ are the barrier potential experienced by the electron and the hole ($i = e$ or h , referring to electron or hole respectively). m_e and m_h are the effective masses of the electron and the hole in the lattice respectively. Also, we may take $V_i(r_i) = 0$ for $r_i < R$ and ∞ for $r_i \geq R$; In a simplified picture, the Coulomb interaction is neglected and $V_C = 0$.

The energy eigenvalues are obtained for the electron ($i = e$) and for the hole ($i = h$)

$$E^i_{n.l} = -\frac{\alpha^2_{n,l}}{m_i}\frac{h^2}{8\pi^2 R^2}, i = h, m$$

The energy levels for the electron and hole are given in eV for dot radius R in units of nm, are given by

$$\begin{aligned} E^h_{n,l} &= -\frac{0.0382}{m'_h R^2}\alpha^2_{n,l} \\ E^e_{n,l} &= -\frac{0.0382}{m'_e R^2}\alpha^2_{n,l} + E_g \end{aligned}$$

where the parameters $\alpha_{n,l}$ have the values for a few cases: $1s$: 3.1416, $1p$: 4.4934, $2s$: 6.2832, $2p$: 7.7253. The band gap energy of the nanocrystal is E^* given by

$$E^* = E_g + \frac{\hbar^2\pi^2}{2R^2}\left[\frac{1}{m_e} + \frac{1}{m_h}\right] - \frac{1.786e^2}{\varepsilon R}$$

This simple model brings out the experimental observation of a $1/R^2$ dependence (known as blue shift).

Optical Nonlinearity in Nanomaterials

The size dependence of optical absorption and fluorescence emission makes quantum dots useful as tunable absorbers and emitters. Nonlinear optical properties are also predictably influenced by quantum confinement. Several reports have appeared on nonlinear optical mechanisms and the size dependence of optical nonlinearity in quantum confined systems [Jain and Lynd, 1983; Woggon, 1997; Rustagi and Flytzanis, 1984; Roussignol et al, 1985; Gaponeko, 2005; Bindra et al, 1993; Wang, 1991]. The continuous energy bands

picture is no longer valid in strongly confined systems and hence the mechanisms of nonlinearity in low quantum dot materials could be different from those in the bulk [Yoffe, 1993]. (The references listed here are those which the authors happened to have noticed and the list is not meant to be exhaustive).

Large nonlinearities have been observed in semiconductor nano crystals using degenerate four wave mixing, z-scan, photoluminescence and femtosecond time resolved pump probe experiments [Wang and Mahler, 1987; Hilinski et al., 1988; Wang et al., 1990; Yao et al., 1996; Miyoshi et al., 2001, Klimov et al, 1996; Klimov et al., 1999; He et al., 2005]. Most of the early work was on semiconductor doped glasses, which have a major limitation of undergoing photodarkening effect. A few reports exist on semiconductor nanocrystals suspended in solutions. The volume fraction of nanocrystals in solutions is small resulting in weak nonlinear response. Thus, polymer-embedded nanomaterials emerge as preferred materials. [Schwerzel 1998; Nandakumar et al, 2000 and 2002; Du et al., 2002; Venkatram et al, 2005 and 2007; Sureshbabu et al, 2007; Pushpa 2008]. In general, resonant nonlinearities have large magnitudes, but are accompanied by a slow response and large linear absorption. On the other hand, off-resonant nonlinearity has ultrafast response.

Nonlinear Absorption and Optical Limiting

A variety of physical mechanisms are operative in semiconductor quantum dot materials and the exact nature of the mechanism depends on parameters such as the wavelength, pulse duration and intensity of the exciting radiation. The surface condition of the cluster, particle size and size distribution are factors which can affect the response. Apart from nonlinear refraction, these materials are also known to exhibit strong nonlinear absorption processes: free carrier absorption, multiphoton absorption, saturable and reverse saturable absorption. Some of these mechanisms lead to optical limiting. Optical limiters are devices which have constant transmittance at low input fluences and a decrease in transmittance at high fluences. These devices are used to protect optical sensors and eyes from laser induced damage. Large nonlinear absorption in nanocrystalline materials can also be used to produce efficient optical limiters. Recent reports are available on enhanced nonlinearity in different materials such as oxide nanostructures, carbon nanotubes, plasmonic structures and graphene-related materials [Manas et al, 2012; Jyotsana,

2011; Polavarapu et al, 2008; Irimpan et al, 2008; Yang et al, 2011; Bonaccorso et al, 2010; Philip, 2012 and Yao and Belyanin, 2013|

8.3.2 Photonic Bandgap Materials

The year 1987 witnessed the publication of two very important papers in the area of optical materials, in the same issue of the journal Physical Review. One of these was by Yablonovitch, |1987|, who was interested in designing efficient lasers by suppressing spontaneous emission. His paper describes how inhibited spontaneous emission could be obtained when an emitter is embedded in a periodic optical structure. The other paper was by Sajeev John [1987], who was interested in localization of light along the lines of Anderson localization of electrons and reported on how to achieve this disordered dielectric superlattices. These papers brought out the immense potential of periodic optical structures in photonics applications while also highlighting the significance of localizing light, leading to extremely high intensities within regions of very small volume. This has led to a large number of investigations, opening up new vistas in linear as well as nonlinear optics.

The Concept of Photonic Bandgap

The basic idea of a photonic crystal can be understood easily by a short revisit of the band theory of solids, which describes the quantum mechanics of electrons in the presence of the periodic potential provided by a crystal lattice. The plot of energy E of the electron as a function of the magnitude of the wave vector $\vec{k}$ (denoted as the E-versus-k diagram) deviates from the parabola corresponding to the free electron. More importantly, energy values exhibit forbidden region for certain values of $\vec{k}$, leading to the band structure of the energy level diagram. The slope of such a curve indicates the group velocity of electrons in the crystal.

An analogous situation arises when light travels through a medium made up of alternating layers of two materials, with different values of refractive index, arranged periodically with a period comparable to the wavelength of light used |Joannopoulos et al, 2008|. This can be realized in one, two or three dimensions. Propagation through such a structure leads to energy bandgaps in a plot of photon frequency as a function of the wave vector, as shown in the figure. The effect of localization of light in photonic crystals ren-

ders them as interesting materials for nonlinear optics [Markowicz et al, 2002 and 2004] .

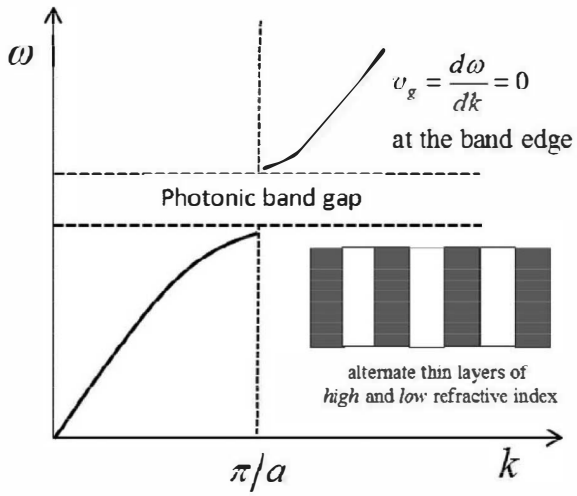


Figure 8.7: A skectch of the plot between frequency and the magnitude of wave vector, showing photonic bandgap; inset : a typical 1D PBG.

Nonlinear Photonic Crystal Fibers and Integrated Circuits

One of the earliest practical application of this concept is that of photonic crystal fibers in where the core is surrounded by photonic bandgap material of appropriate design to prevent radial leakage of the light propagating through the core. This renders these fibers very efficient with reduced need for repeaters. Apart from their superior efficiency in comparison with conventional fibers in communications, the nonlinear optical response of photonic crystal fibers is also of considerable interest [Agrawal, 2012].

Photonic crystal fibers are also very important as media for the realization of one of the most interesting and rather more recent nonlinear optical effect, namely, that of supercontinuum generation. This is an effect based on an interplay of various nonlinear

optical mechanisms that occur when a optical pulse of a very high intensity and a very short duration interacts with matter, which eventually results in the generation of laser emission with a broad spectral band with reasonably high intensities [Alfano, 2006; Dudley et al 2010]. Apart from functioning as tunable laser sources on wavelength filtering, such media are also very useful for applications such as multi-wavelength microscopy, optical information processing and high resolution imaging. A combination of nonlinear optical effects in fibers together with their intrinsic linear dispersion render them as excellent media for supercontinuum generation [Wadsworth et al, 2002; Solli, et al 2007; Agrawal, 2012].

Optical waveguides also plays an important role in integrated optics. High power densities can be attained with moderate values of total power in view of beam confinement in fibers, leading to increased interaction lengths and efficiency of interaction. The dependence of refractive index on intensity in the nonlinear regime permits the operation of integrated optical devices in an *all-optical* mode. Some of the commonly used elements of nonlinear integrated circuits include light sources, waveguiding structures, detectors, grating and prism couplers, grating reflectors, directional couplers, and Mach-Zehnder interferometers [Stegeman et al, 1988]. Polymer-based materials with high transparency and stability appear to be attractive candidate materials for applications in nonlinear integrated optics in view of their large optical nonlinearity coupled with the scope of control of the nonlinear response through structure modification and molecular engineering [Tomme et al, 1991].

8.3.3 *Slowing* of Light and the Effect on Nonlinearity

The speed of light gets reduced when it propagates in any medium other than vacuum and the obtainable speed is determined basically by the dielectric constant of the medium and is described in terms of the refractive index of the material involved. However, this reduction is much less than an order of magnitude. On the other hand, schemes have been designed to reduce the group velocity of light by several orders of magnitude, almost to zero. The slope of the curve in the plot of photon energy as a function of the magnitude of the wave vector (Fig 8.7) gives the speed of light. The plot indicates that the speed remains constant except for near-band-edge regions, where the slope reduces and eventually approaches zero. The physics of slowing of light and the processes involved and the

experimental methods of achieving slow light have been described in detail [Hau et al, 1999; Boyd and Gautheir, 2009; Notomi, 2010; Khurgin, 2011; Warrier and Vijayan, 2013].

One of the experimental techniques employed for slowing light is utilization of the phenomenon of electromagnetically induced transparency which arises due to certain subtle quantum effects in specific energy level systems. This leads to interesting spectral profiles of optical absorption which in turn manifests as the kind of dispersion of the group refractive index required for slowing of light. Another way of obtaining slow light is by utilizing certain specific features of the photonic band gap of suitably designed metamaterials. Photonic crystals can permit extremely low values of group velocity under certain conditions as a result of the propagation of light in a periodic arrangement of two different materials with alternating high and low values of refractive index, as can be judged by noting the slope at the photonic band edges in fig 8.7. The nature of the dispersion relations and hence the actual shape of the dispersion curve in a photonic crystal are determined by the geometry and dimensionality of the photonic crystal. This provides scope for designing efficient media for slowing of light. Light-matter interaction can be expected to get enhanced as interaction time gets larger at the band edges. Design of photonic crystal structure with flat regions of dispersion is crucial in a variety of slow-light effects, such as enhancement of the photonic density of states, lasing and enhanced nonlinear effects.

The physical basis of slowing of light in photonic crystals can be understood in terms of backscattering and omnidirectional reflection within the structure. Each unit cell of the photonic crystal, comprising of a region of high and low dielectric constant, acts as a backscattering point and light is coherently scattered, as in a one dimensional Bragg grating. If the forward and back scattered waves match with each other in phase and amplitude, they form a standing wave implying a slow mode with zero group velocity. Slow light can induce remarkable modifications in the manner in which matter interacts with light, paving way for novel forms of physical processes that can revolutionize the design of optoelectronic and photonic devices. Nonlinear optical response with extremely large efficiency is expected when intense slow light interacts with material media [Boyd, 2011]. Also, slow light media based on photonic crystals permit easy incorporation onto a chip by means of lithography at room temperatures. This enhanced nonlinearity alongwith a possible re-

duction in size of devices is capable of ushering in new paradigms of design of several technologically important devices such as photonic switches, optical memory elements, diodes and modulators, wavelength converters and other components useful in the control of information transfer and information storage as well as processing, paving the way for the realization of the long cherished dreams of all optical computing technologies of communication and control |Baba, 2008|. While the basic physics of slow light and its interaction with matter is quite intriguing at a fundamental level, recent results on the experimental front highlight the scope of photonic-crystal-based slow-light-structures in shaping up new, efficient and economic avenues of this emerging technology |Khurgin, 2011|.

8.4 Explorations

1. An optical material having second order nonlinearity is under a harmonic electric field with magnitude $E = E_m \cos(\omega t)$. Express the DC and second harmonic electric polarizations in the medium in terms of the relevant susceptibility, the amplitude and angular frequency of the electric field.

2. Often, thermal lens effects tend to overshadow the true electronic contributions to nonlinearity in experiments to probe the mechanisms of nonlinearity. Suggest methods by which this can be minimized.

3. Sketch the variation of the intensity-dependent absorption coefficient of a medium at a given wavelength of excitation as a function of the intensity of the incident light. Define saturation intensity. What is its physical significance?

4. A spherical quantum dot of radius 2.0 nm is formed out of a semiconductor material with a bulk band gap 2.40 eV. Using a simple model outlined in this chapter, estimate the energies (in eV) of the transitions $1s(h) \rightarrow 1s(e)$ and $1p(h) \rightarrow 1p(e)$ for the Mott-Wannier exciton. Take $m_h = m_0$ and $m_e = 0.7m_0$.

5. What is the difference between a Frenkel exciton and a Mott-Wannier exciton? Is the equation given in this chapter for the Bohr radius applicable in both the cases?

6. Calculate the first Bohr radius of the MW exciton in Silicon crystal. Take the hole and electron effective masses to be respectively $m_h = 0.16m_0$, $m_e = 0.92m_0$ and the static dielectric constant of Silicon to be 11.7. [Kittel, 2004].

7. Estimate the energies for the $1s(hole) \longrightarrow 1s(electron)$ and the $1p(hole) \longrightarrow 1p(electron)$ transitions for the Mott-Wannier exciton in a semiconductor quantum dot of radius 2.0 nm assuming a band gap of 2.4 eV.

8. Consider a beam of light passing through an infinite medium consisting of ultrathin layers of equal thickness a (of the order of a few hundreds of wavelength) arranged along the $x-$axis with alternate high and low values of refractive index. The layers are kept parallel to one another and the beam passes in a direction perpendicular to the plane of the layers. Representing the input beam as e^{ikx} (with k being the magnitude of the wave vector) and assuming the reflectivity at each interface to be r, add up the contribution due to each reflection, sending a part of light in the negative $x-$ direction. Sum up the infinite series and hence show that the transmission can be zero for certain value of the wavelength. What is the significance of such a structure?

Bibliography

1. Agrawal, G., *Applications of Nonlinear Fiber Optics*, Academic Press (2010).

2. Agrawal, G., *Nonlinear Fiber Optics (Optics and Photonics)*, Academic Press (2012).

3. Banyai, L. and Koch, Stephan W., *Semiconductor Quantum Dots*, World Scientific (1993).

4. Bloembergen Nicolaas , *Nonlinear Optics*, World Scientific (1996)

5. Boyd, R. W., *Nonlinear Optics*, 3rd edition, Academic Press, USA, (2008)

6. Boyd, R. W. (ed), *Self-focusing: Past and Present*: Springer, Topics in Applied Physics, **114**, (2009)

7. Butcher, P. and Cotter, D., *The Elements of Nonlinear Optics*, Cambridge University Press, Cambridge, (1990)

8. Marcuse Dietrich , *Engineering Quantum Electrodynamics,* Harcourt, Brace & World, Inc. (1970)

9. Ferreira, M., *Nonlinear Effects in Optical Fibers* Wiley-OSA; (2011).

10. Fisher, R. A., *Optical Phase Conjugation*, Academic Press; (1983).

11. Gaponenko, S.V., *Optical Properties of Semiconductor Nanocrystals* (Cambridge Studies in Modern Optics), Cambridge University Press (2005)

12. Garmire Elsa, *Am. J. Phys.* **79**(3), 245, (2011).

13. Ghatak Ajoy and Thyagarajan, K., *An Introduction to Fiber Optics*, Cambridge University Press (1998)

14. Gibbs, H. M., *Optical Bistability: Controlling Light with Light*, Academic, Orlando, USA, (1985).

15. Guo Y. et al, *Nonlinear Photonics: Nonlinearities in Optics, Optoelectronics and Fiber Communications*, Springer, (2010)

16. He G. S. and Liu, S. H, *Physics of Nonlinear Optics*, World Scientific, New Jersey (2000).

17. Ho Kuang-Sheng, Guang S. He, Guang S. and Liu, H., *Physics of Nonlinear Optics*, World Scientific (2000).

18. Joannopoulos, J. D., *Photonic Crystals: Moldin the Flow of Light*, 2nd edition, Princeton University Press USA (2008).

19. Kittel, Charles *Introduction to Solid State Physics*, Wiley, (2004)

20. De Martino, R.N., Choe, E. W., Khanarian, G., Stuitz, D, Tomng C. C. and Yoon, H, in *"Nonlinear Optical and Electroactive Polymers"* ed. Prasad, Paras N. and Ulrich, Donald R., Plenum Press, New York, pp169-188 (1988)

21. Nalwa, Hari Singh, *Nanostructured Materials and Nanotechnology: Concise Edition*, Acad Press. (2001).

22. New, Geoffrey, *Introduction to Nonlinear Optics*, Cambridge University Press (2011)

23. Porsezian, K., *Optical Solitons: Theoretical and Experimental Challenges*, Springer, (2010)

24. Powers, Peter E., *Fundamentals of Nonlinear Optics*, CRC Press (2011)

25. Shen, Y. R, *The Principles of Nonlinear Optics* (Wiley Classics Library), Wiley-Interscience; (2002)

26. Stegeman, George I and Stegeman, Robert A., *Nonlinear Optics: Phenomena, Materials and Devices* (Wiley Series in Pure and Applied Optics) Wiley (2012)

27. Sutherland,R. L, *Handbook of Nonlinear Optics*, Marcel Dekker, New York 2003

28. Trillo, S and Torruellas, W, *Spatial solitons*, Springer (2001)

References

Agrawal, G., *Applications of Nonlinear Fiber Optics*, Academic Press, (2010).

Agrawal, G., *Nonlinear Fiber Optics (Optics and Photonics)*, Academic Press, (2012).

Alivisatos, A . P., *J. Phys. Chem.*, **100** (31), 13226 (1996)

Alfano, R. R., *The Supercontinuum Light Source*, Springer, (2006).

Ashcroft N. W. and Mermin M. D., *Solid State Physics*, Cengage Learning, (1976).

Baba, T., *Nature Photonics*, **2**, 465 (2008)

Banyai, L. and Koch, S. W., *Semiconductor Quantum Dots*, World Scientific (1993).

Barettand, H. H. and Jacobs, S. F., *Opt. Lett.,* **4** , 190, (1979).

Bindra, K. S., Oak, S. M., Rustagi, K. C., *Physical Review B* **59**, 2968, (1999)

Bindra, K. S. and Kar., A. K., *Appl. Phys. Lett.* **79**, 3761 (2001)

Bloembergen N., *Nonlinear Optics*, World Scientific (1996)

Bonaccorso, F., Sun, Z ., Hasan ,T. and Ferrari, A. C., *Nature Photonics*, **4**, 611 (2010)

Boyd, R. W., *Nonlinear Optics*, Academic Press, USA, (2008)

Boyd, R .W. (ed), *Self-focusing: Past and Present*: Springer, Topics in Applied Physics, **114**, (2009)

Boyd, R. W. and Gautheir, D. J., *Science 326*, 1074 (2009).

Boyd, R. W., *J. Opt. Soc. Am. B* **28**(12), A 38, (2011)

Brignon, A. and Jean-Pierre H. (Ed.), *Phase Conjugate Laser Optics*, John Wiley Interscience, (2003).

Brus, L. E., *J. Chem. Phys.* **80**, 4403 (1984)

Butcher, P. and Cotter, D., *The Elements of Nonlinear Optics*, Cambridge University Press, Cambridge, (1990)

Chang, T. Y. and Hellwarth, R .W., *Opt. Lett.*, **10**, 408, (1985).

Chemla, D. S., *Rep. Prog. Phys.* **43** 1191 (1980)

Chemla, D. S. and Zyss, J., *Nonlinear optical properties of organic molecules and crystals*, Academic Press (1987)

Chen, Chin -Hui, Matsuo, S., Nozaki, K. , Shinya, A., Sato, T., Kawaguchi, Y., Sumikura, H. and Notomi, M., *Optics Express*, **19**(4) 3387 (2011)

Chin-Hui, C. and Matsuo, S. , *Optics Express*, **19**, 3387, (2011).

Caro, R .G., and Grower, M. C., *IEEE J. Quantum Electron.*, **18** (1982), 1376, (1982)

Cui, M. and Yang, C., *Optics Express*,**18**, 3444 (2010)

Du, H., Xu, G. Q., Huang, L., Chin , W. S. and W. Ji, *Chem. Mater.* **14**, 4473 (2002)

Dudley and Taylor, J., R., (Eds.), *Spercontinuum Generation in Optical Fibers,* Cambridge University press (2010)

Fieste, U., Ludwig , R., Schmidt, C., Dietrich, E., Diez, S., Ehrke, H. J., Patzak, E., Weber, H. G. and Merker, T., *IEEE Photonics Technology Letters* **11**, 1063, (1999).

Feinberg, J. and Hellwarth, R. W., *Opt. Lett.*, **5** 519 (1980); erratum: *Opt. Lett.* **6 257** (1981)

Ferreira, M., *Nonlinear Effects in Optical Fibers* Wiley-OSA; (2011).

Fisher, R. A., *Optical Phase Conjugation*, Academic Press; (1983).

Franz, W. and *Naiturf, Z.*, **13a**, 484 (1958).

Gaponenko, S. V., *Optical Properties of Semiconductor Nanocrystals* (Cambridge Studies in Modern Optics), Cambridge University Press (2005)

Garmina E., *Am. J. Phys.* **79**(3), 245, (2011).

Garrett, C. G. B. and Robinson, F. N. H., *IEEE J. Q. Electronics* **QE 2**, 328 (1966)

Ghatak, A. and Thyagarajan, K., *An Introduction to Fiber Optics*, Cambridge University Press (1998)

Gibbs, H. M, *Optical Bistability: Controlling Light with Light*, Academic, Orlando, USA, (1985).

Gita, B., Sundararajan, G., Vijaya, R. and Murti, Y. V .G. S., *Opt. Mat.* **4**, 663 (1995)

Giuliano, C. R., *Physics Today*, **34**, 27, (1981).

Gower, M., Proch, D. (Ed), *Optical Phase Conjugation*, Springer-Verlag (1994).

Gu,C., Xu, Y., Liu, Y., Pan, J. J., Zhou, F. and He, H., *Optical Materials* **23**, 219 (2003).

Guo,Y., Kao, C. K., Li, H. E. and Chiang, K. S., *Nonlinear Photonics: Nonlinearities in Optics, Optoelectronics and Fiber Communications*, Springer, (2010).

Gupta, J., Lim, Xiaodai, Sow, C. H., and Vijayan, C., *Journal of Nanoscience and Nanotechnology* **11**(5),4029 (2011)

Gupta, J., Vijayan, C., Maurya, S. K, and Goswami, D., *Materials Letters* **65**(5), 3 (2012)

Haret, D, L., Tanabe, T., Kuramochi, E. and Notomi, Masaya, *Optics Express* **17**, 21108 (2009)

Hau, L. V., Harris, S. E., Dutton, Z., and Behroozi, C. H., *Nature*, **397**, 594, (1999).

He, G. S. and Liu, S. H., *Physics of Nonlinear Optics*, World Scientific, New Jersey (2000).

He, G. S., *Progress in Quantum Electronics*, **26**, 131 (2002).

Hecht, E., *Optics*, Addison Wesley, 4th edition (2001)

Hellwarth, R., *J., Opt. Soc. Amer.* **67**, 1 (1977).

Hilinski, F., Edwin, Lucas, A .P. and Wang, Y. *J., Chem. Phys.* **89**, 3435 (1988);

Hirooka,T. and Hasegawa,A., *Electronics Letters*, **34**, 2056 (1998).

Hutchings, D. C., Sheik-Bahai, M., Hagan, D. J. and van Stryland E. W., *and Quantum Electronics*, **24**, 1 (1992).

Ibach, H. and Lüth, H., *Solid-State Physics: An Introduction to Principles of Materials Science*, Springer (2002)

Ioerdman, J. P., *Opt. Comm.* **2** , 212 (1970).

Jain, R. K. and Lind, R. C., *JOSA*, **73**, 647 (1983).

Joannopoulos, J. D., *Photonic Crystals: Molding the Flow of Light*, Princeton University Press USA (2008).

Kajzar, F. and Reinisch, R. (Ed), *Beam Shaping and Control with Nonlinear Optics*, Plenum Publishing coorporation, USA, (1998).

Keldysh, L. V., *Soviet Phys. JETP*, **7**, 788 (1958).

John K. A., Udayakumar, D., Chandrasekharan, K., Ahdikari, A. V., Shashikal, H. D. and Philip, R., *Optics Communications*, **271**(1), 236 (2007)

John, S., *Phys. Rev. Lett.* **58**, 2486 (1987)

Khurgin, J. B., *Adv. Opt. Photon.*, **2**, 287 (2011).

Khurgin, J. B., *Progress in Slow/Fast/Stopped Light*, in Advanced Photonics, OSA Technical Digest, Optical Society of America (2011).

Kittel, C. , *Introduction to Solid State Physics*, Wiley, (2004)

Kivshar,Y. and Agrawal, G., *Optical solitons: from fibers to photonic crystals*, Academic Press (2003).

Kleinman, D. A, *Phys. Rev.* **126**, 1977 (1962)

Klimov, V. I., Schwarz, Ch. J. and McBranch, D. W., *Phys. Rev. B* **60**, R2177 (1999).

Klimov, V. I., A. A. Mikhailovsky, Xu Su, Malko A., Hollingsworth, J. A., Leatherdale, C. A., Eisler H, J and Bawendi, M, G., *Science*, **290,** 314 (2000)

Korteweg, D. J. and Vries, G. de, *Phil. Mag.,* 5th series **39**: 422, (1895).

Krishnamurthy, C. V. and Murti, Y. V. G. S., *Nonlinear Optics* **2** 337 (1992)

Haret, Laurent-Daniel, Tanabe, T., Kuramochi, E. and Notomi, M., *Optics Express*, **17**, p. 21108 (2009).

Irimpan, L., Krishnan, B., Nampoori, V. P. N. and Radhakrishnan, P., *Optical Materials*, **31** (2), 361 (2008).

Lu, H., Xue, Chun-hua , Jiang, Hai-tao and Chen, Hong, *JOSA B*, **28**(4) 856 (2011).

Mabuchi, H., *Appl. Phys. Lett.* **98**, 193109 (2011).

Majles Ara, M. H., Vijayan, C. and Murti,Y. V. G. S, *Nonlinear Optics*, **17**, 1 (1997)

Majles Ara, M. H., Vijayan, C. and Murti,Y. V. G. S, *Nonlinear Optics*, **26**, 313 (2001)

Markowicz, P., Friend, C., Shen, Y., Swiatkiewicz, J., Prasad, N. P. , Toader, O., John, S. and Boyd, R. W. *Opt. Lett.* **27**, (5), 351 (2002).

Przemyslaw P. M., Hanifi T., Haridas P., Paras N. P., Nick N. Lepeshkin and Robert W. Boyd, *Phys Rev Lett.* **92**(8), 083903 (2004).

De Martino, R. N., Choe, E. W., Khanarian, G., Stuitz, D., Tomng, C. C. and Yoon, H., in *"Nonlinear Optical and Electroactive Polymers"* ed. Prasad, P. N and Ulrich, D. R, Plenum Press, New York, 169 (1988)

Merker, T. and Meissner, P., *IEEE Journal of Selected Topics in Quantum Electronics,* **6**(2), 258 (2000).

Miller, R. C., *App. Phys. Lett* **5,** 17 (1964)

Minardi, S., Eilenberger, F., Kartashov, Y. V., Szameit, A., Röpke, U., Kobelke, J., Schuster, K., Bartelt, H., Nolte, S., Torner, L., Lederer, F., Tünnermann, A., and Pertsch, T., *Phys. Rev. Lett.* **105**, 263901 (2010).

Miwa, T., Jimbo, M. and Date,E., *Solitons: Differential Equations, Symmetries and Infinite Dimensional Algebras* Cambridge University Press, (2000)

Murti, Y. V. G. S., Nandakumar, P. and Vijayan, C., *Physics Education (India)*, 229 (1999).

Nandakumar, P., Vijayan, C. and Murti, Y. V. G. S., *Optics Communications*, **185**, 457, (2000).

Nandakumar, P., Vijayan , C. and Murti,Y. V. G. S., *Jl. of Appl. Physics* **91**(3), 1509, Feb (2002).

Nair, R. V. and Vijaya, R., *Progress in Quantum Electronics*, **34**(3), 89 (2010)

Neumann, F. E., *Vorlesungen über die Theorie der Elasticität der festen Körper und des Lichtäthers*, Meyer, O. E., Ed.; B. G. Teubner-Verlag: Leipzig, Germany (1885).

Notomi, M., *Rep. Prog. Phys.*, **73**, 096501, 57 (2010)

Oak, S. M, Bindra, K. S., Chari, R. and Rustagi, K. C., *JOSA B* **10**, 613 (1993).

Parida, M. R., Vijayan, C., Rout, C. S., Suchand Sandeep, C. S. and Philip, R., *Applied Physics Letters*, **100**, 121119 (2012)

Park, S. H, Morgan, R. A., Hu, Y. Z., Lindberg, M., Koch, S. W. and Peyghambarian, N., *JOSA B*, **7** (10) 2097 (1990)

Pégard, N. C. and Fleischer, J. W., *Novel Techniques in Microscopy (NTM)*, Monterey, California, April (2011).

Lucarini, V., Saarinen, J. J., Peiponen, Kai-Erik and Vartiainen E. M, *Kramers-Kronig Relations in Optical Materials Research*, Springer (2005).

Peiponen, Kai-Erik, Vartiainen E. M and Asakura T, *Dispersion, Complex Analysis and Optical Spectroscopy*, Springer (2010).

Pepper, D. M., *Opt. Eng.* **21**(2), 212156 (1982).

Pepper, D. M., *Scientific American,* **254**, 76, (1986).

Pernice, W. H. P., Mo L. P., and Tang, H. X., *Optics Express*, **18**, p. 18438, (2010).

Philip, R., Chantharasupawong, P., Qian, H., Jin,R. and Thomas J., *Nano Letters*, **12**(9), 4661 (2012).

Polavarapu, L., Xu, O., Dhoni, M. S. and Wei, Ji, *Appl. Phys. Lett.* **92**, 263110 (2008).

Kurien, P. A, *Ph. D. Thesis,* Indin Institute of Technology, Madras, INDIA (2008).

Kurian, P., Sathiyamoorthy, K., Vijayan, C., Sandeep, S. and Philip, R. *Nanoscale Research Letters*, **2**, 561 (2007)

Kurian, P. A., Vijayan, C., Suchand Sandeep, C. S., Philip, R. and Sathiyamoorthy, K., *Nanotechnology* **18**, 075708 (2007)

Roussignol, P., Ricard, D., Lukasik, J., Flytzanis, C., *JOSA B*, **4**(1), 5 (1987)

Roussignol, P., Ricard, D., Rustagi, K. C. and Flytzanis,C. *Optics Communications* **55**(2), 143 (1985)

Russel, J. S., *Report of the fourteenth meeting of the British Association for the Advancement of Science*, York, 311, (1844).

Rustagi, K. C., Flytzanis, C., *Optics Letters* **9**, 344(1984)

Sathiyamoorthy, K., Vijayan, C. and Varma, S., *Langmuir*, **24**, 7485 (2008)

Schwerzel, R. E., Spahr, K. B., Kurmer, J. P., Wood, V. E. and Jenkins, J. A, *J. Phys. Chem.* A **102**, 5622 (1998).

Shen, Y. R., *The Principles of Nonlinear Optics* (Wiley Classics Library), Wiley-Interscience; (2002)

Sheik-bahae, M., Said, A. A., Wei, T., Hagen, D. J. and Stryland, E. W. V, *Opt. Lett.* **14**, 955, (1989).

Sheik-bahae, M., Said, A. A., Wei,T., Hagon, D. J and Stryland, E. W. V, *IEEE Journal of Quantum Electronics*, **26,** 760 (1990).

Shkunov, V. and Zel'dovich, Y. B, *Scientific American*, **253**, 40, (1985).

Unnikrishnan, K. P., Thomas, J., Nampoori,V. P. N. and Vallabhan, C. P. G. *Chem. Phys.*, 279, 209, (2002).

Singh, V. A., Ranjan, V. and Kapoor, M., *Bull. Materials Sci.*, **22**, 563 (1999)

Smith, C. S., *'Macroscopic symmtery and properties of crystals', Solid State Physics*, **6**, Ed. F. Seitz and D. Turnbull, (1958).

Smith, S .D., *Appl. Opt.* **25**, 1550 (1986).

Soljacic´, M., Ibanescu, M., Johnson, S. G., Fink, Y. and Joannopoulos, J., D., *Phys. Rev. E*, 66, 055601R (2002).

Solli, D., R., Ropers C., Koonath, P. and Jalali, B., *Nature* **450**, 1054 (2007).

Stegeman, G.I., Wright, E. M., Finlayson, N., Zanoni, and Seaton, C. T., *J. Lightwave Technology* **6**, 953 (1988).

Stepanov, B.I., Ivakin, E.V. and Rubanov, A. S., *Sov. Phys.-Dokl., Tech. Phys.* **15**, 46 (1971).

Suresh Babu, K., Vijayan, C. and Devanathan, R., *Materials Letters*, **58**(7-8), 1223 (2004)

Suresh Babu, K., Vijayan, C. and Haridoss, P., *Materials Research Bulletin*, **42**(**6**),996 (2007)

Suhara, T. and Fujimura, M., *Waveguide Nonlinear-Optic Devices*, (Springer Series in Photonics), Springer (2010)

Sutherland, R. L., *Handbook of Nonlinear Optics*, Marcel Dekker, New York 2003

Takagahara, T., *Phys. Rev. B* **36**, 9293 (1987)

Tomme E. V., Van Daele P. P., Baets, R. G. and Lagasse, P. E., *IEEE J. Quantum Electronics* **27**, 778 (1991)

Trillo, S. and Torruellas, W., *Spatial solitons*, Springer (2001);

Van Vechten, J. A. and Aspnes, D. E., *Physics Letters A*. **30**(6), 346, (1969)

Venkatram, N., Narayana Rao, D. and Akundi, M. A., *Optics Express*, **13**(3) 867 (2005)

Venkatram, N., Sathyavathi, R. and Narayana Rao, D. *Optics Express*, **15**(19) 12258 (2007)

Venkatram, N., Narayana Rao, D., Giribabu, L, Venugopal Rao, S., *Chemical Physics Letters*, **464**, 211 (2008)

Vijaya, R., Murti, Y. V. G. S., Sundararajan, G. and Prasada Rao, T. A., *Optics Commun.* **76**, 256 (1990).

Vijaya, R., Murti, Y. V. G. S., Prasada Rao,T.A. and Sundararajan,G. *J. Appl. Phys.* **69**, 3429 (1991).

Vijaya, R., Murti, Y. V. G. S., and Prasada Rao,T.A *J. Mod. Optics* **39**, 115 (1992).

Vijaya, R., Murti, Y. V. G. S., Sundararajan, G., Mathews, C. K. and Vasudeva Rao, P. R., *Optics Commun.* **94**, 353 (1993).

Vijaya, R., Murti, Y. V. G. S., Vijayaraj,T. A. and Sundararajan, G., *Opt. Quant. Electr.*, **25**, 723 (1993).

Vijaya, R., Murti, Y. V. G. S., Vijayaraj, T. A. and Sundararajan, G. *Curr. Sci.* **72**, 507 (1997).

Wadsworth, W. J., Ortigosa-Blanch, A., Knight, J. C., Birks, T. A., Man, T. -P. M. and Russel, P.St. J.,*JOSA A*, **19**, 2148 (2002)

Wang, Y. *Acc. Chem. Res.*, **24**(5), 133 (1991)

Wang, Y. and Herron, N., *J., Phys. Chem.*, **95**(2), 525 (1991).

Wang, Y. and Mahler, W., *Optics Communications* **61**(3), 171(1987).

Warrier, Anita R. and Vijayan, C., *Resonance,***18**, 1015 (2013).

Woggon, U., *Optical Properties of Semiconductor Quantum Dots*, Springer Tracts in Modern Physics 136 Springer, Berlin (1997).

Yablonovitch, E., *Physical Review Letters* **58** (20), 2059 (1987)

Yang, H. Z., Feng, X. B., Wang, Q., Huang, H., Chen, W., Wee, A. T. S., Ji, W., *Nano Letters* **11**, 2622 (2011).

Yaqoob, Z., Psaltis, D., Feld, M. S. and Yang, C., *Nature Photon.*, **2**, 110 (2008).

Yariv, A., *IEEE J. Quant. Electron. QE* **14,** 650 (1978).

Yariv, A.*Quantum Electronics*, John Wiley, New York (1989).

Yao, X. and Belyanin, A. *Proc. SPIE* **8604**, 860412 (2013);

Yoffe, A. D. *Advances in Physics* **42**(2), 173 (1993)

Zel'Dovich, B. Y., Pilipetskii, N. F.,Ragul'ski, V. V. and Shuknov, V. V., *Sov. J. Quant. Electron.*, **8**, 1021 (1978).

Zel'Dovich, B. Y., Popovichev, Ragulskii, V. V., and Faisullov, F. S., *JETP Letters,***15**, 109 (1972); **16**, 435 (1972).

Index

A
Aberration 111
Abrosprion, saturable 135
Absorption 135
Absorption, multi-photon 5
Absorption, nonlinear 135
Absorption, optical 132
Absorption, reverse saturable 135
Absortion, two-photon 144
Airy 121
Anharmonicity 149
Anisotropy 93
Aperture 130

B
Bahae, Sheik 129
Band filling 157
Band gap 2
Band gap, Photonic 1
Beam 126
Beam, Gaussian 126
Berra 29
Bistability, optical 7
Bloembergen 7
Bottleneck, materials 5
Boyd 126
Brillouin 15

C
Carrol 125
Cartesian 17
Centrosymmetric 43
Chirp 138
Chirp, negative 138
Chirp, positive 138
Coefficient
Coherence 93
Color center 55
Conducting media
Conduction band 157
Conservation 23
Coulomb 165
Crystal, centrosymmetric 43
Crystal, photonic 8
crystal, uniaxial 29
Crystalline 6
Cubic 30

D
Delocalization 149
density matrix 55
Devices 3
Devices, nonlinear optical 4
Dielectric constant 47
Dimension 6
Dipole moment 12
Dirac 55
Dispersion 8
Dispersion, group velocity 140
Displacement vector 47
Double integral 68

E
Effective mass 158
Efficiency
Einstein 1
Electric field 15
Electromagnetically induced transparency 170
Electromagnetism 78
Electron 2
Electron-hole pair 164

Electronic 3
Electrostatic 25
Ellipsoid 47
Emission, spontaneous 167
Emission, stimulated 15
Energy 2
Energy transfer 77
Energy, Coulomb 165
Engineering, bandgap 7
Equation of motion 55
Etalon 101
Exciton 7
Exciton Bohr radius 164
Expectation value 56
Extraordinary 11

F
Far field 130
Feynman 77
Fiber optics 173
Fluorescence 165
Four wave mixing 15
Fourier transform 21
Free space 4
Frequency 4
Frequency mixing 5
Frequency, instantaneous 138

G
Gaussian 126
Grating 112
Grating, Bragg 112
Group velocity 140

H
Hamilton 56
Harmonic generation 5
Hexagonal 30
Hydrogen 45

I
Imaginary 15
Induced transparency 135
Intensity 3
Intensity, high 3
Intensity-depend refractive index 15
Interaction 2
Ion-implantation 7
Irradiance 116
Isotropic 4

K
keldysh 157
Kerr effect 27
Kittel 148
Kleinman 45
Kortweg 141
Kramers-Kronig 148
Krishnamurti 199

L
Laser 2
Light bullet 143
Light, slow 170
Liquid crystals 6
Loaclization, Anderson 167
loss 88
Low Dimensional 162

M
Macroscopic 12
Magnetic field 9
Material 1
MaxwellŠs equations 81
Mechanism 8
Mechanism, band gap filling 149
Mechanism, orientational 149
Mechanism, thermal 149
Microscopic 114
Modulation 113
Modulation, phase 113
Modulation, phase
Modulation, self phase 114

Molecular 7
Momentum 56
Monochromatic 14
Monoclinic 30

N
Nanomaterial 165
Nanoparticle 135
Neumann 29
Non-degenerate 141
Nonlinear Optics 2
Non-magnetic 85
Non-parabolicity 149
Nonradiative 71

O
Operator 52
Optical absorption 124
Ordinary 11
Organic 6
Orthorhombic 30

P
Parametric mixing 74
Particle in a box 163
Permeability 84
Perspective 148
Perturbation 61
Phase 8
Phase conjugate mirror 109
Phase matching 77
Phase shift 117
Phase velocity 50
Photoluminescence 166
Photon 2
Photonics 1
Photorefractive 153
Polarization 4
Pockels effect 14
Point group 30
Polarizability 12
Polarizability, atomic 159
Polymer 6
Polymer, conjugate
Probe beam 105
Process 2
Profile, beam 8
Profile, spectral 170
Prototype 152
pulse width 136
Pump 91

Q
Quantum confinement 7
Quantum dot 162
Quantum Well 162

R
Radiative 71
Raman 15
Real 16
Rectification 14
Reflection, nonlinear 110
Reflectivity 108
refractive index 5
Relaxation 71
Rose 11
Round trip 117

S
Scattering 15
Second harmonic generation 14
Self focusing 115
Self phase modulation 114
Self trapping 125
Semiconductor 6
Shröedinger 142
Slowly varying envelope approximation 105
Soliton 8
Soliton, spatial 127
Soliton, temporal 140
Stimulated 15
Susceptibility 15

Susceptibility tensor 29
Susceptibility, linear 30
Susceptibility, nonlinear 70
Switching, photonic 15
Symmetry 18
Symmetry, crystal 30
Symmetry, time reversal 103

T
Tagore 101
Technology 1
Tetragonal 30
Thermal 8
Threshold 8
Time reversal 53
Transition 7
Transition, nonradiative 71
Transition, radiative 74
Triclinic 30

U
Ultrafast 8
Uniaxial 29

V
Valence band 157
Velocity, group 140
Velocity, phase 50
Visualize 144

W
Wave equation, linear 86
Wave equation, nonlinear 86
Wave function 56
Wave mixing 3
Wavefront 101
Wavelength 89

Y
Yariv 103

Z
z-scan 129
z-scan, closed 131
z-scan, open 131

The last page ...

"Every beginning
is but a continuation,
and the book of events
is never more than half open."
Wislawa Szymborska

"*There is no end to education. It is not that you read a book, pass an examination, and finish with education. The whole of life, from the moment you are born to the moment you die, is a process of learning*".
Jiddu Krishnamurti

The bottom line

Optics is NOT *light* work; it is making light *work*!